Supplementary Information

Precision polymer nanofibers with a responsive polyelectrolyte corona designed as a modular, functionalizable nanomedicine platform

Steven T. G. Street,[1,2,3]† Yunxiang He,[1]‡ Robert L. Harniman,[1] Juan Diego Garcia-Hernandez[2] and Ian Manners[2,3]*

[1] School of Chemistry, University of Bristol, Bristol BS8 1TS, United Kingdom

[2] Department of Chemistry, University of Victoria, Victoria, BC V8W 3V6, Canada

[3] Centre for Advanced Materials and Related Technology (CAMTEC),

University of Victoria, 3800 Finnerty Rd, Victoria, BC, V8P 5C2, Canada

* Corresponding Author: imanners@uvic.ca

Contents

Supplemental Results and Discussion

Investigating the self-assembly landscape of PFTMC$_{16}$-*b*-PDMAEMA$_{131}$ (P1)

More detailed investigations into the self-assembly of PFTMC$_{16}$-*b*-PDMAEMA$_{131}$ (**P1**) are discussed here. DMSO and THF were studied as common solvents, whilst MeOH, EtOH, iPrOH and water were studied as selective solvents. As the ratio of common solvent to selective solvent is an important parameter for controlling particle morphology, several ratios of common:selective solvent were examined: 5:95 and 20:80 *v/v* for samples with DMSO as the common solvent, and 5:95, 10:90 and 20:80 *v/v* for samples with THF as the common solvent. Initial results focused on annealing the samples at 70°C for 30 mins to facilitate CDSA, however good results were also obtained for samples prepared at room temperature. Morphologically pure nanofibers were obtained in 13 out of 40 different conditions screened (33%) as well as 7 out of 10 conditions screened using MeOH as the selective solvent. Such versatility and robustness in self-assembly is necessary for future efforts to produce functional polymer nanofibers through CDSA.

Results from utilizing DMSO as the common solvent (Figure S31-Figure S32) revealed that 20% *v/v* DMSO was sufficient to yield morphologically pure nanofibers in MeOH, EtOH and iPrOH. Mixtures of DMSO:water (20:80) yielded predominantly nanospheres, with some short nanofibers also observable. This result is consistent with the challenge of obtaining morphologically pure nanofibers via CDSA in water.[S1,S2] 20% *v/v* DMSO favoured nanofiber formation over 5% *v/v* DMSO. Morphologically pure nanofibers were obtained in DMSO:MeOH (20:80), however a mixture of nanofibers and nanospheres were obtained for DMSO:EtOH and DMSO:iPrOH (20:80 *v/v*) mixtures. Interestingly, mixing at room temperature in water yielded larger spherical aggregates (possibly vesicles, $D_n = 395$ nm, $Đ = 1.05$, $\sigma = 86$ nm), with a relatively low dispersity. Comparing trends in alcoholic solvents across both Figure S31 and Figure S32, it was clear that annealing the sample prior to self-assembly reversed the order of

preference from MeOH > EtOH > iPrOH for samples mixed at room temperature, to iPrOH > EtOH > MeOH for samples annealed at 70°C for 30 mins. This effect was especially pronounced for samples with 5% *v/v* DMSO: At room temperature, MeOH is the favoured solvent, yielding morphologically pure nanofibers whilst EtOH yields a mixture of nanofibers and nanospheres, and iPrOH yields morphologically pure nanospheres. After annealing to 70°C, iPrOH is the favoured solvent, yielding morphologically pure nanofibers whilst MeOH and EtOH yield mixtures of nanofibers and nanospheres.

Use of THF as the common solvent (Figure S33-Figure S34) revealed morphologically pure nanofibers under several conditions. Annealing at 70°C (Figure S33) yielded morphologically pure nanofibers in: THF:MeOH (10:90 and 20:80 *v/v*), THF:EtOH (10:90 *v/v*), and THF:iPrOH (20:80 *v/v*). Additionally, THF;MeOH (5:95 *v/v*) yielded nanofibers with a small quantity of nanospheres, whilst THF:EtOH (5:95 and 20:80 *v/v*), and THF:iPrOH (5:95 and 10:90 *v/v*) yielded mixtures of nanofibers and nanospheres. Interestingly, results in water revealed relatively low dispersity aggregates with triangular faces, as well as nanospheres. Results from mixing at room temperature (Figure S34) revealed morphologically pure nanofibers in THF:MeOH (5:95, 10:90 and 20:80 *v/v*), THF:EtOH (10:90) and THF:iPrOH (20:80 *v/v*) as well as mixtures of nanofibers and nanospheres in THF/EtOH (5:95 and 20:80 *v/v*) and THF/iPrOH (10:90 *v/v*). THF/EtOH (20:80 *v/v*) and THF/iPrOH (5:95 *v/v*) both exhibited oligomers and aggregates of nanospheres, which in the case of THF/iPrOH (5:95 *v/v*) appeared as large, sheet-like structures. These could possibly be intermediate species that yield insights into the mechanism of formation of nanofibers, though this requires further investigation. The analogous THF/iPrOH (5:95 *v/v*) sample that was annealed at 70°C was a mixture of nanofibers and nanospheres, indicating that annealing the samples at 70°C helps facilitate nanofiber growth, and suppresses the aggregation of nanospheres. THF/water (5:95 and 20:80 *v/v*) also exhibited the relatively low dispersity aggregates with triangular faces, as well as nanospheres. THF/water (10:90 *v/v*) yielded morphologically pure nanospheres.

When these self-assembly results are taken together, several observations can be made. Firstly, in all samples that yielded disperse nanofibers it was found that the nanofibers exhibited a strong tendency to aggregate and entangle, often forming spherical supermicelle aggregates that were tens of microns in diameter (Figure S35). Regarding the effects of common solvent: for some samples, merely ensuring the unimer is dissolved in common solvent prior to addition of selective

solvent is sufficient to yield morphologically pure nanofibers at any ratio of common solvent to selective solvent. However, increasing the amount of common solvent present generally leads to a lower fraction of nanospheres, and an increased fraction of nanofiber micelles. This presumably occurs though increasing the solubility of the core-forming block, which better facilitates exchange from nanospheres into unimer, which can then undergo epitaxial growth to increase the fraction of nanofibers present. Thus, increasing the percentage of common solvent present in a sample is a useful tool for reducing the presence of nanosphere impurities and generating morphologically pure nanofibers. Annealing the sample is another method for reducing the presence of nanosphere impurities. Comparing the effects of the nature of both the common and selective solvents, it was clear that the selective solvent plays a much more important role in dictating the resulting morphology. Whilst differences between DMSO and THF were observed for the common solvent, these were typically more subtle. THF was selected as the common solvent of choice, as its lower boiling point better facilitates transfer of samples into water. The selective solvent is important, balancing solvent polarity with the solubility of both the core- and corona-forming blocks of the unimer. If the solvent is too polar and the unimer solubility is too low (as is the case in water), unimer aggregation occurs quickly and unimer exchange is unable to occur, leading to kinetically trapped nanospheres. Conversely, if the solvent polarity is lower, the core-forming block exhibits a better solubility and crystallization occurs at a slower rate, but this cannot compensate for the reduced solubility of the corona, which again leads to nanospheres. The effects of the selective solvent were inherently tied to the effects of annealing the sample before self-assembly. In general, annealing the sample for 30 mins before self-assembly occurs was sufficient to favour nanofiber growth and supress the formation of nanospheres, however morphologically pure nanofibers can still be obtained through mixing and aging at room temperature. In many cases, the morphologies observed differed between the annealed and non-annealed samples, with more unique morphologies observed after mixing and aging at room temperature. It was clear that MeOH worked well as a selective solvent under most conditions, however annealing samples in iPrOH frequently increased the fraction of nanofibers, whilst annealing samples in EtOH seemed to have little effect. Self-assembly of the intermediate PFTMC$_{16}$-b-(PDMAEMA·HCl)$_{124}$ was also attempted, using DMSO/MeOH (5:95 v/v) and DMSO/water (5:95 v/v) after annealing at 70°C for 30 mins (Figure S36). Unfortunately, nanospheres were obtained in both cases. Protonation of the amine residues in the PDMAEMA corona would be expected to facilitate inter-coronal affinity

between separate PDMAEMA chains through electrostatic interactions and hydrogen bonding. This increased inter-coronal affinity might be sufficient to supress crystallization of the PFTMC core, and hence provide an explanation for why PFTMC$_{16}$-b-(PDMAEMA·HCl)$_{124}$ cannot form nanofiber micelles through CDSA.

Assessing the long-term colloidal stability of P1 nanofibers and nanospheres

This section details additional discussion on the long-term colloidal stability of **P1** nanofibers and nanospheres. Previous DLS studies suggest that molecularly dissolved polymers (unimers) should exhibit a D_h of less than ca. 10 nm, whilst discrete nanofibers or nanospheres would have a D_h of between ca. 50 and 200 nm, and aggregates of nanoparticles would have a D_h of greater than 200 nm. The initial D_h values for the 137 nm **P1** nanofibers ($Đ = 1.05$, $\sigma = 30$ nm, Figure S45) and 14 nm **P1** nanospheres ($Đ = 1.05$, $\sigma = 3$ nm, Figure S46) under the conditions studied are displayed in Figure S50A. The 137 nm nanofibers exhibited D_h values ranging from 77 – 132 nm indicative of unaggregated nanofibers. A shift in D_h was observed for the 137 nm **P1** nanofibers ($Đ = 1.05$, $\sigma = 30$ nm) from 82 ± 1.4 nm in 5 mM NaCl to 132 ± 1.0 nm in 20 mM HEPES + 5 wt% glucose pH 7.4 (HBG), which is consistent with an increase in coronal swelling due to protonation of the secondary amine residues in the PDMAEMA corona. After 2 months, the D_h and ζ-potential of the 137 nm **P1** nanofibers ($Đ = 1.05$, $\sigma = 30$ nm) was recorded again (Figure S50B-C). The 137 nm **P1** nanofibers ($Đ = 1.05$, $\sigma = 30$ nm) remained colloidally stable and unimeric in THF/MeOH (2:98 v/v). The D_h of 137 nm **P1** nanofibers ($Đ = 1.05$, $\sigma = 30$ nm) and 14 nm **P1** nanospheres ($Đ = 1.05$, $\sigma = 3$ nm) in 5 mM NaCl after 4 months was comparable to the initial values and indicated that both **P1** nanofibers and **P1** nanospheres were colloidally stable upon dilution into 5 mM NaCl from water (Figure S50D).

The ζ-potential of **P1** nanofibers and **P1** nanospheres exhibited diverging changes over a four-month period (Figure S50E). 137 nm **P1** nanofibers ($Đ = 1.05$, $\sigma = 30$ nm) increased from $+18 \pm 0.6$ mV initially to $+22 \pm 0.6$ mV after 2 months and $+31 \pm 0.5$ mV after 4 months, indicating a long-term trend towards increasing surface charge over time. In comparison, the ζ-potential of the 14 nm **P1** nanospheres ($Đ = 1.05$, $\sigma = 3$ nm) changed from $+26 \pm 0.4$ mV initially to $+11 \pm 0.5$ mV after 4 months. Particle morphology therefore appears to influence surface charge, with **P1** nanospheres exhibiting a higher initial ζ-potential than the corresponding **P1** nanofibers. Over a period of months however, the ζ-potential of the nanofibers and nanospheres diverge, rising for **P1** nanofibers and decreasing for **P1** nanospheres.

To date, the longest timeframe that materials produced through living CDSA have been studied over is one year.[S3,S4] To expand upon this, we stored **P1** nanofibers at room temperature (23°C) for 2 years either in their preparation conditions (THF/MeOH 20:80 v/v, L_n = 93 nm, $Đ$ = 1.05, σ = 22 nm) or in water (L_n = 94 nm, $Đ$ = 1.10, σ = 30 nm), analysing them via TEM (Figure 6 and Figure S51). After 2 years of storage at room temperature, colloidal stability was maintained for both samples with morphologically pure nanofibers observed via TEM (Figure 6B, E). In THF/MeOH (20:80 v/v), the length of 93 nm **P1** nanofibers ($Đ$ = 1.05, σ = 22 nm) had increased to 282 nm ($Đ$ = 1.76, σ = 246 nm, Figure 6A-C) which was accompanied by a significant increase in nanofiber width from 10 nm ($Đ_W$ = 1.03, σ = 2 nm) to 29 nm ($Đ_W$ = 1.06, σ = 7 nm, Figure S51A-B) and an increase in both length- and width-dispersity. The limited evidence of nanofibers shorter than 93 nm indicates that fragmentation was not an issue. The large population of nanofibers that were longer and wider than the original sample implies that micelle fusion had occurred. Similar observations of end-to-end micelle fusion have been made previously,[S5–S7] however in this case it appears to result from side-to-side micelle fusion as well as end-to-end fusion. Additional evidence for micelle fusion is the observation of a central line running down the middle of many nanofibers (Figure S51A). It appears that long-term storage of **P1** nanofibers in THF/MeOH is favourable for the fusion of nanofibers and unfavourable for fragmentation, leading to a gradual increase in nanofiber length and dispersity. After 2 years of storage at 23°C in water (Figure 6D-F and Figure S51C-D), nanofiber length decreased from 94 nm ($Đ$ = 1.10, σ = 30 nm) to 69 nm ($Đ$ = 1.46, σ = 47 nm), with a more modest increase in dispersity (σ of 47 nm) whilst nanofiber width remained consistent (W_n = 13 nm, $Đ_W$ = 1.02, σ = 2 nm). The primary driver for the observed increase in length-dispersity in water was nanofiber fragmentation. Micelle fusion appears to exhibit a greater contribution to the increase in length-dispersity than fragmentation, hence why storage in water is superior to storage in THF/MeOH. A sample of **P1** nanospheres was also observed after 2 years of storage at room temperature in water, with no changes (Figure S52). This is in direct contrast to the behaviour of nanospheres produced from PFTMC$_{20}$-b-PEG$_{490}$.[S8]

Assessing the enzymatic biodegradability of P1 nanofibers and nanospheres

This section details additional discussion of the enzymatic biodegradability experiments. DLS studies on the degradation process revealed that 14 nm **P1** nanospheres ($Đ$ = 1.05, σ = 3 nm) with TLL reached a maximum D_h of 7606 ± 1209 nm after 30 mins, before decaying down to a

minimum D_h of 12 ± 4 nm after 20 h (Figure 7). This value is lower than the initial D_h of the 14 nm **P1** nanospheres (Đ = 1.05, σ = 3 nm) without TLL present (123 ± 3 nm), suggesting that micelle degradation had occurred. After 6 h, the D_h had reached 7% of the peak at 30 min. In contrast, 137 nm **P1** nanofibers (Đ = 1.05, σ = 30 nm) with TLL reached a maximum D_h of 5345 nm ± 1167 nm after 3 h, before reaching a D_h of 47 ± 49 nm after 60 h. This was also lower than the starting size of the **P1** nanofibers (82 ± 1 nm), indicative of micelle degradation. The aggregation process observed for both micelles is presumably related to the active micelle/TLL complexes that perform the degradation, as lipases such as TLL are known to form bimolecular aggregates in solution.[S9] The decrease in size of these aggregates over time is presumably related to the progress of the degradation process, yielding smaller and smaller aggregates until no more intact micelles exist. The count rate for the 14 nm nanospheres (Đ = 1.05, σ = 3 nm) revealed a sharp decrease in the number of particles in solution from a maximum at 1 h until 6 h, after which a slower decay occurred, reaching a minimum of 4% of the highest count rate after 20 h (Figure S54). The 137 nm **P1** nanofibers (Đ = 1.05, σ = 30 nm) also exhibited an initial decay from a maximum at 5 mins to a low of 14% of the highest count rate after 12 h after which the derived mean count rate becomes more erratic, reaching a minimum of 2% of the highest count rate after 84 h.

MALDI-TOF MS analysis of the degradation of 103 nm **P1** nanofibers (Đ = 1.07, σ = 27 nm) revealed negligible detectable signal from either the PFTMC core-forming block or the *9H*-fluorene-9,9-dimethanol degradation product[S10] up to 48 h post TLL addition (Figure S57). After 72 h, a distribution of signals from <2,000 m/z to ca. 4,500 m/z was obtained with a peak at 2,536 m/z that corresponds to a PFTMC DP_n of 10 (Figure S57A). The repeat unit was consistent with PFTMC homopolymer, whilst end-group analysis revealed hydroxyl end groups that are consistent with the degradation products of **P1**. Analysis of the mass spectrum over a lower mass range (m/z = 100-1000) revealed no detectable PFTMC oligomers or *9H*-fluorene-9,9-dimethanol (Figure S57B). It was observed that in contrast to FTMC and PFTMC, the precipitate formed was insoluble in CD_2Cl_2 and THF-d_8. NMR studies on the precipitate were conducted in DMSO-d_6 (Figure S57C-F) however the spectra resembled that of lyophilized TLL, with the only detectable component being propylene glycol.

Comparison of the cellular toxicity of P1 nanofibers and nanospheres with conventional polymeric nucleic acid delivery vectors

Additional discussion of the cytotoxicity results is detailed here. Comparing the molar EC_{50} values (determined using the M_n) allows us to consider the cytotoxic effects per polymer chain, accounting for differences in chain length and molecular weight (Table S6). PEI_{53} exhibited the lowest EC_{50} values (and therefore highest cytotoxicity) in all experiments, as expected.[S11,S12] EC_{50} values for reductive metabolism (alamarBlue™) were consistent for PEI_{53} between both cell lines: 110 nM for HeLa and 114 nM for WI-38. In comparison, the EC_{50} values for cell viability (calcein AM) were lower for the primary WI-38 cells at 68 nM compared to 374 nM for HeLa cells, which is understandable given that primary cells are known to be more sensitive than robust cancer cell lines such as HeLa. $PDMAEMA_{249}$ and **P1** nanofibers and nanospheres were all less cytotoxic than PEI_{53}. For all three samples, EC_{50} values for cell viability were again consistent with primary human cells being more susceptible to cell death than HeLa cervical carcinoma cells. The EC_{50} values for reductive metabolism indicate that the remaining HeLa cells had a lower reductive metabolism than the remaining WI-38 cells.

Producing segmented and blended nanofibers

This section details additional discussion of the preparation of segmented and blended nanofibers. Segmented nanofibers have been observed to have increased susceptibility towards fragmentation upon transfer from organic media to water,[S13] so we were curious as to how blended nanomaterials would compare. Both nanofibers were designed to contain equal amounts of **P1**, **P2** and **P3**, with similar overall lengths that corresponded to a total u/s ratio of 4 (**P2** u/s = 2, **P3** u/s = 2). This corresponds to each nanomaterial consisting of 20 wt% **P1** unimer, 40 wt% **P2** unimer and 40 wt% **P3** unimer. The pentablock segmented nanofibers ($L_n = 101$ nm, $Đ = 1.12$, $\sigma = 36$ nm) had **P2** segments that were 11 nm long on average, and **P3** segments that were 25 nm long on average. Blended nanofibers ($L_n = 134$ nm, $Đ = 1.10$, $\sigma = 42$ nm) were produced from 22 nm **P1** seeds ($Đ = 1.11$, $\sigma = 7$ nm) via the simultaneous addition of **P2** and **P3** unimer (u/s = 2 for each), resulting in mixed **P2**/**P3** blocks that were each 56 nm long. Nanospheres with a diameter of 32 nm ($Đ = 1.11$, $\sigma = 11$ nm) were also prepared using a mixture of **P1**, **P2**, and **P3** unimer that was equal to the composition of the analogous segmented nanofibers (Figure S62).

The discrepancy in observed vs expected segment length for segmented nanofibers could be attributed to factors such as lateral unimer addition at the core-corona interface, nanofiber fusion, competing self-nucleation, or fragmentation. Morphologically pure nanofibers were observed in all cases, so any self-nucleation present must have generated nanofibers and not nanospheres. Examination of the width of random blend nanofibers ($W_n = 12$ nm, $Đ = 1.07$, $\sigma = 3$ nm) revealed no observable change in width compared to pristine **P1** nanofibers, so lateral unimer addition seems unlikely for this sample. It is important to note that when segmented nanofibers are formed, the junctions between blocks appear especially weak, and fragment easily (unpublished observations). Furthermore, the rate of epitaxial growth of unimer 'B' onto the end of nanofibers formed from unimer 'A' appears slower than epitaxial growth of the unimer 'B' onto nanofibers with ends that consist of the unimer 'B'. Thus, the rate of initial crystallization of unimer B onto nanofiber A is slow, followed by a rapid growth of unimer B from nanofibers with B ends, similar to that which is observed for heteroepitaxial growth.[S14] This leads to asymmetric growth of the nanofiber segments, with each end of a nanofiber undergoing initial epitaxy at different times, followed by a more rapid epitaxy once the initial crystallization of unimer B onto the end of nanofiber A is complete. Thus, the block lengths of the two matching segments in a particular nanofiber are not equal.

Several advantages exist when comparing segmented and blended nanofibers with blended nanospheres. Firstly, the production of segmented nanospheres or 'Janus' nanospheres is especially challenging and would require a redesign of the chemical structure of the unimers,[S15] whilst segmented nanofibers can be easily produced from simple diblock copolymers bearing the same core-forming block. Additionally, control over the size of blended nanospheres is more challenging than control over 'pristine' nanospheres, which are already difficult to produce with size control. Thus, segmented or blended nanofibers are the simplest way to produce more complex nanomaterials with controlled surface chemistry. Several challenges remain for both segmented and blended nanofibers though. There is a general increase in dispersity that is associated with the formation of segmented and blended nanofibers that consist of multiple unimers as compared to 'pristine' nanofibers produced from a single unimer. This is magnified by an increased propensity for fragmentation upon transfer into water, which can lead to a further increase in dispersity and possible changes in nanofiber length.

General Experimental Considerations

All reagents and solvents were purchased from Sigma-Aldrich, Acros, Fluka, Fisher Chemical and Alfa Aesar, and used as received unless otherwise noted. The PEI_{53} used was branched ($M_n = 25$ kDa by light scattering), and purchased from Sigma Aldrich (CAS no: 9002-98-6). Lipase from *Thermomyces lanuginosus* was purchased from Sigma Aldrich ($>1\times10^8$ U/L). All reactions were carried out in an MBraun MB150B-G glove box under nitrogen atmosphere or using standard Schlenk line techniques. Solvents used for self-assembly were HPLC grade and were filtered through PTFE, nylon or cellulose membranes with a pore size of 200 nm before use. Anhydrous solvents were obtained using a modified Grubbs system of alumina columns manufactured by Anhydrous Engineering.[S16] RAFT polymerizations were performed in custom-made Schlenk-vials to fit dry heating blocks. Ring-opening polymerization (ROP) reactions were conducted in oven-dried glass vials. 1,8-Diazabicyclo[5.4.0]undec-7-ene (DBU) was dried over CaH_2, and purified by distillation under reduced pressure. Reagents for ROP were dried via vacuum desiccation over phosphorus pentoxide for ~2 days before being brought into the glovebox. Reactions were monitored by thin layer chromatography (TLC) on Kieselgel 60 F_{254} (Merck). Aromatic compounds were detected with UV light (254 or 365 nm), and amines were detected by staining with ninhydrin. Flash column chromatography was performed according to Still and co-workers,[S17] using silica gel [Merck, 230−400 mesh (40−63 µm)]. The crude material was applied to the column by pre-adsorption onto silica, as appropriate. Solvents for flash column chromatography (FCC) and TLC are listed in volume:volume percentages (*v/v*). Extracts were concentrated *in vacuo* using both a Heidolph Hei-VAP Advantage rotary evaporator (bath temperatures up to 50°C) at a pressure of 15 mmHg (diaphragm pump), and a high vacuum line at room temperature. HeLa and WI-38 cells were purchased from ATCC through LGC Standards (UK). Cell culture media and additives were purchased from Gibco (Thermo Fischer Scientific). The Dulbecco's Minimal Essential Medium (DMEM) formulation contained high glucose (4.5 g/L), Sodium Pyruvate (0.11 g/L), GlutaMAX™, and Phenol Red (15 mg/L), and was missing HEPES (catalogue number: 10569044). The Minimal Essential Medium (MEM) formulation contained GlutaMAX™, and Phenol Red (10 mg/L), and was missing HEPES (catalogue number: 41090101). Phosphate Buffered Saline (PBS) contained NaCl (9 g/L), KH_2PO_4 (144 mg/L) and Na_2HPO_4-7.H2O (795 mg/L, catalogue number: 10010049). TrypLE Express™ was provided with EDTA (458 mg/L) and without Phenol Red (catalogue number: 12604021).

Instrumentation

Matrix-assisted laser desorption/ionization time of flight mass spectrometry (MALDI-TOF MS)

MALDI-TOF MS measurements were performed using a Bruker Ultraflextreme running in reflector mode. MALDI-TOF samples were prepared by depositing approximately 1 µL of the sample (2 mg/mL in THF) onto a stainless-steel sample plate, followed by the deposition of approximately 2 µL of *trans*-2-[3-(4-*tert*-butylphenyl)-2-methyl-2-propenylidene]malononitrile matrix (20 mg/mL in THF), and the sample was allowed to dry in air. If the crystalline matrix could not be observed on the plate, a further aliquot of matrix was added, and the sample dried in air until crystallization was observed. For all samples, a second spot was also prepared with the addition of sodium trifluoroacetate (20 mg/mL in THF) to supress K^+ adducts. The best spectrum was selected for each sample (with/without sodium trifluoroacetate). This was without sodium trifluoroacetate for Figure S1-Figure S2 and Figure S57, but with sodium trifluoroacetate for Figure S3.

Gel permeation chromatography (GPC)

GPC was conducted on a Viscotek VE2001 GPCmax chromatograph equipped with a refractive index (RI) and UV-Vis detector array. *n*-Bu$_4$NBr/THF (0.1 w/w %) was used as the eluent, with the flow rate set at 1 mL/min. The columns used were of grade GP5000HHR followed by GP2500HHR (Viscotek) at a constant temperature of 30 °C. The calibration of the RI detector was carried out using polystyrene standards (Viscotek). Samples were prepared at 2 mg/mL in eluent and filtered through a Ministart SRP 15 filter (polytetrafluorethylene membrane, pore size = 0.45 µm).

NMR Spectroscopy

^{1}H and ^{13}C NMR spectra were obtained at 25 °C in the solvent specified with Varian or Bruker spectrometers (some equipped with a cryoprobe), operating at the field strengths listed. Chemical shifts are quoted in parts per million with spectra referenced to the residual solvent peak. Multiplicities are abbreviated as: br (broad), s (singlet), d (doublet), t (triplet), q (quartet), p (pentet), m (multiplet) and *app.* (apparent) or combinations thereof. Assignments of ^{1}H-NMR and ^{13}C-NMR signals were made where possible, using COSY, HSQC and HMBC experiments.

DOSY NMR experiments were processed using the 'Bayesian DOSY Transform' function of MestreNova.

Ultrasonication

Micelle sonication was carried out using a Hielschur UP100H sonication probe (100W total output power) at 80% power.

Transfer of samples into water

Samples were transferred into water through dialysis, using dialysis membranes from Sigma Aldrich with a molecular weight cut-off (MWCO) of 12,000 – 14,000 Da. Samples were manually shaken for ~10 s, and then vortex mixed for ~10 s before transfer into the dialysis membrane. Samples were transferred at 2× the desired final concentration, with the volume being corrected gravimetrically post-dialysis. To confirm that no mass loss was occurring during this process, an aliquot of nanofiber solution (700 µL, 1 mg/mL, H_2O) was dried to a solid and weighed. The resulting mass (0.7 mg) confirmed that any mass loss was negligible.

Transmission electron microscopy (TEM)

TEM images were obtained on either a JEOL 1400 microscope with a Gatan Orius SC1000 CCD camera, operated at 120 kV or a JEOL 1011 microscope with an 11 Megapixel CCD camera, operated at 80 kV. Samples were prepared by drop casting 1.5 µL of the micelle solution onto a carbon coated copper grid. Negatively stained samples were additionally drop cast with uranyl acetate in EtOH (8 µL, 3 wt%). Copper grids (400 or 500 mesh) were purchased from Agar Scientific and carbon films (ca. 6 nm) were prepared on mica sheets by carbon sputtering with an Agar TEM Turbo Carbon Coater or a Leica ACE 600 carbon coater. The carbon films were deposited onto the copper grids by floatation on water using the Smith Grid Coating Trough (Ladd Research Industries) and the carbon coated grids were allowed to dry in air.

For micelle contour length analysis, a minimum of 200 micelles were traced manually using the Fiji (ImageJ) software package developed at the US National Institute of Health. The number average micelle length (L_n), width (W_n) or diameter (D_n) and weight average micelle length (L_w), width (W_w) or diameter (D_w) were calculated using eq. S1-2 from measurements of the contour lengths/widths (L_i) of individual micelles, where N_i is the number of micelles of length L_i, and n is the number of micelles examined in each sample. The distribution of micelle lengths/widths

(termed *Đ*) is characterized by both L_w/L_n (*Đ*$_L$) or W_w/W_n (*Đ*$_W$) or D_w/D_n (*Đ*$_D$) and σ (standard deviation, σ_L, σ_W and σ_D).

$$L_n = \frac{\sum_{i=1}^{n} N_i L_i}{\sum_{i=1}^{n} Ni} \qquad L_w = \frac{\sum_{i=1}^{n} N_i L_i^2}{\sum_{i=1}^{n} NiLi} \qquad\qquad \text{(eq. S1-2)}$$

In some negatively stained images, darker micelles are observed on the grid in addition to the lighter ones. These correspond to micelles adhered to the reverse-side of the TEM grid. This was confirmed by flipping the grid upside down, and imaging the sample again, whereby the inverse distribution of light / dark micelles was observed. For future reference, this may be suppressed through the addition of a lower volume of uranyl acetate solution (ca. 1.5 µL instead of the 8 µL used here) or by using a more dilute sample solution.

Atomic Force Microscopy

Atomic-force microscopy (AFM) analyses were performed in ambient conditions using a Bruker Multimode VIII atomic force microscope equipped with a ScanAsyst-HR fast scanning module and a ScanAsyst-Air-HR probe (tip radius, 2 nm), utilising peak force feedback control.

Samples for AFM were prepared by either drop casting 8 µL of micelle colloidal solution onto freshly cleaved mica and drying with a gentle stream of nitrogen, or prepared on carbon-coated TEM grids using the procedure mentioned above for TEM sample preparation. For Figure 4, superior results were obtained using TEM grids, so this is the data presented.

Data was processed and visualized using Gwyddion (http://gwyddion.net/), using the levelling and align rows tools to subtract the background.

Dynamic Light Scattering (DLS)

Dynamic light scattering (DLS) experiments were carried out using a Zetasizer Pro or Zetasizer ZS (Malvern Panalytical). Samples were prepared at concentrations of 0.1 mg/mL, diluted using filtered solvents (0.45 µm membrane filter). The cuvette used was a low-volume quartz cuvette (ZEN2112, 100 µL volume, 10.0 mm light path). A minimum of five measurements per sample were taken. The correlation function was acquired in real time and analysed with a function capable of modelling multiple exponentials (Cumulant analysis). This process enabled the diffusion coefficients for the component particles to be extracted, and these were subsequently expressed as effective hydrodynamic diameter using the Stokes-Einstein relationship for coated nanospheres in

H_2O, with core properties of polystyrene latex (RI = 1.590, Absorption = 0.010, dispersant RI = 1.33, dispersant viscosity = 0.887, dispersant dielectric constant 78.5). As these measurements assume that the particles are spherical, measurements of nanofiber size via DLS are not absolute, but still provide a useful method for monitoring the colloidal stability of the samples and providing relative comparisons. Particle degradation, pH and temperature experiments were performed on a single sample, with each data point representing the average of 5 repeat measurements taken over a period of 5-10 minutes, using the 'equilibration time' function of the ZS Xplorer software to automate data acquisition.

ζ-Potential Measurements

ζ-potential measurements were recorded on a Zetasizer Pro (Malvern Panalytical), following the Smoluchowski approximation at 25 °C. Samples were diluted to 100 µg/mL in 5 mM NaCl buffer, with each cuvette containing 700 µL of micelle solution. A minimum of five measurements per sample were taken, each consisting of between 10 and 100 cycles per run. The average ζ-potential was calculated from the individual measurements taken, with error represented as σ.

Confocal Laser Scanning Microscopy (CLSM)

CLSM imaging was performed in the Wolfson Bioimaging Facility at the University of Bristol on a Lecia SP8 AOBS confocal laser scanning microscope attached to a Lecia DM I6000 inverted epifluorescence microscope with 'Adaptive Focus Control' to correct focus drift during time-courses (BBSRC Alert 13 capital grant (BB/L014181/1). All images were taken at 37 °C using a 63×1.4 oil-immersion lens. The excitation laser was operated at 633 nm, and confocal images were obtained using a digital detector with an observation window between 640-700 nm (BODIPY$^{630/650\text{-}X}$). The images were processed using LAS X (Lecia) and Fiji software (ImageJ).

Samples for CLSM were prepared by pipetting sample solution (10 µL, 0.1 mg/mL) onto a clean microscope slide, then a coverslip was placed on top of the solution and sealed in place with clear nail polish.

Synthetic Procedures
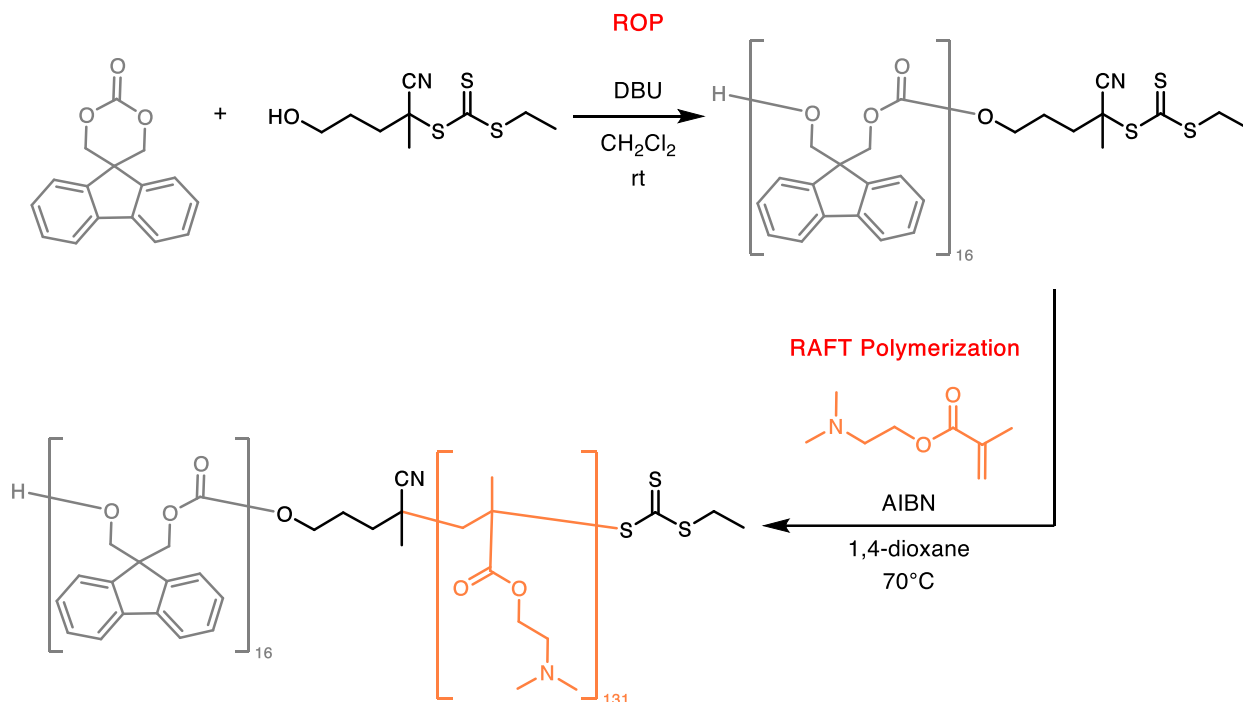
Scheme S1. Synthesis of PFTMC$_{16}$-*b*-PDMAEMA$_{131}$ (**P1**) via sequential ring opening polymerization (ROP) and reversible addition-fragmentation chain-transfer (RAFT) polymerization.

Spiro[fluorene-9,5´-[1,3]-dioxan]-2´-one (FTMC)
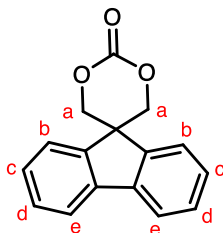
Fluorenetrimethylene carbonate (FTMC) was prepared according to a modified procedure reported by Finnegan et al.[S8] A solution of *9H*-fluorene-9,9-dimethanol[S18] (2.65 g, 11.7 mmol, 1 eq) in THF (120 mL) was cooled to 0 °C. Ethylchloroformate (4.49 mL, 46.9 mmol, 4 eq) was added, and the reaction mixture was stirred at 0 °C for 15 min at which point a blue UV active spot was observed via TLC (hexanes/EtOAc, 1:1, R$_f$ = 0.3). To the reaction mixture, NEt$_3$ (6.8 mL, 48.8 mmol, 4 eq) was added in a dropwise fashion, and the reaction mixture was allowed to warm to rt, and was stirred for 4.5 h until complete consumption of the starting material was observed by TLC

(hexanes/EtOAc, 1:1, product R_f = 0.6). The crude reaction mixture was filtered, and all volatiles were removed *in vacuo*. EtOAc was then added (30 mL) at which point a white precipitate was observed. The reaction mixture was then washed with 1M HCl (2 × 30 mL) and water (2 × 30 mL). It was observed that the reaction mixture became homogenous upon the addition of HCl. The organic layer was dried over $MgSO_4$ and concentrated *in vacuo* to yield crude FTMC as a colourless solid. Recrystallisation from toluene yielded a colourless solid (977 mg, 33 %). **¹H-NMR** (400 MHz, DMSO-*d6*) δ 7.98 (2H, d, *J* = 7.5 Hz, He), 7.52 (4H, m, Hb and Hd), 7.42 (2H, td, *J* = 7.5, 1.1 Hz, Hc), 4.67 (4H, s, Ha); **¹³C-NMR** (101 MHz, DMSO-*d6*) δ 147.8 (*C*=O), 143.1 (Ar-*C*), 140.1 (Ar-*C*), 129.0 (Cd), 128.0 (Cc), 124.0 (Cb), 120.9 (Ce), 74.1 (Ca), 46.4 (CH₂*C*CH₂). Proton and Carbon NMR were consistent with literature data.[S8]
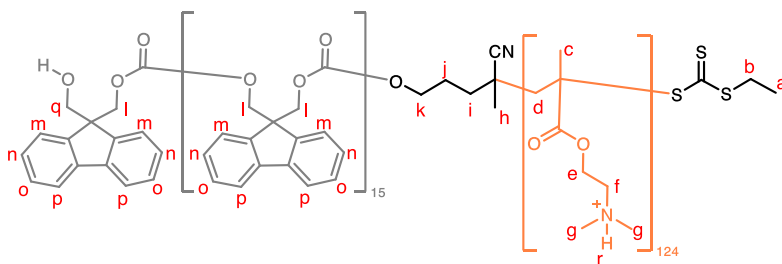
PFTMC₁₆-CTA
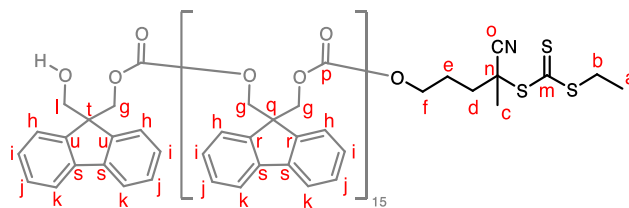
To a solution of 2-cyano-5-hydroxypentan-2-yl ethyl carbonotrithioate (**CTA-OH**, 50.0 mg, 0.200 mmol, 1.0 eq)[S1] in anhydrous CH_2Cl_2 (500 µL), 1,8-Diazabicyclo[5.4.0]undec-7-ene (24 µL, 0.160 mmol, 0.8 eq) was added and stirred at rt for 15 mins. In a separate oven dried glass vial, FTMC (1.02 g, 4.01 mmol, 20 eq) and anhydrous CH_2Cl_2 (6 mL) was added and stirred at rt until all of the FTMC had dissolved, at which point it was added to the first solution of initiator and catalyst. The reaction mixture was then stirred at room temperature for 30 mins, until complete consumption of the starting material was observed via NMR. The crude reaction mixture was quenched by the addition of benzoic acid (100 mg) and purified by precipitation into ice-cold diethyl ether three times, before being dried *in vacuo* to yield PFTMC₁₆-CTA as a yellow solid (878 mg, 83 %). Analysis of the ¹H-NMR integrals of Hf, Hl and Hb revealed a 94 % end capping with the CTA. **¹H-NMR** (500 MHz, CD₂Cl₂) δ 7.76 (40H, dt, *J* = 14.4, 6.9 Hz, Hh), 7.61 – 7.47 (40H, m, Hk), 7.40 (40H, dt, *J* = 13.9, 7.2 Hz, Hi), 7.28 (40H, dt, *J* = 25.3, 7.4 Hz, Hj), 4.50 – 4.17 (80H, m, Hg), 4.09 (2H, t, *J* = 5.9 Hz, Hf), 3.71 (2H, s, Hl), 3.33 (2H, q, *J* = 7.4 Hz, Hb), 2.25 – 2.14 (1H, m, Hd), 2.03 (1H, ddd, *J* = 16.5, 13.8, 7.4 Hz, Hd), 1.92 – 1.83 (2H, m, He), 1.81 (3H,

s, Hc), 1.32 (3H, t, J = 7.4 Hz, Ha), DP_n = 20; **^{13}C-NMR** (126 MHz, CD_2Cl_2) δ 218.3 (Cm), 155.8 (Cp), 155.2 (Cp), 155.1 (Cp), 155.0 (Cp), 145.5 (Cu), 144.3 (Cr), 144.2 (Cr), 141.4 (Cs), 141.3 (Cs), 129.4 (Ci), 129.3 (Ci), 128.9 (Ci), 128.1 (Cj), 127.8 (Cj), 125.6 (Ck), 125.5 (Ck), 120.9 (Ch), 120.7 (Ch), 119.8 (Co), 75.5 (Cg), 69.8 (Cg), 69.7 (Cg), 69.5 (Cg), 67.5 (Cf), 65.2 (Cl), 56.2 (Ct), 53.7 (Cq), 47.3 (Cn), 35.9 (Cd), 32.0 (Cb), 25.2 (Cc), 24.8 (Ce), 13.12 (Ca); **MALDI-TOF MS** for $C_{265}H_{207}NO_{49}S_3K^+$ $[M_{16}+K]^+$, calculated: 4,321.3; found: 4,322.1, DP_n = 16; **GPC** (n-Bu_4NBr/THF, PS standard): M_n = 3,700 g/mol, $Đ_M$ = 1.17.
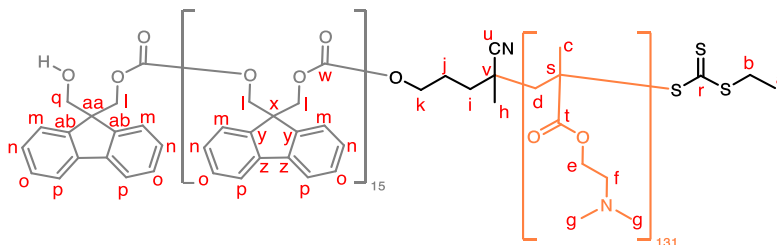
$PFTMC_{16}$-b-$(PDMAEMA \cdot HCl)_{124}$

To a solution of $PFTMC_{16}$-CTA (250 mg, 0.047 mmol, 1.0 eq) and 2-(dimethylamino)ethyl methacrylate (DMAEMA, 1,194 µL, 7.08 mmol, 150 eq) in 1,4-dioxane (10 mL), a solution of AIBN in 1,4-dioxane was added (1.6 mg, 0.010 mmol, 0.2 eq in 62 µL). The reaction mixture was stirred until homogenous before undergoing three freeze-pump-thaw cycles, and then heated to 70 °C for 24 h. The crude reaction mixture was quenched by submersion in liquid nitrogen, and purified by precipitation into hexanes, whereby the solution was shaken in a centrifuge tube until the polymer had agglomerated against the walls of the tube, and the solution was transparent. The supernatant was decanted off, the polymer dried, and precipitated from THF into hexanes twice more. PFTMC homopolymer was removed by the addition of conc. HCl (2×100 µL) to a solution of the crude polymer in CH_2Cl_2 (20 mL). Note: the addition of further conc. HCl was found to cause a turbid solution to form and should thus be avoided. Upon shaking the solution, a colourless precipitate was observed that was collected by centrifugation (5,400 rpm for 10 minutes). The supernatant was removed, and the polymer was washed three times with THF (20 mL) followed by centrifugation (5,400 rpm for 10 minutes) and dried *in vacuo* to yield $PFTMC_{16}$-b-$(PDMAEMA \cdot HCl)_{124}$ as a colourless solid (71.8 mg kept for further analysis and self-assembly experiments). **^{1}H-NMR** (400 MHz, DMSO-$d6$) 11.34 (108H, s, Hr), 7.89 – 7.12 (131H, m, Hm,

Hn, Ho & Hp), 4.64 – 4.02 (246H, m, Hl & He), 3.51 (app. 217H, s, Hf), 2.89 (742H, s, Hg), 2.21 – 1.69 (app. 31H, m, Hd), 1.35 – 0.55 (331H, m, Hc). GPC was not possible due to insolubility in THF.
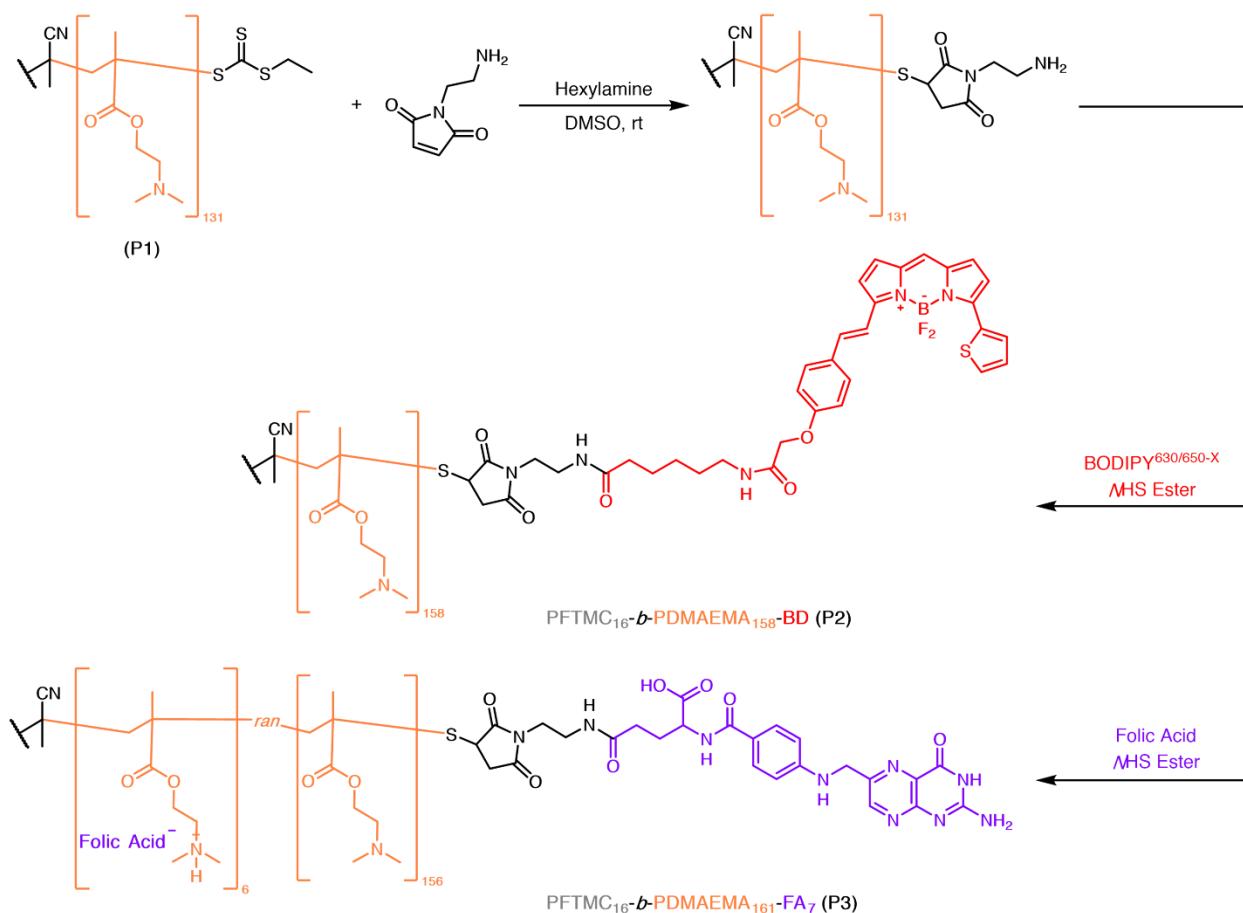
PFTMC$_{16}$-*b*-PDMAEMA$_{131}$ (P1)

PFTMC$_{16}$-*b*-PDMAEMA$_{131}$ (**P1**) was formed through deprotonation of the PDMAEMA block of PFTMC$_{16}$-*b*-(PDMAEMA · HCl)$_{124}$. PFTMC$_{16}$-*b*-(PDMAEMA · HCl)$_{124}$ (all minus the 71.8 mg kept for further experiments) was added to sat. Na$_2$CO$_3$ (20 mL) and shaken until complete dissolution had occurred, and a thin organic layer had appeared. The pH of the aqueous layer was confirmed to be basic (pH > 7). CH$_2$Cl$_2$ (20 mL) and brine (20 mL) were added, and the organic layer was collected. Note: if an emulsion forms, this may be resolved by centrifugation. The aqueous layer was further washed with CH$_2$Cl$_2$ (20 mL), and the combined organic layer was dried over MgSO4, and concentrated *in vacuo* to furnish PFTMC$_{16}$-*b*-PDMAEMA$_{131}$ (**P1**) as a colourless solid (479 mg, 35 % from PFTMC$_{16}$-CTA). **^{1}H-NMR** (500 MHz, CD$_2$Cl$_2$) δ 7.79 – 7.69 (33H, m, Hm), 7.59 – 7.47 (33H, m, Hp), 7.45 – 7.33 (36H, m, Hn), 7.26 (33H, dq, *J* = 18.9, 7.6 Hz, Ho), 4.49 – 4.26 (66H, m, Hl), 4.04 (263H, p, *J* = 6.6 Hz, He & Hk), 3.70 (2H, s, Hq), 3.25 (1H, h, *J* = 7.8 Hz, Hb), 2.54 (259H, dq, *J* = 7.5, 4.5, 3.7 Hz, Hf), 2.30 – 2.20 (763H, m, Hg), 1.91 (82H, d, *J* = 6.2 Hz, Hd [*rm*]), 1.81 (132H, dq, *J* = 6.2, 2.8 Hz, Hd [*rr*]), 1.72 (3H, d, *J* = 3.9 Hz, Hh), 1.68 (2H, s, Hj), 1.52 – 1.38 (29H, m, Hd [*mm*]), 1.33 – 1.19 (28H, m, Ha & Hc [*mm*]), 1.03 (129 H, d, *J* = 7.4 Hz, Hc [*rm*]), 0.95 – 0.76 (241H, m, Hc [*rr*]), DP$_n$ PFTMC = 16, DP$_n$ PDMAEMA = 131; **^{13}C-NMR** (126 MHz, CD$_2$Cl$_2$) δ 178.5 (Ct), 178.2 (Ct), 177.9 (Ct), 177.3 (Ct), 177.1 (Ct), 155.0 (Cw), 144.2 (Cy), 141.3 (Cz), 129.3 (Cn), 128.8 (Cn), 128.0 (Co), 127.8 (Co), 125.5 (Cp), 125.5 (Cp), 120.9 (Cm), 120.7 (Cm), 69.5 (Cl), 65.2 (Cq), 63.6 (Ce), 57.8 (Cf), 57.7 (Cf & Cb), 56.2 (Cd), 55.1 (Cd), 54.7 (Cd), 53.7 (Cd), 46.1 (Cg), 45.6 (Cg), 45.2 (Cg), 30.3 (Cc [*mm*]), 19.0 (Cc [*rm*]), 17.2 (Cc [*rr*]); **GPC** (*n*-Bu$_4$NBr/THF, PS standard): M_n = 9,700 g/mol, $Đ_M$ = 1.55.

PDMAEMA₂₄₉
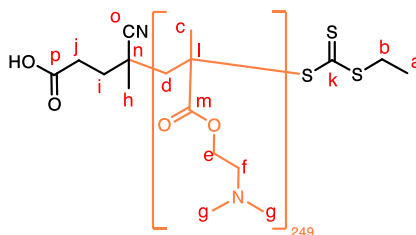
To a solution of 4-cyano-4-((((ethylthio)carbonothioyl)thio)pentanoic acid[S1] (20.0 mg, 0.076 mmol, 1.0 eq) and 2-(dimethylamino)ethyl methacrylate (DMAEMA, 3,844 µL, 22.8 mmol, 300 eq) in 1,4-dioxane (3 mL), a solution of AIBN in 1,4-dioxane was added (3.75 mg, 0.023 mmol, 0.3 eq in 75 µL). The reaction mixture was stirred until homogenous before undergoing three freeze-pump-thaw cycles, and then heated to 70 °C for 15 h. The crude reaction mixture was quenched by submersion in liquid nitrogen, diluted in THF (10 mL) and purified by precipitation into hexanes, whereby the solution was shaken in a centrifuge tube until the polymer had agglomerated against the walls of the tube, and the solution was transparent. The supernatant was decanted off, the polymer dried, and precipitated from THF into hexanes twice more and dried *in vacuo* to furnish PDMAEMA₂₄₉ as a colourless, viscous gum (3.53 g, 98 %). **^{1}H-NMR** (500 MHz, CD$_2$Cl$_2$) δ 4.15 – 3.90 (498H, m, He), 3.30 – 3.22 (2H, m, Hb), 2.69 – 2.45 (496H, m, Hf), 2.43 – 2.07 (1501H, m, Hg), 2.06 – 1.34 (496H, m, Hd), 1.32 – 0.63 (787H, m, Hc), DP$_n$ PDMAEMA = 249; **^{13}C-NMR** (126 MHz, CD$_2$Cl$_2$) δ 178.2 (Cm), 177.9 (Cm), 177.2 (Cm), 63.6 (Ce), 63.5 (Ce), 57.9 (Cf), 57.8 (Cf), 55.2 (Cd), 54.8 (Cd), 46.2 (Cg), 45.6 (Cg), 45.3 (Cg), 32.2 (Cl), 23.2 (Cc [*mm*]), 19.0 (Cc [*rm*]), 17.2 (Cc [*rr*]), 14.5 (Ca); **GPC** (*n*-Bu$_4$NBr/THF, PS standard): M_n = 63,100 g/mol, $Đ_M$ = 1.17.

Scheme S2. Synthesis of BODIPY$^{630/650-X}$ (BD) and folic acid (FA) functionalized polymers **P2** and **P3** (termed PFTMC$_{16}$-*b*-PDMAEMA$_{158}$-BD and PFTMC$_{16}$-*b*-PDMAEMA$_{161}$-FA$_7$ respectively) via modification of the terminal trithiocarbonate. 6 equivalents of FA also reacted with the PDMAEMA corona to yield a total of 7 equivalents of FA present in **P3**.

PFTMC$_{16}$-*b*-PDMAEMA$_{158}$-NH$_2$
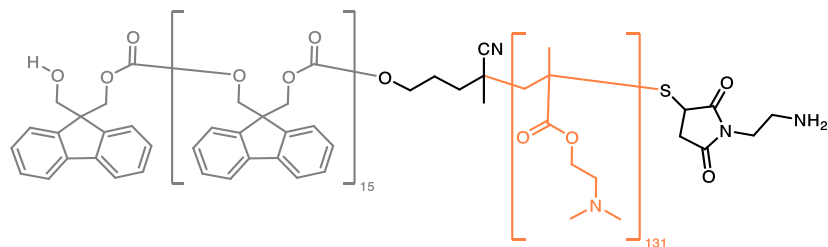
PFTMC$_{16}$-*b*-PDMAEMA$_{131}$ (**P1**, 20.0 mg, 0.80 umol, 1.0 eq) was dissolved in anhydrous DMSO (1 mL) in a glass vial. In a separate vial, hexylamine (5 µL) was dissolved in anhydrous DMSO (495 µL). An aliquot of the hexylamine solution (11 µL, 0.81 µmol, 1.0 eq) was transferred to the polymer solution, and the reaction mixture was stirred at rt for 1 h. N-(2-aminoethyl)maleimide

trifluoroacetate salt (1.0 mg, 3.9 µmol, 49 eq) was added and the reaction mixture was stirred for a further 16 h. The crude reaction mixture was purified by precipitation into ice-cold diethyl ether (40 mL) three times. The polymer was re-dissolved in methanol (1mL) and dialyzed against methanol for 24 h to remove excess N-(2-aminoethyl)maleimide trifluoroacetate salt, before being dried in vacuo to yield PFTMC$_{16}$-b-PDMAEMA$_{158}$-NH$_2$ as a colourless solid (15 mg, 75 %). The polymer was used immediately in the next step without further characterization.

General Procedure for the synthesis of P2 and P3 from PFTMC$_{16}$-b-PDMAEMA$_{158}$-NH$_2$

To a solution of PFTMC$_{16}$-b-PDMAEMA$_{158}$-NH$_2$ (1.0 eq) in anhydrous DMSO, BODIPY$^{630/650\text{-X}}$ or folic acid NHS ester was added (1.2 - 10 eq). The reaction mixture was stirred at room temperature for 16 h. The crude reaction mixture was purified by precipitation into ice-cold diethyl ether (20 mL) until no fluorescence could be detected in the supernatant under UV light (at least three times). The polymer was dried in vacuo to yield either PFTMC$_{16}$-b-PDMAEMA$_{158}$-BD (**P2**) or PFTMC$_{16}$-b-PDMAEMA$_{161}$-FA$_7$ (**P3**) as a blue or colourless solid respectively.

PFTMC$_{16}$-b-PDMAEMA$_{158}$-BD (P2)
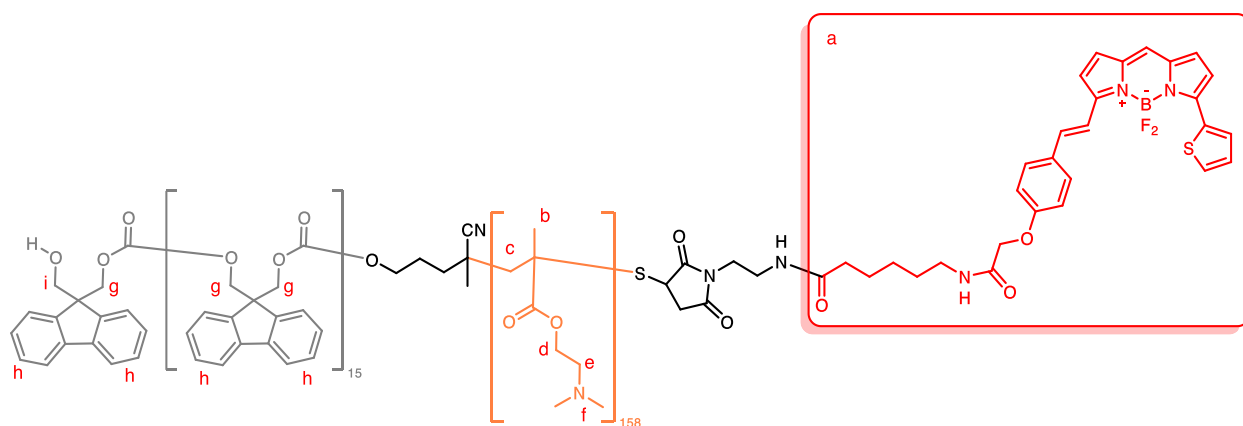
^{1}H-NMR (500 MHz, DMSO-d_6) δ 7.93 (1H, d, J = 7.7 Hz, Ha), 7.81 (33H, s, Hh), 7.55 (1H, d, J = 7.5 Hz, Ha), 7.53 – 7.31 (67H, m, Hh), 7.30 – 7.16 (33H, m, Hh), 7.09 (1H, d, J = 7.9 Hz, Ha), 6.65 (1H, s, Ha), 6.52 (4H, br s, Ha), 5.39 (2H, s, Hi), 5.32 (2H, t, J = 5.1 Hz, Ha), 5.23 (2H, s, Ha), 4.27 (69H, s, Hg), 4.21 – 3.93 (292H, m, Hd), 2.70 (316H, s, He), 2.46 – 2.16 (817H, m, Hf), 2.13 – 1.36 (310H, m, Hc), 1.35 – 0.41 (462H, m, Hb), DP$_n$ PFTMC = 16, DP$_n$ PDMAEMA = 158.

PFTMC16-*b*-PDMAEMA161-FA7 (P3)
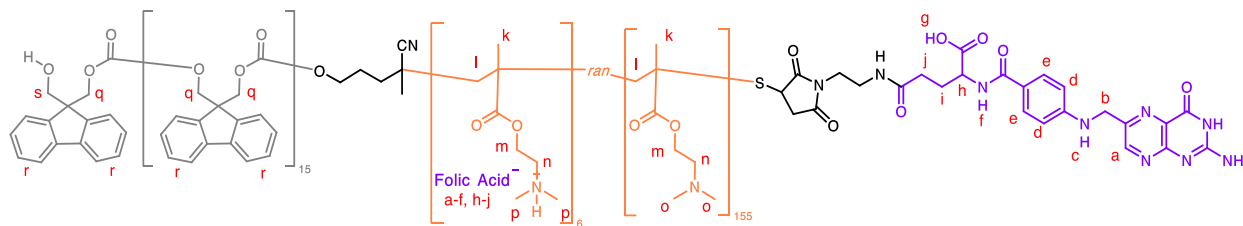
¹H-NMR (500 MHz, DMSO-d_6) δ 11.46 (1H, s, Hg), 8.64 (7H, s, Ha), 8.13 (7H, s, Hf), 7.53 – 7.30 (33H, m, Hr), 7.65 (14H, d, J = 8.4 Hz, He), 7.38 (67H, s, Hr), 7.20 (33H, s, Hr), 6.94 (7H, t, J = 6.0 Hz, Hc), 6.65 (14H, s, Hd), 5.78 – 5.69 (2H, m, Hs), 5.61 (7H, s), 4.49 (14H, s, Hb), 4.33 (7H, s, Hh), 4.36 – 4.20 (80H, m, Hq), 4.10 (287H, br s, Hm), 3.66 – 3.54 (372H, m, Hn), 2.82 (322H, br s, Hp), 2.52 – 2.29 (727H, m, Ho & Hj), 2.04 – 1.40 (429H, m, Hl & Hi), 1.33 – 0.60 (465H, m, Hk) DP_n PFTMC = 16, DP_n PDMAEMA = 161.

Self-assembly procedures

General procedure for the self-assembly of P1 and PFTMC$_{16}$-*b*-(PDMAEMA · HCl)$_{124}$

Unimer solutions (either 20 mg/mL or 200 mg/mL) of either **P1** or PFTMC$_{16}$-*b*-(PDMAEMA · HCl)$_{124}$ were prepared by dissolution in common solvent (either THF or DMSO as indicated). An aliquot of this solution was then further diluted in an amount of common solvent appropriate to the final concentration of polymer and desired solvent composition. To this solution, selective solvent (either MeOH, EtOH, iPrOH, or H$_2$O as indicated) was added slowly, and the vial was sealed, manually shaken for 10 s and then vortexed mixed for a further 10 s.

For samples annealed at 70 °C: Where indicated, the sample was then annealed at 70 °C for 30 min and allowed to cool in the heating block until it reached rt (23 °C), before being aged for 24 h.

For samples aged at 23 °C: Where indicated, the sample was then aged at 23 °C for 24 h.

Example procedure for the self-assembly of PFTMC$_{16}$-*b*-PDMAEMA$_{131}$ (P1)

An aliquot of **P1** unimer solution (50 µL, 200 mg/mL in THF) was diluted in THF (50 µL). To this solution, MeOH was then slowly added (900 µL), and the sample was manually shaken for 10 s, then vortex mixed for 10 s, and aged at 23 °C for 24 h. The resulting disperse nanofibers were then imaged via TEM.

General Procedure for the preparation of seed nanofibers from disperse nanofibers

Disperse **P1** nanofibers (ranging from 1 mg/mL to 10 mg/mL) were sonicated for at least 3 h using a Hielschur UP100H sonication probe, according to the setup outlined in Image S1. The temperature was kept between 0 °C and 23 °C using an ice bath. The resulting seed nanofibers were then imaged via TEM.

Note: If the lab has recirculating chilled water condensers, the sample may be immersed into a larger water bath equipped with a stirrer bar and a submersed condenser, and used in place of the ice bath. This provides consistent temperatures (ca. 18 °C from our experience), negating the need to continually check the levels of ice in the ice bath.
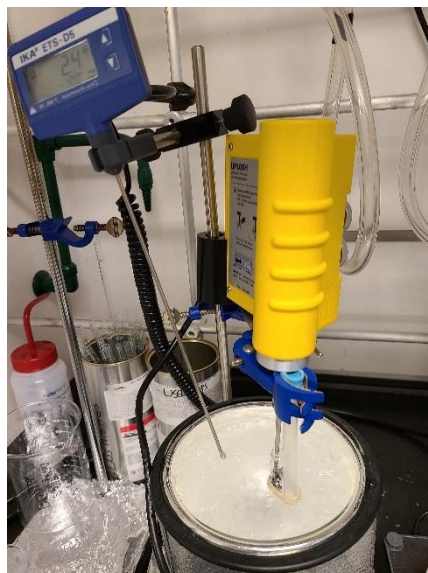
Image S1. Photograph of the setup for the sonication of disperse nanofibers into seed nanofibers.

Example procedure for the preparation of seed nanofibers from disperse nanofibers

Disperse **P1** nanofibers (1 mL, 10 mg/mL) were sonicated for 3 h using a Hielschur UP100H sonication probe, with the temperature kept between 0 °C and 23 °C using an ice bath. The resulting seed nanofibers (**seeds 6**) were then imaged via TEM (L_n = 34 nm, $Đ$ = 1.10, σ = 11 nm). It was observed that the solution of nanofibers became noticeably less viscous and more transparent after sonication.

General Procedure for the one-step preparation of seed nanofibers

Unimer solution (either 20 mg/mL or 200 mg/mL) of **P1** was prepared by dissolution in common solvent (THF). An aliquot of this solution was then further diluted in an amount of common solvent appropriate to the final concentration of polymer and solvent composition. To this solution, selective solvent (MeOH) was added slowly, and the vial was sealed, manually shaken for 10 s and then vortexed mixed for a further 10 s. This solution was sonicated immediately for at least 3 h using a Hielschur UP100H sonication probe, according to the setup outlined in Image S1. The temperature was kept between 0 °C and 23 °C using an ice bath. After sonication, the solution was aged at 23 °C for 24 h. The resulting seed nanofibers were then imaged via TEM.

Example Procedure for the one-step preparation of seed nanofibers

P1 unimer solution (50 µL, 200 mg/mL, THF) was diluted in THF (150 µL). To this solution, MeOH was then slowly added (800 µL), and the sample was manually shaken for 10 s, then vortex mixed for 10 s, and sonicated immediately for 3 h using a Hielschur UP100H sonication probe, with the temperature kept between 0 °C and 23 °C using an ice bath. The solution was then aged at 23 °C for 24 h. The resulting seed nanofibers were then imaged via TEM.

General procedure for the preparation of low dispersity nanofibers from seed nanofibers using the seeded-growth method (living CDSA)

A solution of seed **P1** nanofibers (between 0.1 mg/mL and 1 mg/mL) were diluted in a volume of selective solvent appropriate to the final concentration of polymer and solvent composition. To this solution, an aliquot of unimer solution in common solvent (THF or DMSO, 20 mg/mL) appropriate to the desired $m_{unimer}:m_{seed}$ ratio was added, the sample was manually shaken for 10 s, then vortex mixed for 10 s, and aged at 23 °C for 24 h. The resulting low dispersity nanofibers were then imaged via TEM.

Samples with an $m_{unimer}:m_{seed}$ ratio of above 10 were added iteratively in aliquots of no more than 10 followed by ageing for 24h between the addition of each aliquot.

Example procedure for the preparation of low dispersity nanofibers from seed nanofibers

34 nm **P1** seeds ($Đ = 1.10$, $\sigma = 11$ nm, 100 µL, 10 mg/mL) were diluted in MeOH (900 µL). To this solution, **P1** unimer solution (15 µL, 200 mg/mL, $m_{unimer}:m_{seed} = 3$) was added, and the sample was manually shaken for 10 s, then vortex mixed for 10 s, and aged at 23 °C for 24 h. The resulting low dispersity **P1** nanofibers were characterized via TEM (Figure S45, $L_n = 140$ nm, $Đ_L = 1.05$, $\sigma_L = 32$ nm, $W_n = 14$ nm, $Đ_W = 1.09$, $\sigma_W = 4$ nm) and DLS ($D_h = 97$ nm ± 1 nm, 0.1 mg/mL, diluted in MeOH).

General procedure for the transfer of low dispersity nanofibers into water

Low dispersity **P1** nanofibers (500 µL – 2 mL, 2 – 5 mg/mL) were manually shaken for 10 s, then vortex mixed for 10 s, before being placed inside a dialysis membrane (Sigma Aldrich, MWCO = 12,000 – 14,000 Da), sealed with clips (Spectrum Chemical), and dialyzed into deionized water (500 mL) for 24 h with a minimum of three dialysate changes. The dialysis

membrane was opened, and the nanofiber solution was transferred to a vial. The solution was weighed, and filtered deionized water was added to make the sample up to 1 mg/mL gravimetrically. The resulting low dispersity **P1** nanofibers were characterized via TEM, DLS, and ζ-potential.

Example procedure for the transfer of low dispersity nanofibers into water

140 nm **P1** nanofibers ($Đ = 1.05$, $\sigma = 32$ nm, 1 mL, 2 mg/mL) were placed inside a dialysis membrane (Sigma Aldrich, MWCO = 12,000 – 14,000 Da), sealed with clips (Spectrum Chemical), and dialyzed into deionized water (500 mL) for 24 h with a minimum of three dialysate changes. The dialysis membrane was opened, and the nanofiber solution was transferred to a vial. The solution was weighed, and filtered, deionized water was added to make the sample up to 1 mg/mL gravimetrically (2 g). The resulting low dispersity **P1** nanofibers were characterized via TEM (Figure S45, $L_n = 137$ nm, $Đ_L = 1.05$, $\sigma_L = 30$ nm, $W_n = 13$ nm, $Đ_W = 1.04$, $\sigma_W = 3$ nm), DLS ($D_h = 77 \pm 1.3$ nm in H_2O, 82 nm ± 1.4 nm in 5 mM NaCl, 0.1 mg/mL), and ζ-potential (*app.* ζ-potential = $+17.6 \pm 0.6$ mV).

General procedure for the preparation of segmented nanofibers

A solution of seed **P1** nanofibers or low dispersity **P1** nanofibers (between 0.1 and 5 mg/mL) were diluted in a volume of selective solvent appropriate to the final concentration of polymer and solvent composition. To this solution, an aliquot of a different unimer solution in common solvent (THF or DMSO, 20 mg/mL) appropriate to the desired m_{unimer}:m_{seed} ratio was added, the sample was manually shaken for 10 s, then vortex mixed for 10 s, and aged at 23°C for 24 h. The resulting segmented low dispersity nanofibers were then imaged via TEM.

Example procedure for the preparation of segmented nanofibers

30 nm **P1** seeds ($Đ_L = 1.08$, $\sigma = 8$ nm, 100 µL, 10 mg/mL) were diluted in MeOH (900 µL). To this solution, PFTMC$_{16}$-*b*-PDMAEMA$_{158}$-BD (**P2**) unimer solution (100 µL, 20 mg/mL in DMSO, m_{unimer}:m_{seed} = 2) was added, and the sample was manually shaken for 10 s, then vortex mixed for 10 s, and aged at 23 °C in the dark for 24 h. The resulting low dispersity nanofibers were characterized via TEM (Figure S61, $L_n = 51$ nm, $L_w/L_n = 1.25$, $\sigma = 25$ nm).

To a solution of these low dispersity nanofibers ($L_n = 51$ nm, $Đ_L = 1.25$, $\sigma = 25$ nm, 1100 µL, 3 mg/mL), PFTMC$_{16}$-*b*-PDMAEMA$_{161}$-FA$_7$ (**P3**) unimer (100 µL, 20 mg/mL in DMSO,

$m_{unimer}{:}m_{seed\ (original)} = 2$, total $m_{unimer}{:}m_{seed} = 5$) was added, and the sample was manually shaken for 10 s, then vortex mixed for 10 s, and aged at 23 °C in the dark for 24 h. The resulting low dispersity nanofibers were characterized via TEM (Figure S61, $L_n = 101$ nm, $Đ_L = 1.12$, $\sigma = 36$ nm).

These segmented nanofibers ($L_n = 101$ nm, $Đ_L = 1.12$, $\sigma = 36$ nm, 1 mL, 4 mg/mL) were placed inside a dialysis membrane (Sigma Aldrich, MWCO = 12,000 − 14,000 Da), sealed with clips (Spectrum Chemical), and dialyzed into deionized water (500 mL) in the dark for 24 h with a minimum of three dialysate changes. The dialysis membrane was opened, and the nanofiber solution was transferred to a vial. The solution was weighed, and filtered deionized water was added to make the sample up to 1 mg/mL gravimetrically (4 g). The resulting low dispersity nanofibers were characterized via TEM (Figure S45, $L_n = 97$ nm, $Đ_L = 1.20$, $\sigma = 44$ nm) and stored in the dark.

Procedure for the preparation of blend nanofibers

22 nm **P1** seeds ($Đ_L = 1.11$, $\sigma = 7$ nm, 100 µL, 10 mg/mL) were diluted in MeOH (900 µL). To this solution, a mixture of $PFTMC_{16}$-*b*-$PDMAEMA_{158}$-BD (**P2**) unimer (100 µL, 20 mg/mL in DMSO, $m_{unimer}{:}m_{seed} = 2$) and $PFTMC_{16}$-*b*-$PDMAEMA_{161}$-FA_7 (**P3**) unimer (100 µL, 20 mg/mL in DMSO, $m_{unimer}{:}m_{seed} = 2$) solutions were added (200 µL total, $m_{unimer}{:}m_{seed} = 4$ overall). The sample was manually shaken for 10 s, then vortex mixed for 10 s, and aged at 23 °C in the dark for 72 h. The resulting low dispersity nanofibers were characterized via TEM (Figure S60, $L_n = 134$ nm, $Đ_L = 1.10$, $\sigma = 42$ nm).

These blend nanofibers ($L_n = 134$ nm, $Đ_L = 1.10$, $\sigma = 42$ nm, 1 mL, 4 mg/mL) were placed inside a dialysis membrane (Sigma Aldrich, MWCO = 12,000 − 14,000 Da), sealed with clips (Spectrum Chemical), and dialyzed into deionized water (500 mL) in the dark for 24 h with a minimum of three dialysate changes. The dialysis membrane was opened, and the nanofiber solution was transferred to a vial. The solution was weighed, and filtered deionized water was added to make the sample up to 1 mg/mL gravimetrically (4 g). The resulting low dispersity nanofibers were characterized via TEM (Figure S60, $L_n = 77$ nm, $Đ_L = 1.18$, $\sigma = 32$ nm) and stored in the dark.

General procedure for the preparation of nanospheres via dialysis

Unimer solutions (20 mg/mL) of **P1**, **P2** and **P3** were prepared by dissolution in common solvent (either THF or DMSO as indicated). Aliquots of these unimer solutions appropriate to the desired composition and concentration of the resulting nanospheres were combined in a vial, and further diluted in an amount of common solvent appropriate to the final concentration of polymer. The sample was manually shaken for 10 s, then vortex mixed for 10 s. This solution (500 µL – 5 mL, 2 – 5 mg/mL) was then placed inside a dialysis membrane (Sigma Aldrich, MWCO = 12,000 – 14,000 Da), sealed with clips (Spectrum Chemical), and dialyzed into deionized water (500 mL) for 24 h with a minimum of three dialysate changes. The dialysis membrane was opened, and the nanosphere solution was transferred to a vial. The solution was weighed, and filtered deionized water was added to make the sample up to 1 mg/mL gravimetrically. The resulting nanospheres were characterized via TEM, DLS, and ζ-potential.

Example procedure for the preparation of P1 nanospheres via dialysis

An aliquot of **P1** unimer solution (250 µL, 20 mg/mL in DMSO) was diluted in DMSO (750 µL). The sample was manually shaken for 10 s, then vortex mixed for 10 s, before being placed inside a dialysis membrane (Sigma Aldrich, MWCO = 12,000 – 14,000 Da), sealed with clips (Spectrum Chemical), and dialyzed into deionized water (500 mL) for 24 h with a minimum of three dialysate changes. The dialysis membrane was opened, and the nanosphere solution was transferred to a vial. The solution was weighed, and filtered deionized water was added to make the sample up to 1 mg/mL gravimetrically (5 g). The resulting nanospheres were characterized via TEM (Figure S46J, D_n = 14 nm, $Đ_D$ = 1.05, σ = 3 nm), DLS (Figure S46K, D_h = 136 ± 8 nm in H$_2$O, 123 nm ± 3 nm in 5 mM NaCl, 0.1 mg/mL), and ζ-potential (*app.* ζ-potential = +25.5 ± 0.4 mV).

Example procedure for the preparation of blend nanospheres via dialysis

An aliquot of **P1** unimer solution (50 µL, 20 mg/mL in DMSO), PFTMC$_{16}$-*b*-PDMAEMA$_{158}$-BD (**P2**) unimer solution (100 µL, 20 mg/mL in DMSO) and PFTMC$_{16}$-*b*-PDMAEMA$_{161}$-FA$_7$ (**P3**) unimer solution (100 µL, 20 mg/mL in DMSO) was diluted in DMSO (750 µL). The sample was manually shaken for 10 s, then vortex mixed for 10 s, before being placed inside a dialysis membrane (Sigma Aldrich, MWCO = 12,000 – 14,000 Da), sealed with clips (Spectrum Chemical), and dialyzed into deionized water (500 mL) in the dark for 24 h with a minimum of three dialysate changes. The dialysis membrane was opened, and the nanosphere solution was

transferred to a vial. The solution was weighed, and filtered deionized water was added to make the sample up to 1 mg/mL gravimetrically (5 g). The resulting nanospheres were characterized via TEM (Figure S62, D_n = 14 nm, $Đ_D$ = 1.05, σ = 3 nm) and stored in the dark.

Procedure for the isolation and storage of seed nanofibers in the solid phase

37 nm **P1** seeds ($Đ_L$ = 1.12, σ = 12 nm) in water (100 µL, 1 mg/mL) were frozen in liquid nitrogen, and placed into a FreeZone Freeze Drier (Labconco Corporation), and lyophilized to a solid. This solid was aged at room temperature for 24 h, before water (100 µL) was added, and the sample was characterized via TEM (Figure S53, L_n = 36 nm, $Đ_L$ = 1.10, σ = 11 nm).

Characterization data for individual samples used in this work

Nanofiber **seeds 7**: TEM (THF/MeOH, 10:90 v/v): Figure S39A, L_n = 28 nm, $Đ_L$ = 1.20, σ_L = 12 nm; (H$_2$O): Figure S39B, L_n = 27 nm, $Đ_L$ = 1.12, σ_L = 9 nm; DLS: D_h = 85 ± 5 nm in H$_2$O, 51 nm ± 1 nm in 5 mM NaCl, 0.1 mg/mL; and ζ-potential: *app.* ζ-potential = +18.6 ± 0.3 mV.

Nanofiber **seeds 7b**: TEM (H$_2$O): Figure S40A, L_n = 7 nm, $Đ_L$ = 1.06, σ_L = 2 nm, W_n = 12 nm, $Đ_W$ = 1.04, σ_W = 2 nm; DLS: D_h = 255 ± 70 nm in H$_2$O, 193 nm ± 49 nm in 5 mM NaCl, 0.1 mg/mL; and ζ-potential: *app.* ζ-potential = +5.8 ± 1.9 mV.

Nanofiber **seeds 8**: TEM (THF/MeOH, 10:90 v/v): Figure S39D, L_n = 37 nm, $Đ_L$ = 1.14, σ_L = 14 nm; (H$_2$O): Figure S39E, L_n = 37 nm, $Đ_L$ = 1.12, σ_L = 12 nm; DLS: D_h = 205 ± 12 nm in H$_2$O, 195 nm ± 10 nm in 5 mM NaCl, 0.1 mg/mL; and ζ-potential: *app.* ζ-potential = +19.5 ± 0.5 mV.

Nanofibers **F1**: TEM (THF/MeOH, 20:80 v/v): Figure S44A: L_n = 93 nm, $Đ_L$ = 1.05, σ_L = 22 nm, W_n = 11 nm, $Đ_W$ = 1.05, σ_W = 2 nm; (H$_2$O): Figure 6D, L_n = 94 nm, $Đ_L$ = 1.10, σ_L = 30 nm, W_n = 12 nm, $Đ_W$ = 1.04, σ_W = 2 nm; (PBS): Figure S44B, L_n = 103 nm, $Đ_L$ = 1.07, σ_L = 27 nm, W_n = 10 nm, $Đ_W$ = 1.03, σ_W = 2 nm; DLS: D_h = 124 ± 8 nm in H$_2$O, 140 nm ± 5 nm in 5 mM NaCl, 0.1 mg/mL; and ζ-potential: *app.* ζ-potential = +26.4 ± 1.1 mV.

Nanofibers **F2**: TEM (THF/MeOH, 20:80 v/v): Figure S45A, L_n = 140 nm, $Đ_L$ = 1.05, σ_L = 32 nm, W_n = 14 nm, $Đ_W$ = 1.09, σ_W = 4 nm; (H$_2$O): Figure S45B, L_n = 137 nm, $Đ_L$ = 1.05, σ_L = 30 nm, W_n = 13 nm, $Đ_W$ = 1.04, σ_W = 3 nm; DLS: D_h = 77 ± 1 nm in H$_2$O, 82 nm ± 1 nm in 5 mM NaCl, 0.1 mg/mL; and ζ-potential: *app.* ζ-potential = +17.6 ± 0.6 mV.

Nanofibers **F3**: TEM (THF;MeOH:DMSO, 2:88:10 *v/v*): Figure S61A, $L_n = 51$ nm, $Đ_L = 1.25$, $\sigma = 25$ nm.

Nanofibers **F4**: TEM (THF;MeOH:DMSO, 2:78:20 *v/v*): Figure S60A, $L_n = 101$ nm, $Đ_L = 1.12$, $\sigma = 36$ nm; (H$_2$O): Figure S60B, $L_n = 97$ nm, $Đ_L = 1.20$, $\sigma = 44$ nm).

Nanofibers **F5**: TEM (THF;MeOH:DMSO, 1:79:20 *v/v*): Figure S60D, $L_n = 134$ nm, $Đ_L = 1.10$, $\sigma = 42$ nm; (H$_2$O): Figure S60E, $L_n = 77$ nm, $Đ_L = 1.18$, $\sigma = 32$ nm.

Nanospheres **S1**: TEM (H$_2$O): Figure S46A, $D_n = 9$ nm, $Đ_D = 1.06$, $\sigma = 0.3$ nm; DLS: Figure S46B, $D_h = 190 \pm 6.4$ nm in H$_2$O, 0.1 mg/mL.

Nanospheres **S2**: TEM (H$_2$O): Figure S46D, $D_n = 15$ nm, $Đ_D = 1.07$, $\sigma = 4$ nm; DLS: Figure **S46**E, $D_h = 222 \pm 12$ nm in H$_2$O, 192 nm $\pm$ 9 nm in 5 mM NaCl, 0.1 mg/mL; and ζ-potential: *app.* ζ-potential $= +20.9 \pm 1.3$ mV.

Nanospheres **S3**: TEM (H$_2$O): Figure S46G, $D_n = 16$ nm, $Đ_D = 1.08$, $\sigma = 5$ nm; DLS: Figure **S46**H, $D_h = 139 \pm 17$ nm in H$_2$O, 90 nm $\pm$ 4 nm in 5 mM NaCl, 0.1 mg/mL; and ζ-potential: *app.* ζ-potential $= +12.0 \pm 2.1$ mV.

Nanospheres **S4**: TEM (H$_2$O): Figure S46J, $D_n = 14$ nm, $Đ_D = 1.05$, $\sigma = 3$ nm; DLS: Figure S46K, $D_h = 136 \pm 8$ nm in H$_2$O, 123 nm $\pm$ 3 nm in 5 mM NaCl, 0.1 mg/mL; and ζ-potential: *app.* ζ-potential $= +25.5 \pm 0.4$ mV.

Nanospheres **S5**: TEM (H$_2$O): Figure S62A, $D_n = 22$ nm, $Đ_D = 1.08$, $\sigma = 6$ nm.

Determination of the linear aggregation number ($N_{agg,L}$)

The linear aggregation number was calculated according to the procedure outlined by Finnegan et. al.[S8]

The $N_{agg,L}$ is defined by the following equation:

$$N_{agg,L} = \frac{number\ of\ molecules\ per\ micelle}{micelle\ length} \qquad \text{(eq. S3)}$$

The average number of molecules per micelle can be determined by the following equation:

$$No.\ of\ molecules\ per\ micelle = \frac{volume\ of\ micelle\ core \times \rho\ core-forming\ block \times N_A}{M_n\ of\ the\ core-forming\ block} \text{(eq. S4)}$$

The volume of the micelle core may be determined by the following equation:

$$volume\ of\ micelle\ core = micele\ core\ width\ \times height\ \times length \qquad (eq.\ S5)$$

The micelle core width (11 nm) and length (103 nm) were taken from TEM data (Figure S44), whilst the micelle height (7 nm) was taken from AFM data (Figure 4). The density of PFTMC ($\rho = 1.33$ g/cm^3) was taken from the literature,[S19] whilst the M_n of the PFTMC core (4,053 Da) was calculated based on a DP$_n$ of 16, which was calculated from MALDI-TOF data (Figure S1). Based on these parameters, the $N_{agg,L}$ was determined to be 15 molecules per nm.

Investigating the pH- and thermo-responsiveness of P1 nanofibers via DLS (Figure S48-Figure S49)

Investigating the pH-responsiveness of P1 nanofibers (Figure S48)

To a solution (10 µL, 1 mg/mL) of 36 nm **P1** nanofibers ($Đ_L = 1.12$, $\sigma = 12$ nm), water (40 µL) and 50 µL of either: 40 mM HNO$_3$ + 20 mM NaCl (pH = 2), 30 mM NaCl (pH = 7) or 40 mM NaOH + 20 mM NaCl (pH = 12) was added. The solution was placed in a low-volume cuvette (Zen 2112, Malvern Panalytical) and placed in the DLS instrument. The results were recorded at 25 °C and plotted in Figure S48.

Investigating the thermo-responsiveness of P1 nanofibers (Figure S49)

To a solution (70 µL, 1 mg/mL) of 36 nm **P1** nanofibers ($Đ_L = 1.12$, $\sigma = 12$ nm), water (280 µL) and NaCl (350 µL, 10 mM) was added. The solution was placed in a low-volume cuvette (Zen 2112, Malvern Panalytical) and placed in the DLS instrument. The sample was heated to from 25 °C to 61 °C in 2 °C increments, and the method set to automatically take 5 size measurements at each temperature, with a 2-minute equilibration time. The results were plotted in Figure S49.

Enzymatic biodegradation of P1 nanofibers and nanospheres

Following the degradation of P1 nanofibers and nanospheres via DLS (Figure 7 and Figure S54-Figure S55)

Figure 7 and Figure S54

To a solution (10 µL, 1 mg/mL) of 137 nm **P1** nanofibers ($Đ_L = 1.05$, $\sigma = 30$ nm) or 14 nm **P1** nanospheres ($Đ_D = 1.05$, $\sigma = 3$ nm), 10mM NaCl (50 µL), water (49 µL) and lipase from

Thermomyces lanuginosus (1 µL, $>1\times10^8$ U/L) was added. The solution was placed in a low-volume cuvette (Zen 2112, Malvern Panalytical) and placed in the DLS instrument. The sample was heated to 37 °C, and the method set to automatically take size measurements at intervals over a 24 h period using the 'equilibration time' function. The results were plotted in Figure 7 and Figure S54.

Figure S55

To a solution (20 µL, 1 mg/mL) of 7 nm **P1** nanofibers ($Đ_L$ = 1.06, σ = 2 nm), water (179 µL) and lipase from *Thermomyces lanuginosus* (2 µL, $>14,000$ U/L) was added. The solution was placed in a low-volume cuvette (Zen 2112, Malvern Panalytical) and placed in the DLS instrument. The sample was heated to 37 °C, and the method set to automatically take size measurements at intervals over a 108 h period using the 'equilibration time' function. The results were plotted in Figure S55.

Following the degradation of P1 nanofibers via TEM, MALDI and NMR (Figure S56-S50 and Table S5)

To a solution of 103 nm **P1** nanofibers ($Đ_L$ = 1.07, σ = 27 nm, 100 µL, 1 mg/mL in PBS), a solution of lipase from *Thermomyces lanuginosus* was added (900 µL, $>1\times10^8$ U/L) and heated to 37 °C. Aliquots (10 µL) were taken at intervals, and analysed via TEM (Figure S56) and MALDI-TOF MS (Figure S57) with samples prepared immediately. After 72 h, an aliquot was taken and analyzed via ^{1}H-NMR (Figure S57C & E-F). It was observed that upon addition of the nanofibers to the lipase solution, effervescence was observed (presumably release of CO_2), and over time a precipitate was obtained.

The solid precipitate was extracted and analysed by repeating the above procedure, but without taking any aliquots for TEM / MALDI-TOF MS analysis. After 7 days, the solution was taken, and centrifuged for 10 mins at 5,400 rpm. The supernatant was decanted, and the solid material was washed with water (10 mL), centrifuged for 10 mins at 5,400 rpm, and the supernatant was removed again. Et$_2$O / MeOH (9:1, 10 mL) was added, and the solid material centrifuged once more for 10 mins at 5,400 rpm. The solid material was then dried and analysed via ^{1}H-NMR (Figure S57D). It was observed that the solid material was insoluble in CD$_2$Cl$_2$, THF, and water.

Cell culture protocols

HeLa (Human cervical carcinoma cells) were grown in DMEM media with high glucose (4.5 g/L), WI-38 (Caucasian fibroblast-like foetal lung cells) were grown in MEM media in a humidified 5% CO_2 incubator at 37°C. All growth media were supplemented with 10% fetal bovine serum (FBS). Confluent cultures (80% or less) were detached from the surface using trypsin (TrypLE Express™) and plated at 5×10^3 - 1×10^4 cells/well in 96-well plates for cytotoxicity studies.

Cell Viability Assays

The influence of 103 nm nanofibers ($Đ_L = 1.07$, $\sigma = 27$ nm) and 9 – 16 nm nanospheres ($Đ_W = 1.06 – 1.08$, $\sigma = 1$ - 5 nm) on WI-38 and HeLa cells was evaluated after 72 h of exposure, and analyzed with a dual calcein / alamarBlue® assay (Table S6, Figure 8, Figure S58 and Figure S59). Cell survival was quantified by measuring calcein AM fluorescence. The fluorescence, retained within live cells only, results from activity of esterases on the (nonfluorescent) calcein AM (Molecular Probes). Changes in cell metabolism were assessed using alamarBlue™ (AB, Life Technologies), a cytosolic substrate for reductive metabolism (resazurin to resorufin) whose fluorescence spectrum changes on reduction by cytosolic enzymes. WI-38 and HeLa cells were incubated with 0-100 µg/mL of sample for 72 h. Each experiment was repeated at least in duplicate in medium with reduced FBS (5%), and each data point was conducted in sextuplicate. Staurosporine (1 µM/mL, Enzo Life Sciences) was used as a positive control. After 72 h, the plates were washed with PBS, and AB (5 % solution) and calcein (3 µM) were added in medium without FBS. After 1 h incubation, the fluorescence of both dyes was read using a plate reader (BMG Labtech CLARIOstar) (AB $\lambda_{ex} = 545$ nm, $\lambda_{em} = 590$ nm, calcein $\lambda_{ex} = 494$ nm, $\lambda_{em} = 517$ nm). Results were expressed as the concentration of sample (in nM) that reduces cell growth by 50 % versus untreated control cells (EC_{50}) using the nonlinear regression function of Prism 7 (GraphPad Software) to fit the data to a sigmoidal curve using the 'log (inhibitor) versus normalized response – variable slope' equation.

Supplementary Figures
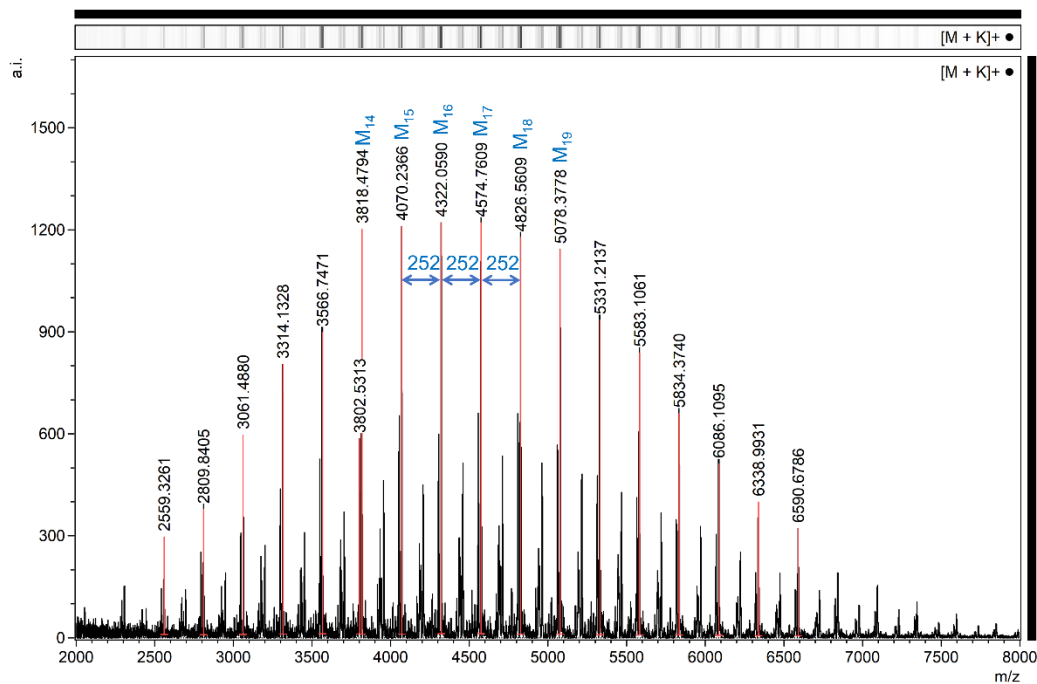
Figure S1. MALDI-TOF mass spectrum of PFTMC$_{16}$-CTA. HRMS for C$_{265}$H$_{207}$NO$_{49}$S$_3$K$^+$ (DP of 16), [M+K]$^+$, calculated: 4,321.3; found: 4,322.1.
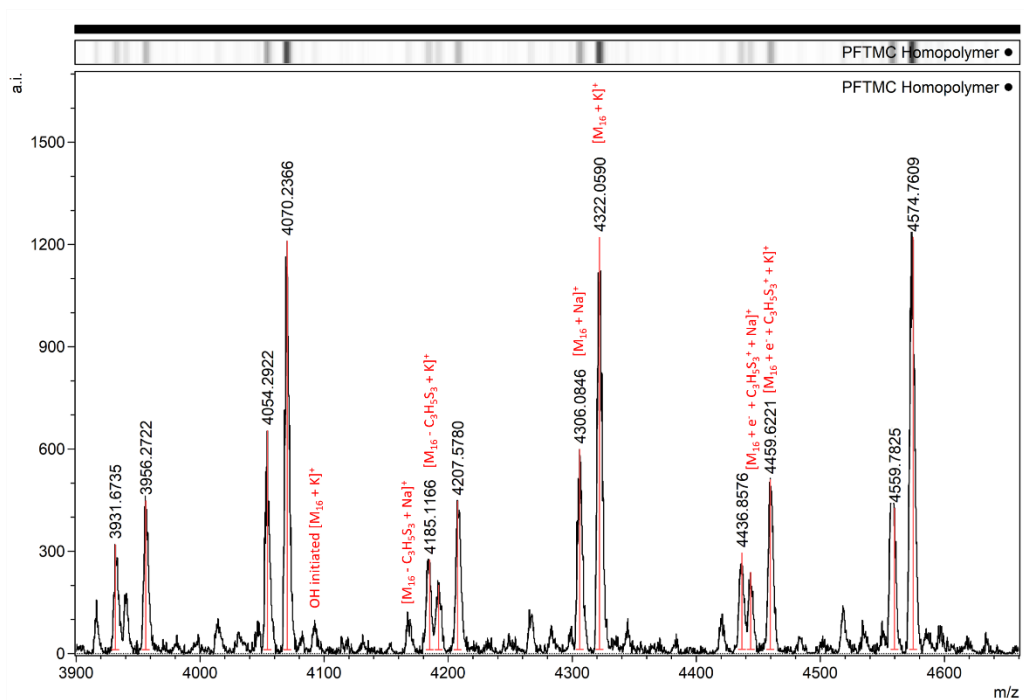
Figure S2. Magnification of MALDI-TOF mass spectrum of PFTMC$_{16}$-CTA, with the various adducts of M$_{16}^+$ labelled.
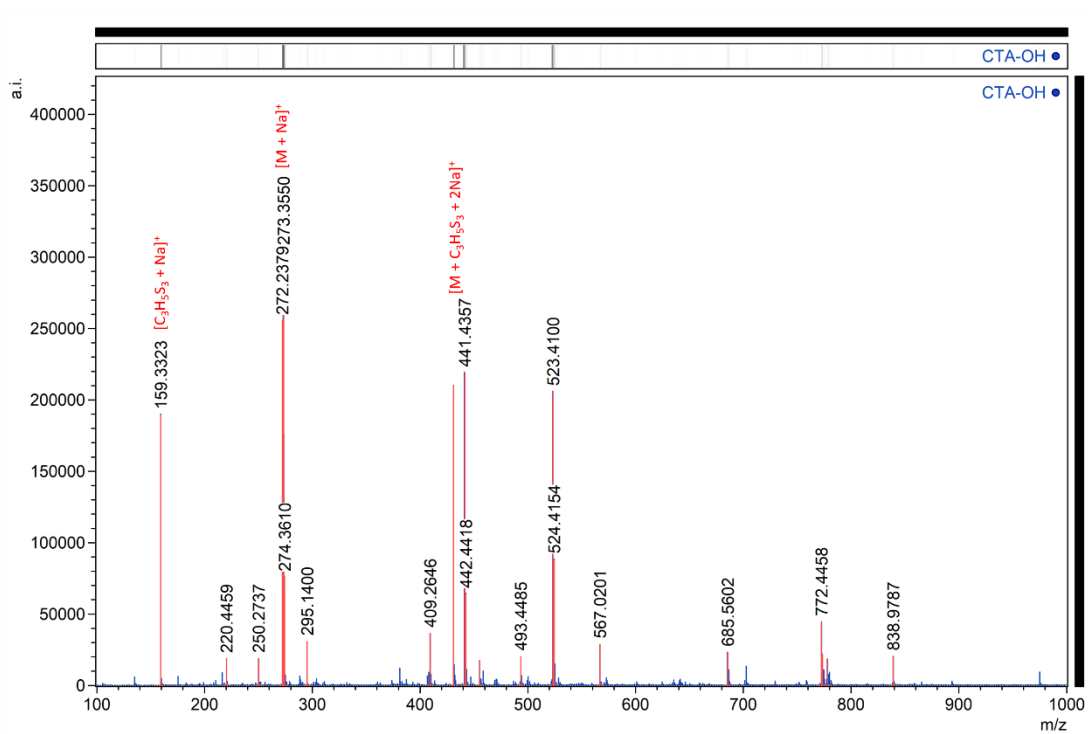
Figure S3. MALDI-TOF mass spectrum of CTA-OH, with key adducts labelled.
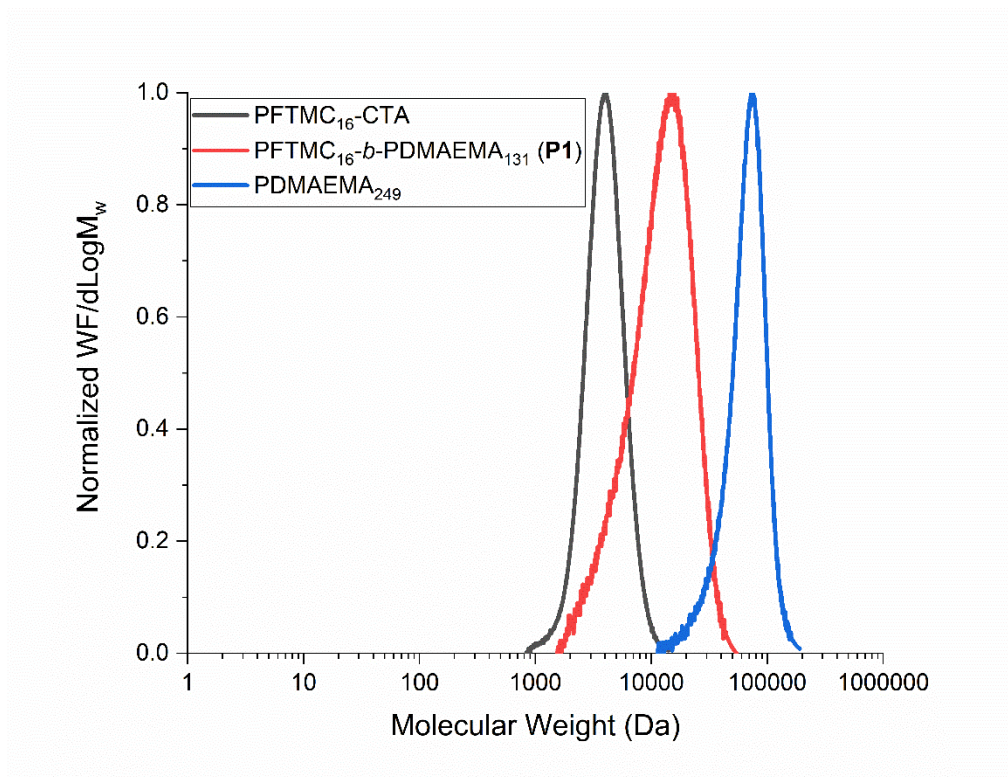
Figure S4. GPC Chromatograms (refractive index detection) in n-Bu₄NBr/THF of PFTMC₁₆-CTA (black trace), PFTMC₁₆-*b*-PDMAEMA₁₃₁ (**P1**, red trace), and PDMAEMA₂₄₉ (blue trace).
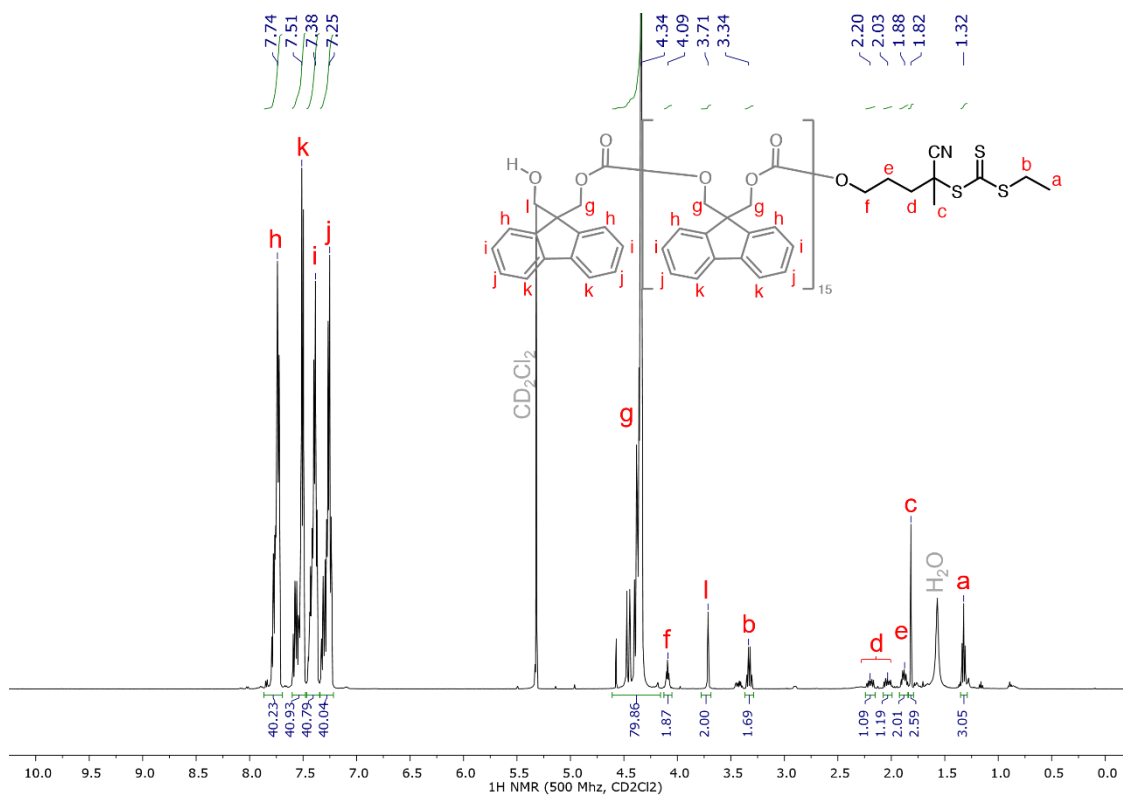
Figure S5. ^{1}H-NMR spectrum of PFTMC$_{16}$-CTA in CD$_2$Cl$_2$ (500 MHz).
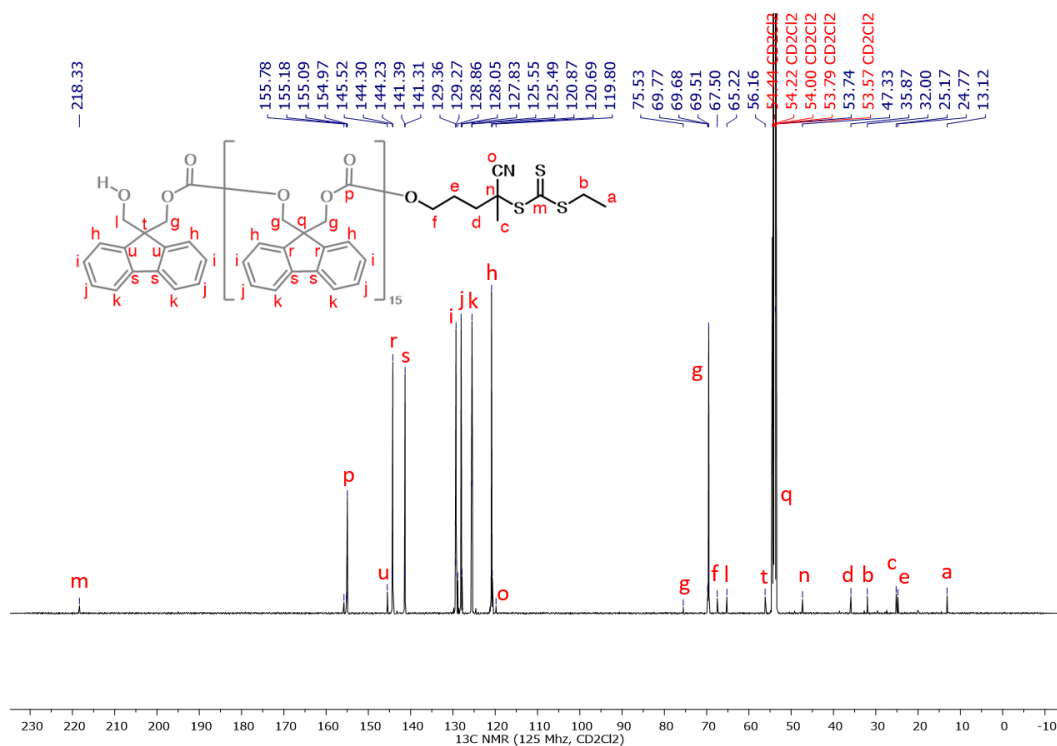
Figure S6. ^{13}C-NMR spectrum of PFTMC$_{16}$-CTA in CD$_2$Cl$_2$ (125 MHz).
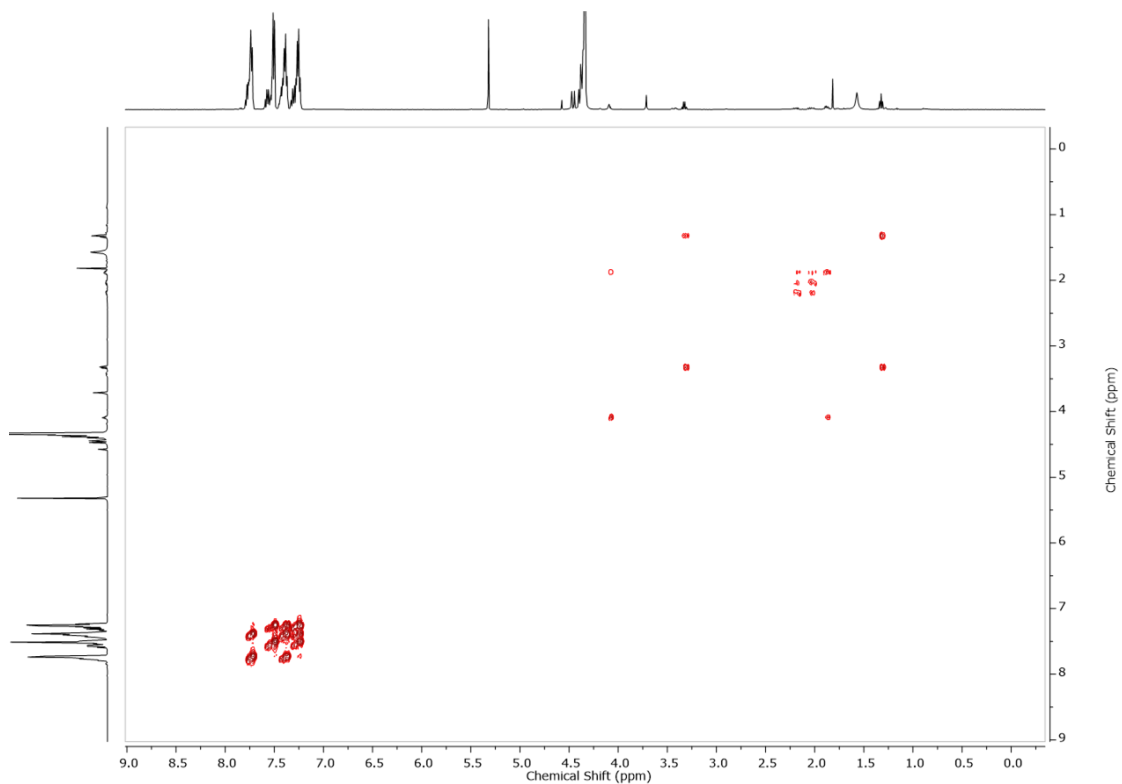
Figure S7. ^{1}H-^{1}H COSY NMR spectrum of PFTMC$_{16}$-CTA in CD$_2$Cl$_2$ (500 MHz).
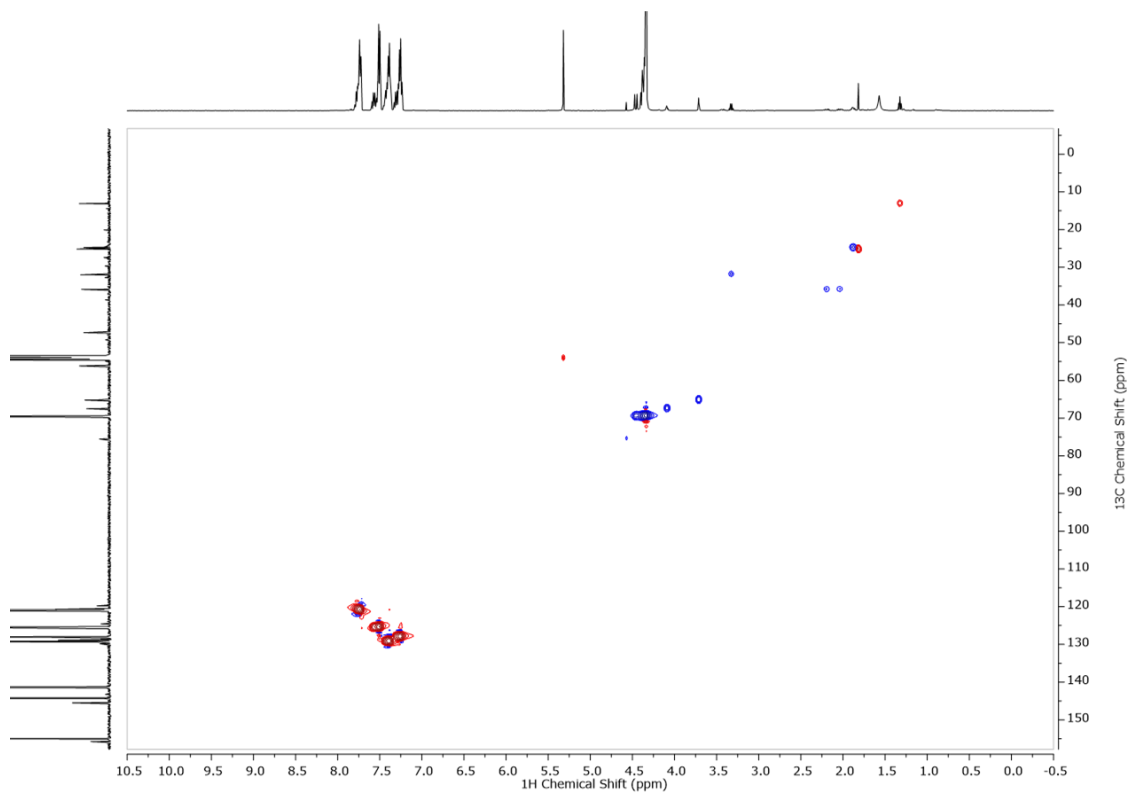
Figure S8. ^{1}H-^{13}C HSQC NMR spectrum of PFTMC$_{16}$-CTA in CD$_2$Cl$_2$ (500 MHz).
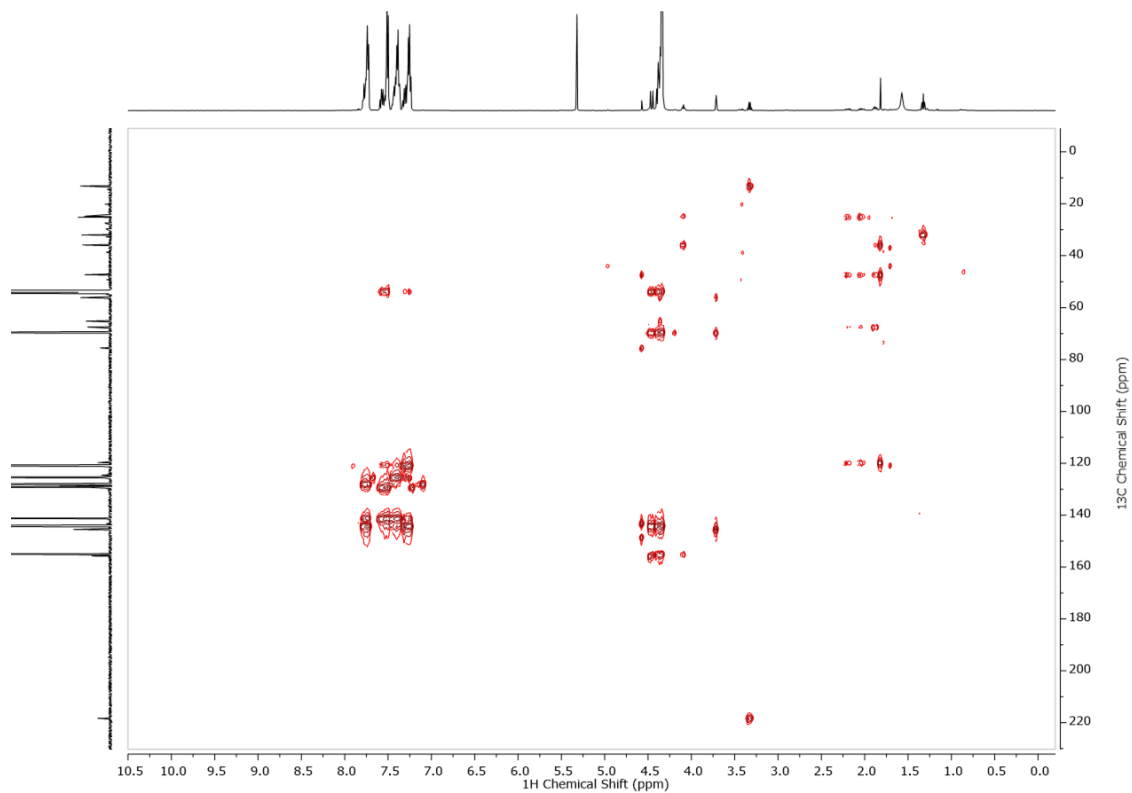
Figure S9. ^{1}H-^{13}C HMBC NMR spectrum of PFTMC$_{16}$-CTA in CD$_2$Cl$_2$ (500 MHz).
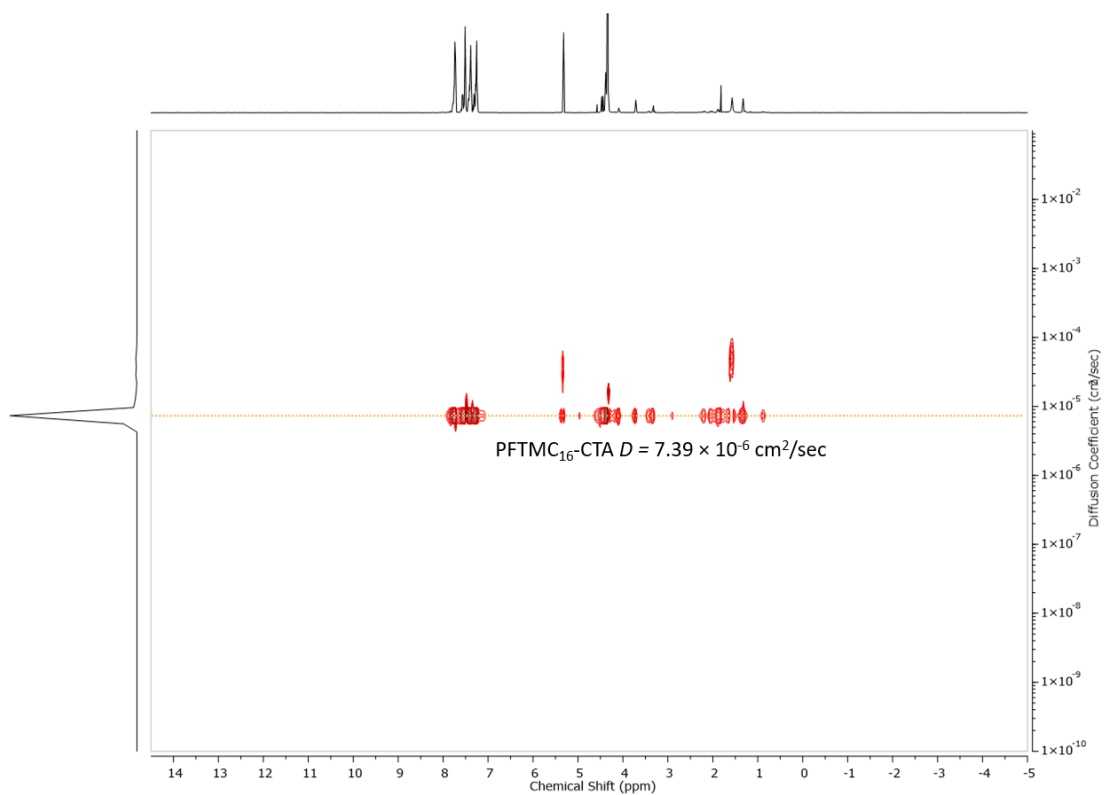
Figure S10. ^{1}H DOSY NMR spectrum of PFTMC$_{16}$-CTA in CD$_2$Cl$_2$ (500 MHz).
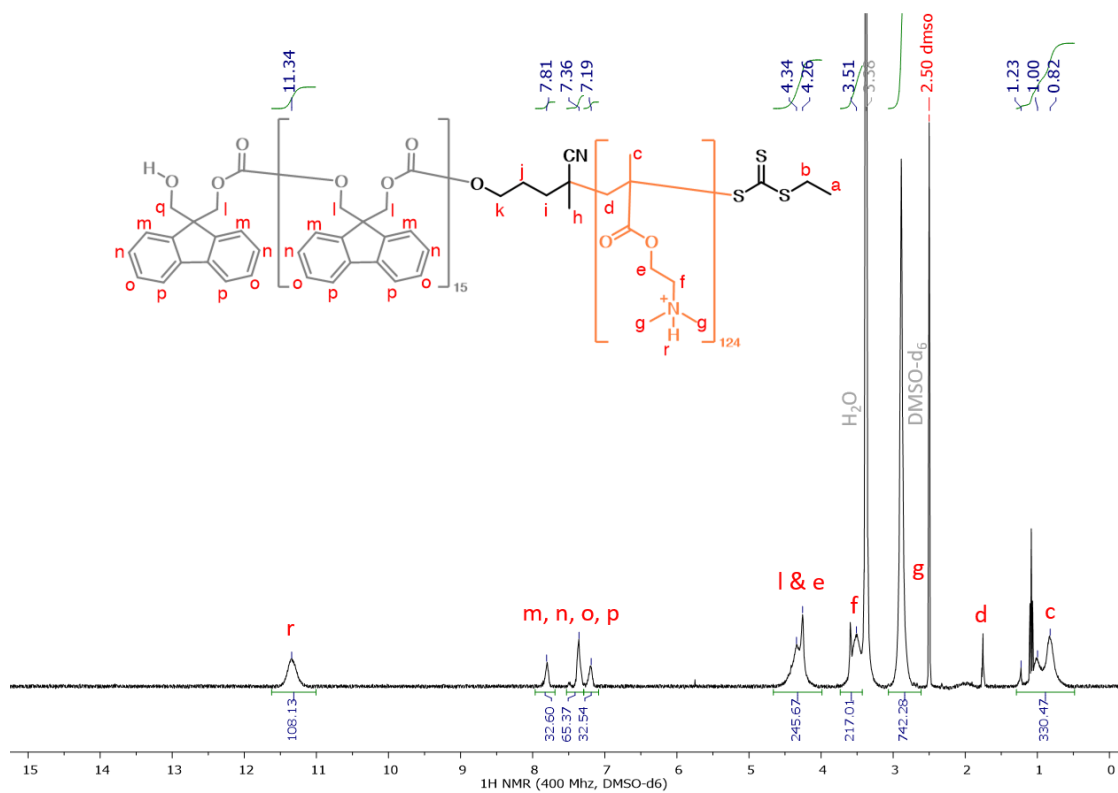
Figure S11. ^{1}H-NMR spectrum of PFTMC$_{16}$-b-(PDMAEMA · HCl)$_{124}$ in DMSO-d_6 (500 MHz).
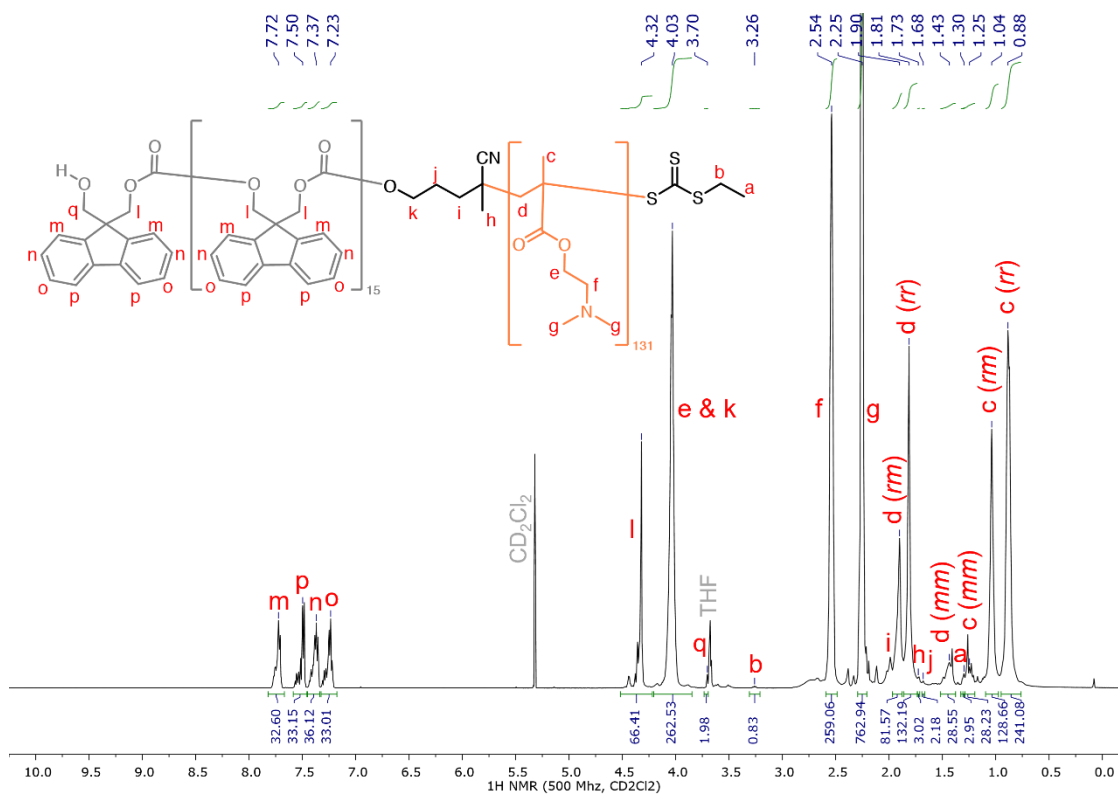
Figure S12. ^{1}H-NMR spectrum of PFTMC$_{16}$-b-PDMAEMA$_{131}$ (**P1**) in CD$_2$Cl$_2$ (500 MHz).
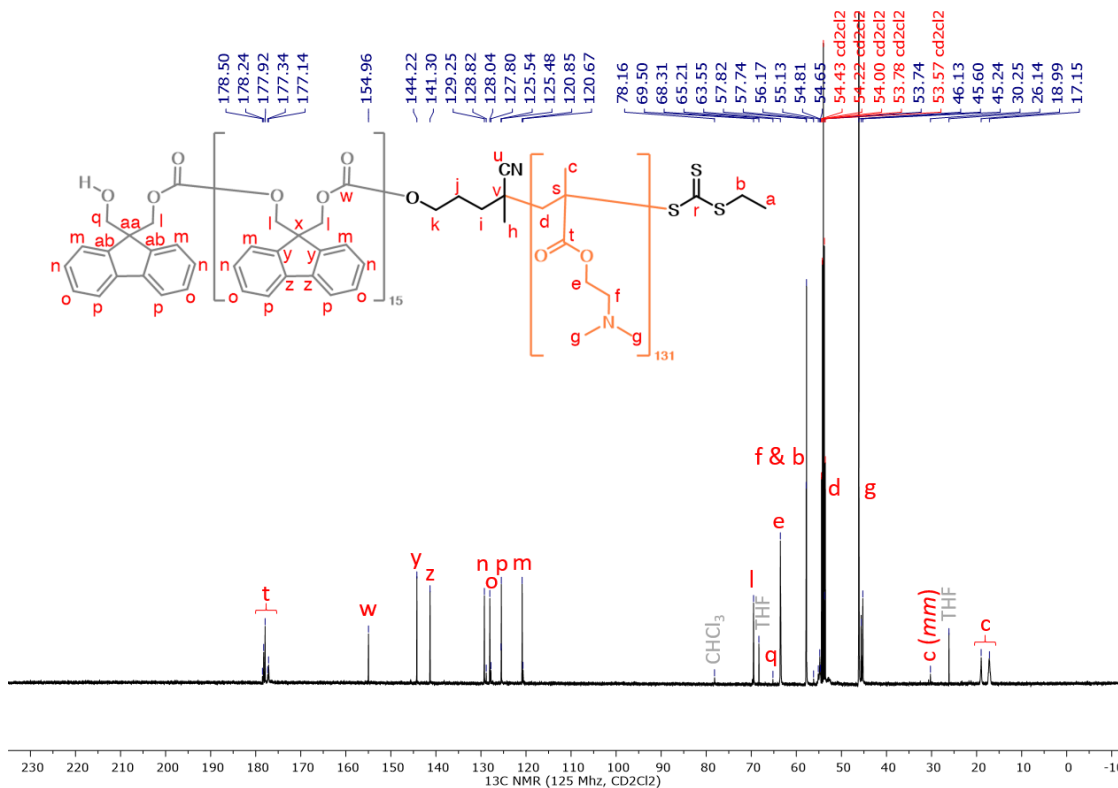
Figure S13. ^{13}C-NMR spectrum of PFTMC$_{16}$-b-PDMAEMA$_{131}$ (**P1**) in CD$_2$Cl$_2$ (125 MHz).
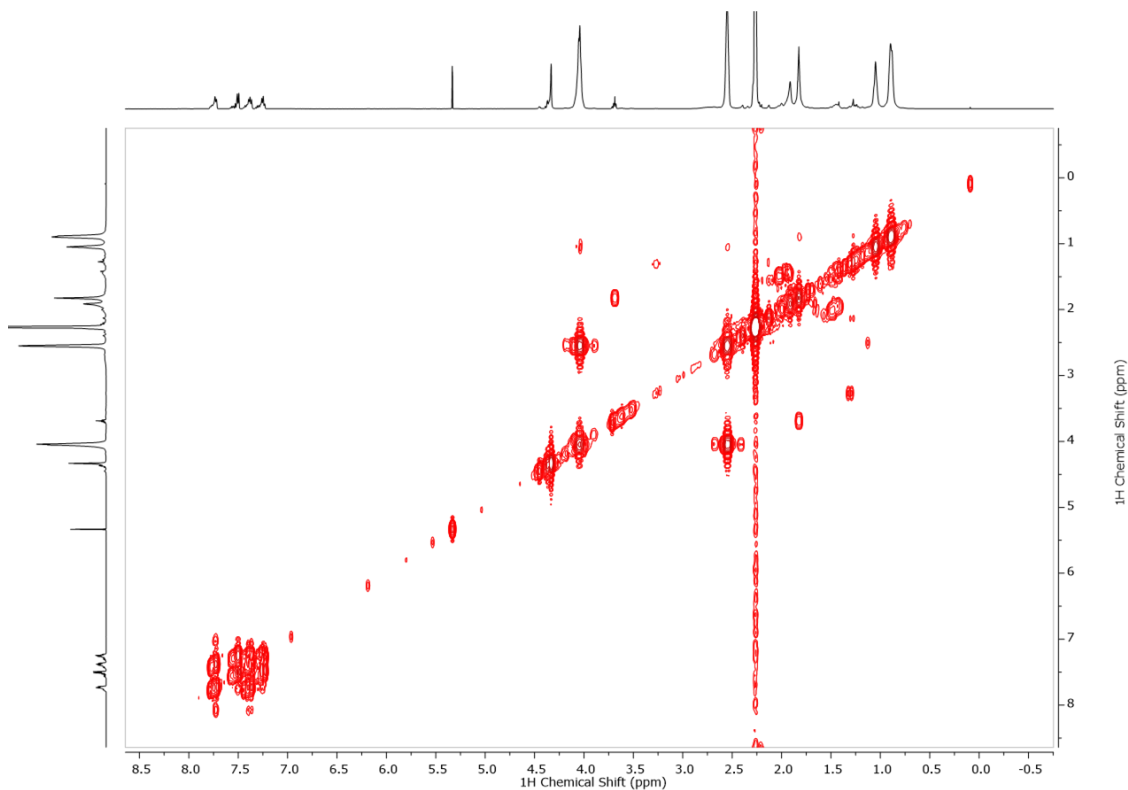
Figure S14. ^{1}H-^{1}H COSY NMR spectrum of PFTMC$_{16}$-b-PDMAEMA$_{131}$ in CD$_2$Cl$_2$ (500 MHz).
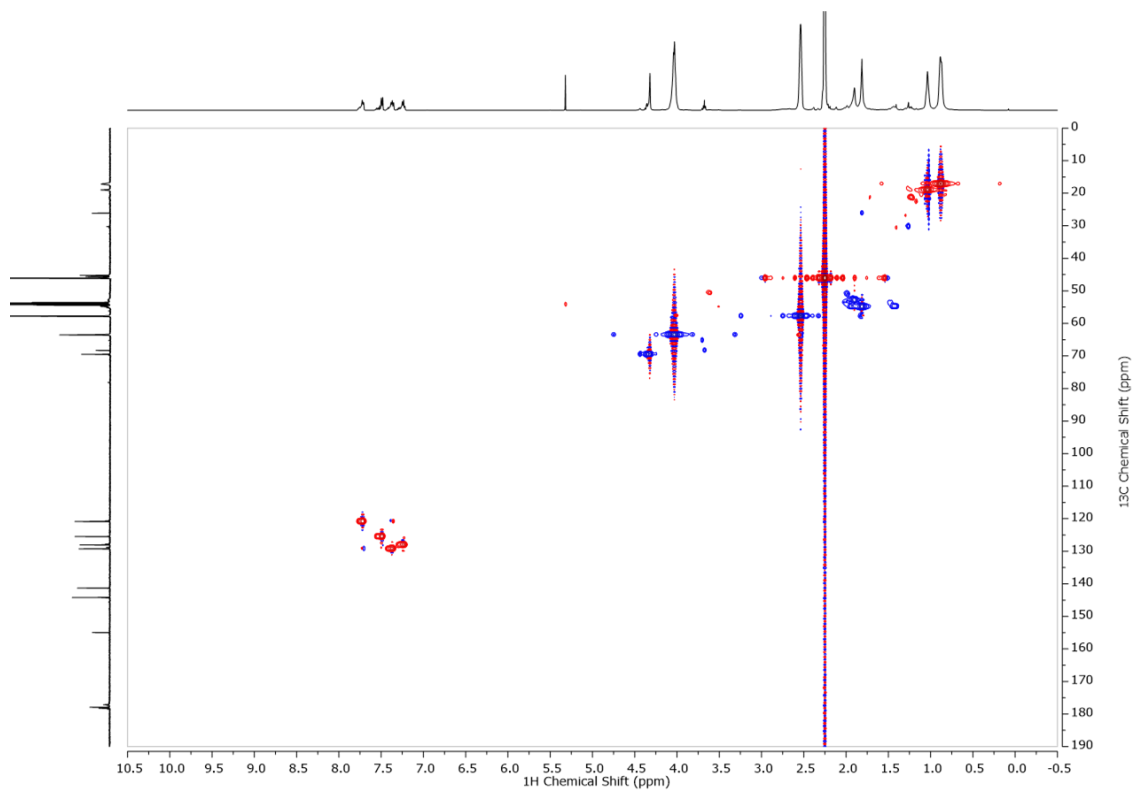
Figure S15. ^1H-^{13}C HSQC NMR spectrum of PFTMC$_{16}$-*b*-PDMAEMA$_{131}$ in CD$_2$Cl$_2$ (500 MHz).
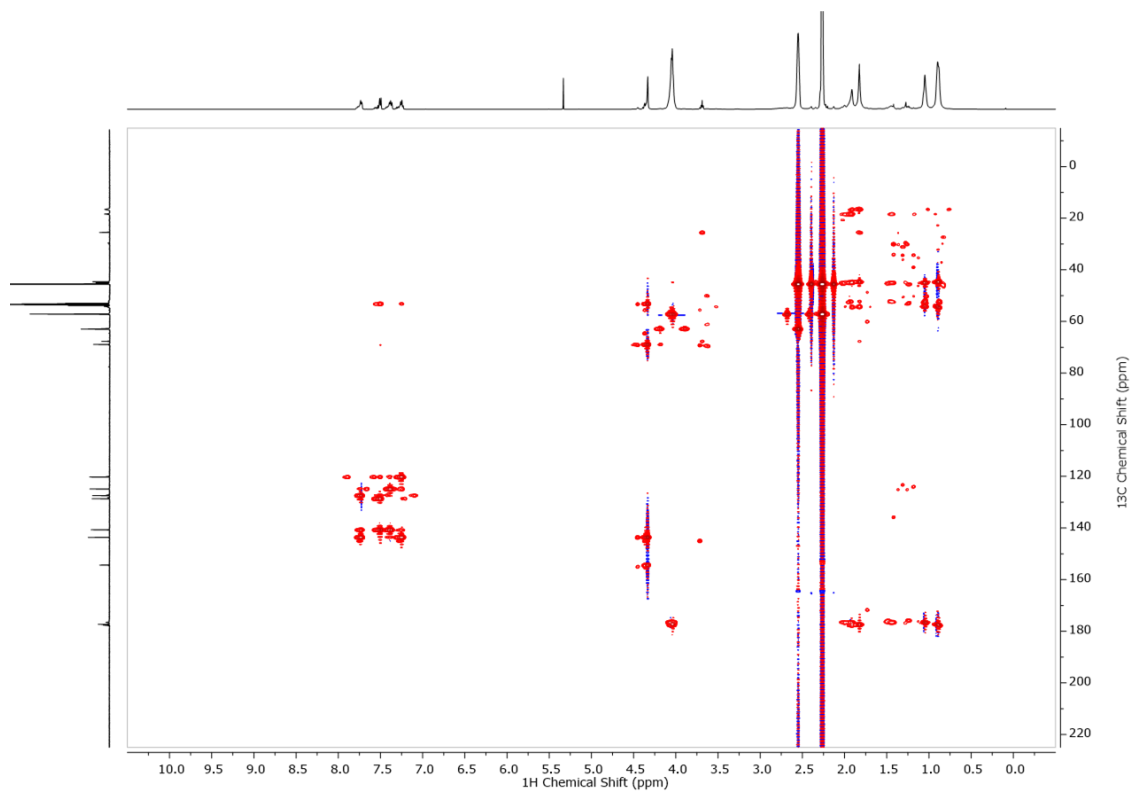
Figure S16. ^1H-^{13}C HMBC NMR spectrum of PFTMC$_{16}$-*b*-PDMAEMA$_{131}$ in CD$_2$Cl$_2$ (500 MHz).
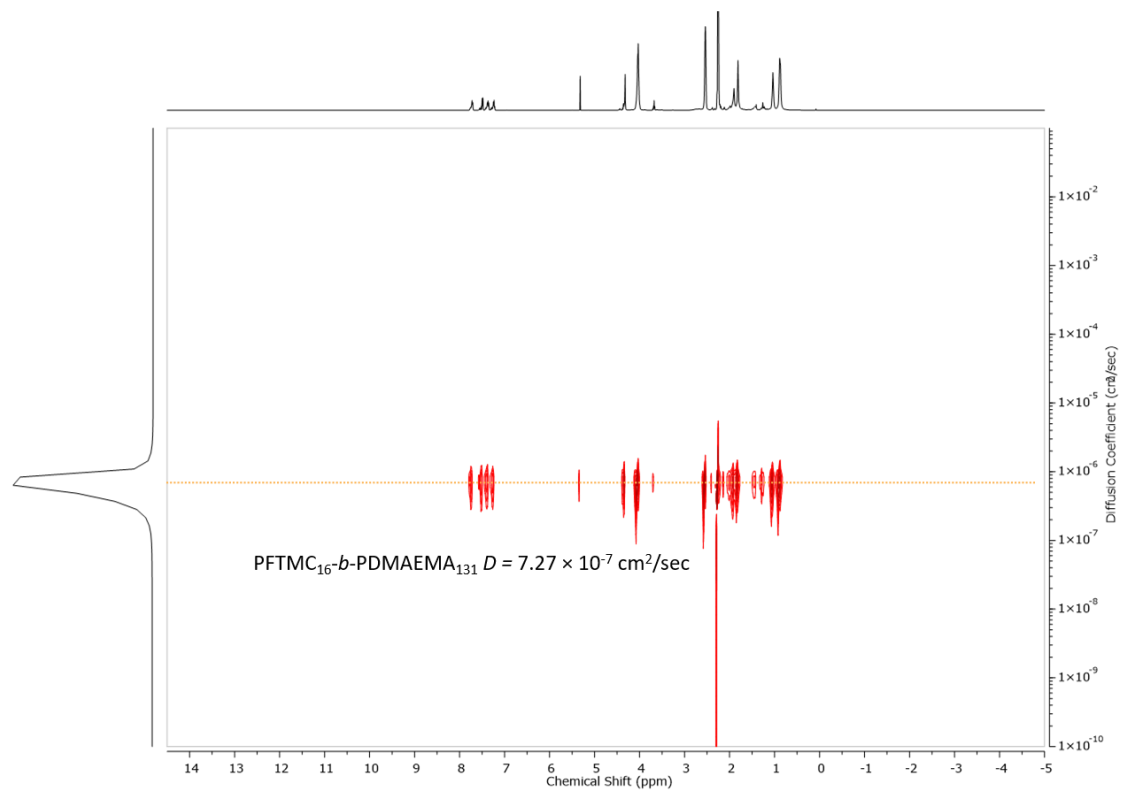
Figure S17. ^{1}H DOSY NMR spectrum of PFTMC$_{16}$-*b*-PDMAEMA$_{131}$ in CD$_2$Cl$_2$ (500 MHz).
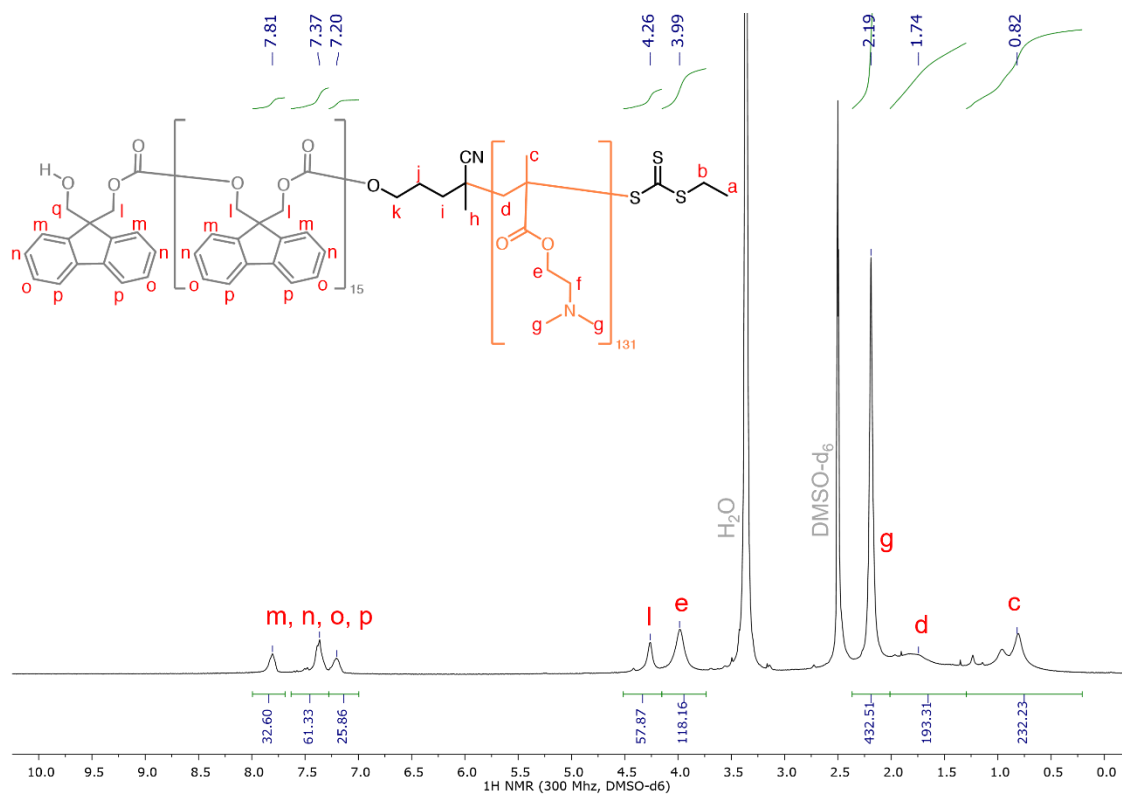
Figure S18. ^{1}H-NMR spectrum of PFTMC$_{16}$-*b*-PDMAEMA$_{131}$ (**P1**) in DMSO-*d$_6$* (500 MHz).
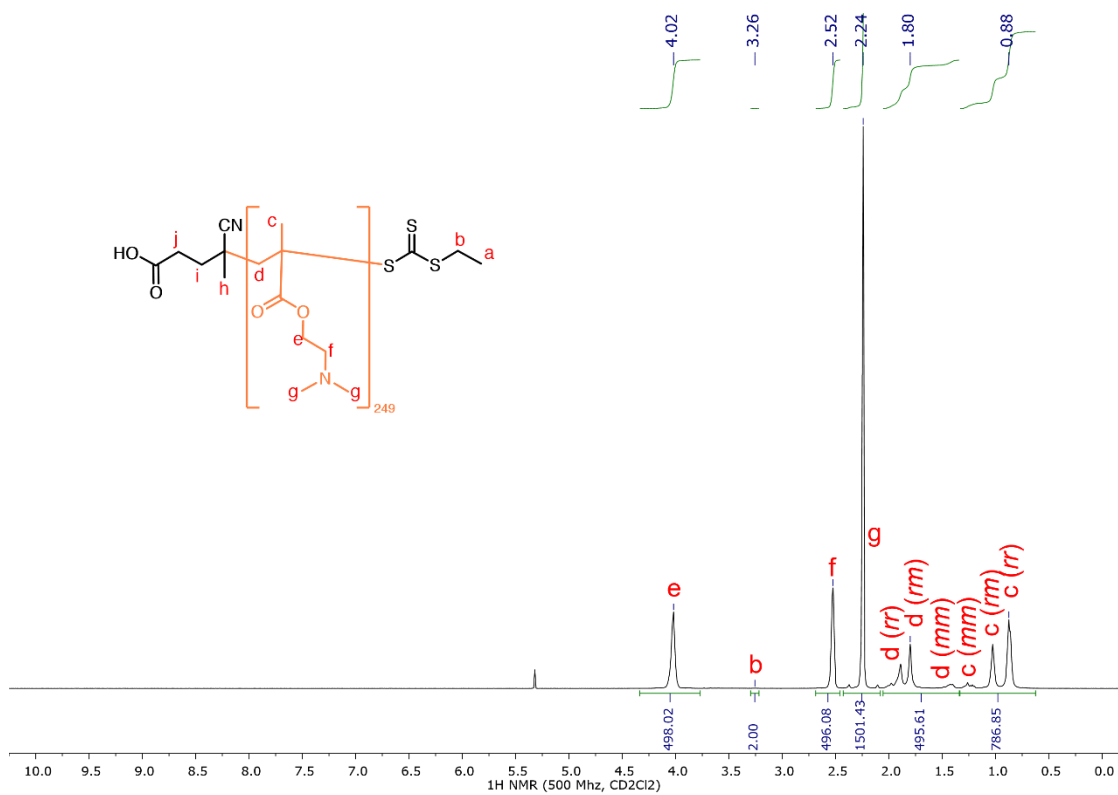
Figure S19. ^{1}H-NMR spectrum of PDMAEMA$_{249}$ in CD$_2$Cl$_2$ (500 MHz).
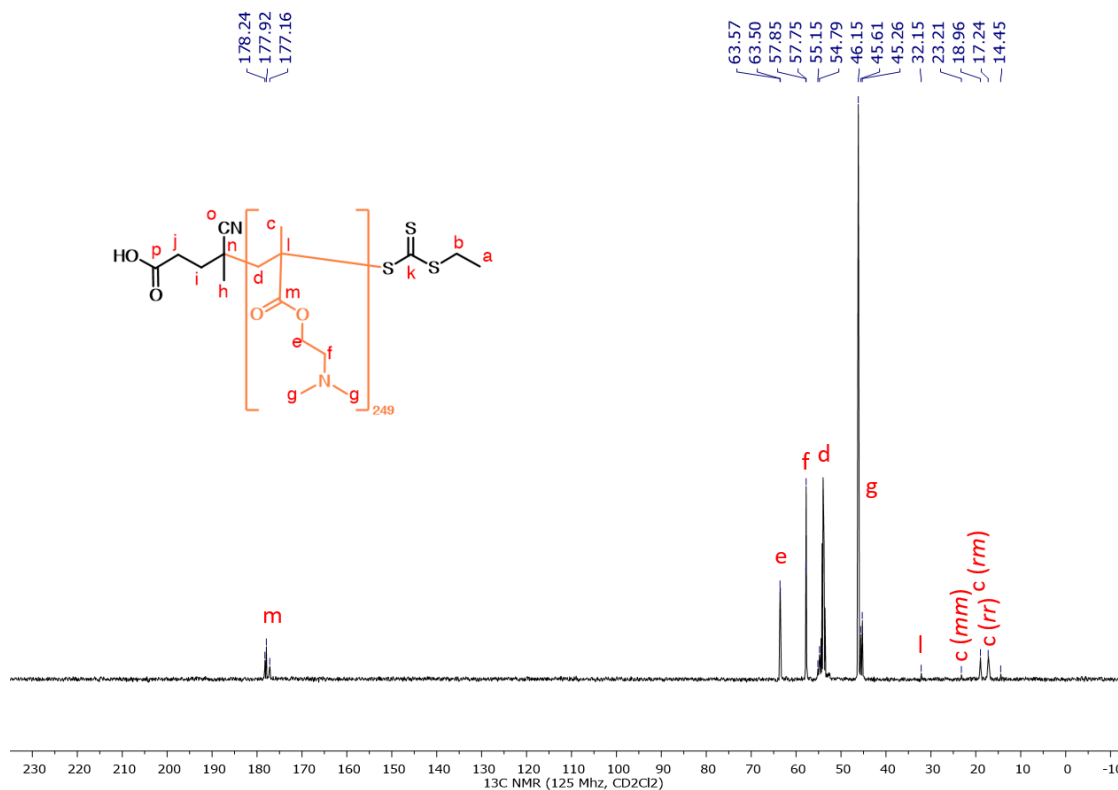
Figure S20. ^{13}C-NMR spectrum of PDMAEMA$_{249}$ in CD$_2$Cl$_2$ (125 MHz).
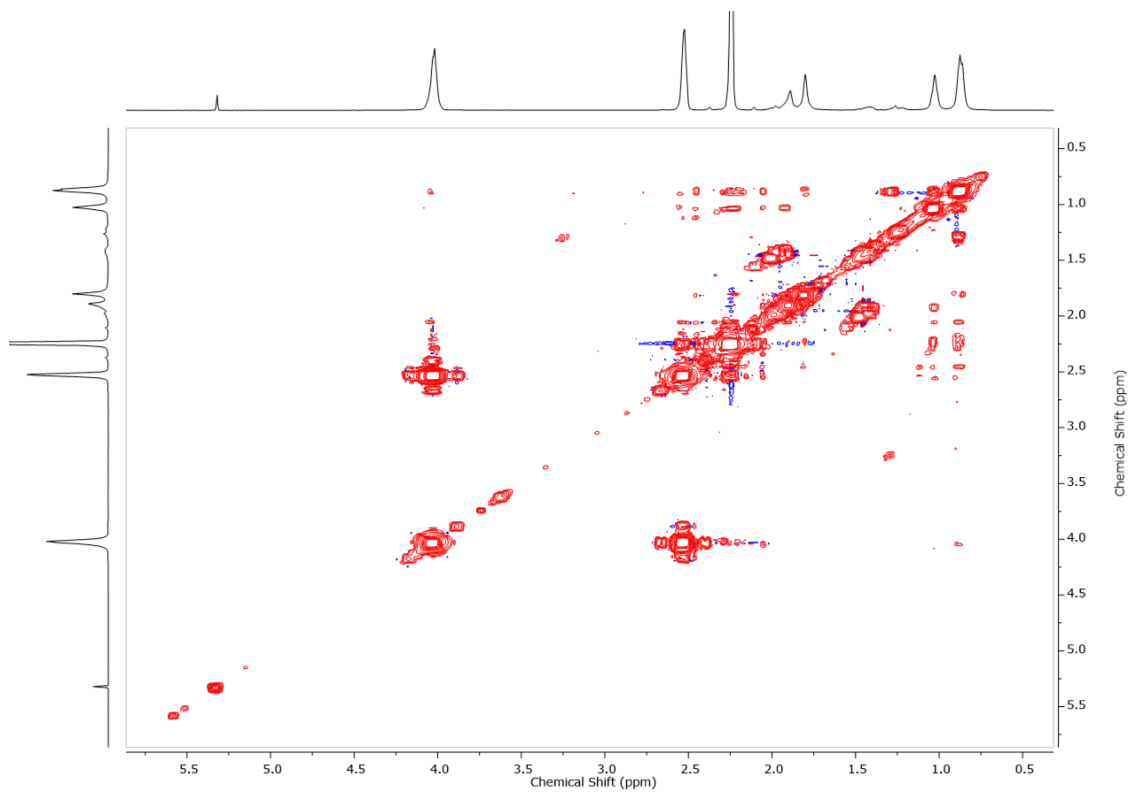
Figure S21. ^{1}H-^{1}H COSY NMR spectrum of PDMAEMA$_{249}$ in CD$_2$Cl$_2$ (500 MHz).
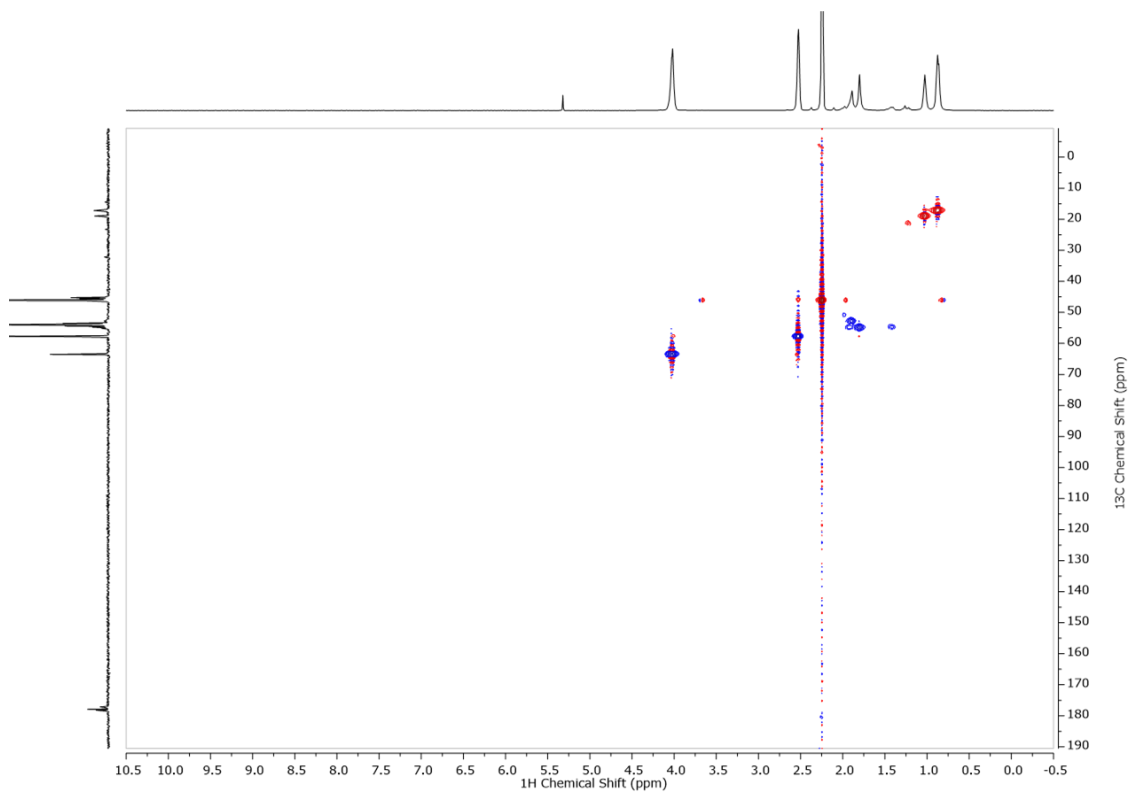
Figure S22. ^{1}H-^{13}C HSQC NMR spectrum of PDMAEMA$_{249}$ in CD$_2$Cl$_2$ (500 MHz).
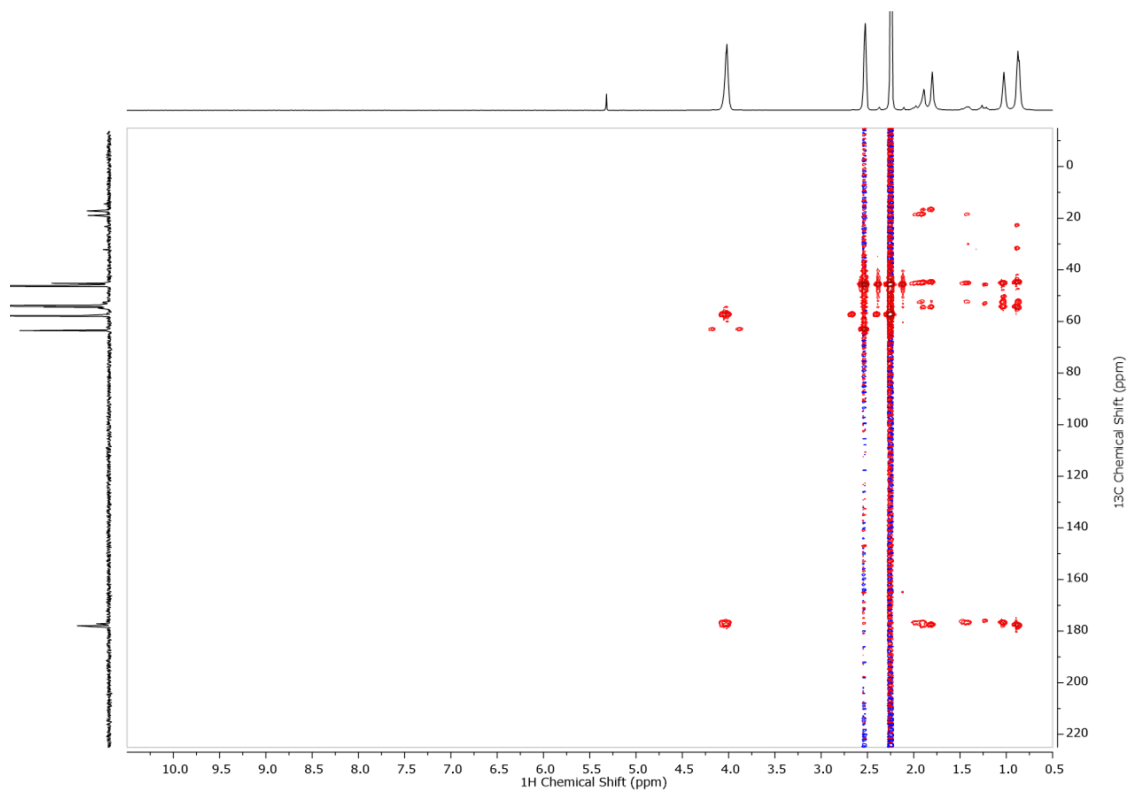
Figure S23. ^{1}H-^{13}C HMBC NMR spectrum of PDMAEMA$_{249}$ in CD$_2$Cl$_2$ (500 MHz).

PDMAEMA$_{249}$ D = 3.81 × 10^{-7} cm^2/sec
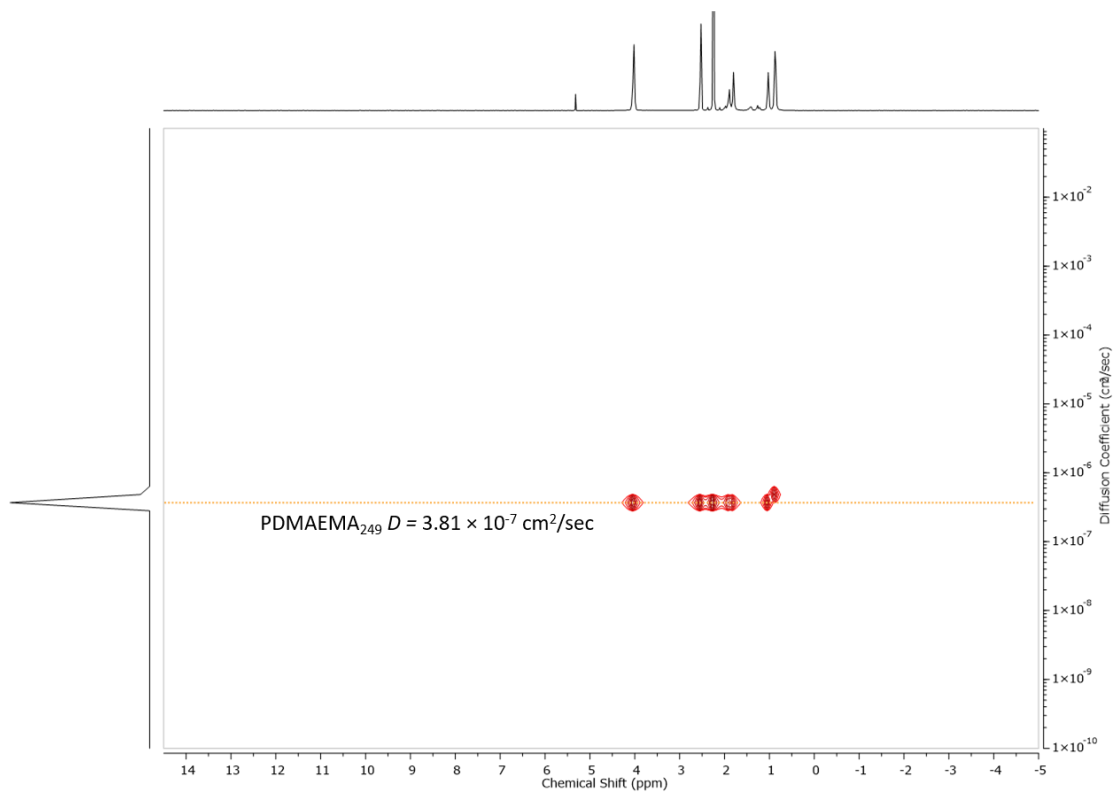
Figure S24. ^{1}H DOSY NMR spectrum of PDMAEMA$_{249}$ in CD$_2$Cl$_2$ (500 MHz).
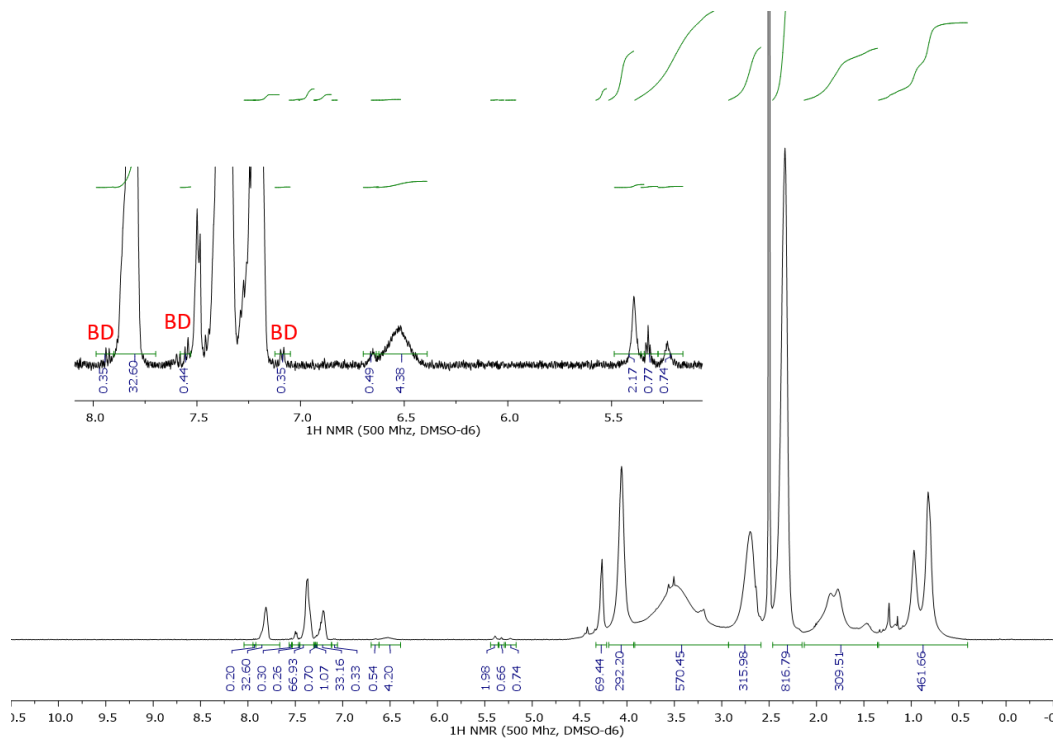
Figure S25. ^{1}H-NMR spectrum of PFTMC$_{16}$-*b*-PDMAEMA$_{158}$-BD (**P2**) in DMSO-*d$_6$* (500 MHz). Observable protons from the BODIPY$^{630/650-X}$ dye are labelled.
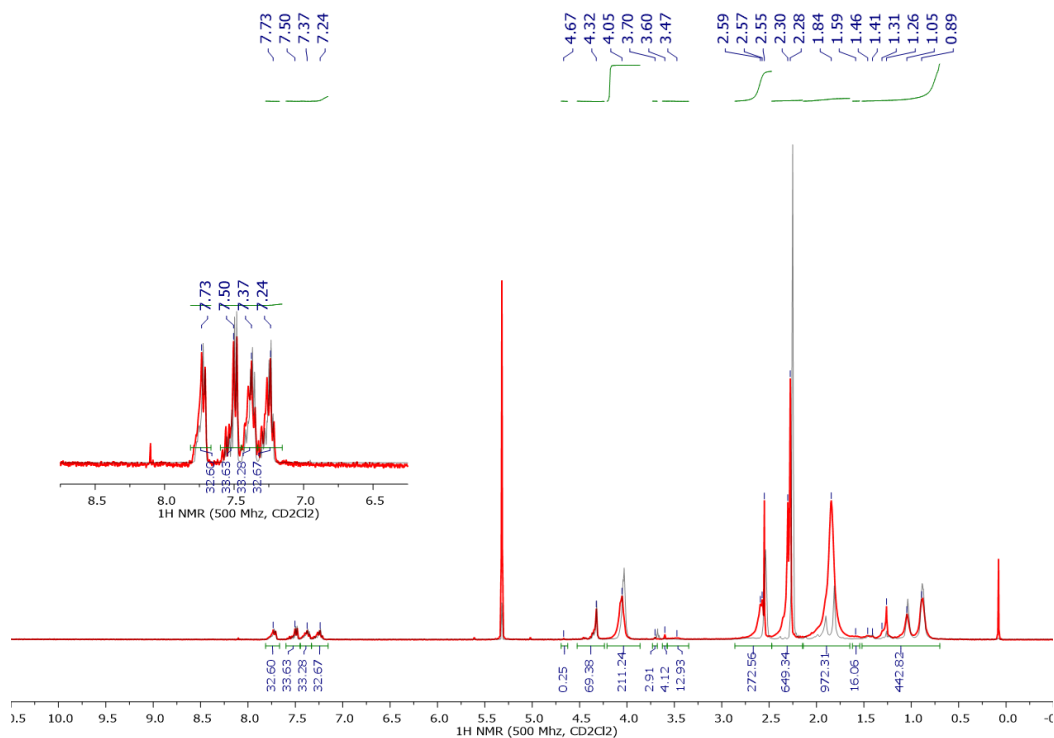

Figure S26. Overlay of ^{1}H-NMR spectra of PFTMC$_{16}$-*b*-PDMAEMA$_{158}$-BD (**P2**, red trace) and PFTMC$_{16}$-*b*-PDMAEMA$_{131}$ (**P1**, black trace) in CD$_2$Cl$_2$ (500 MHz).
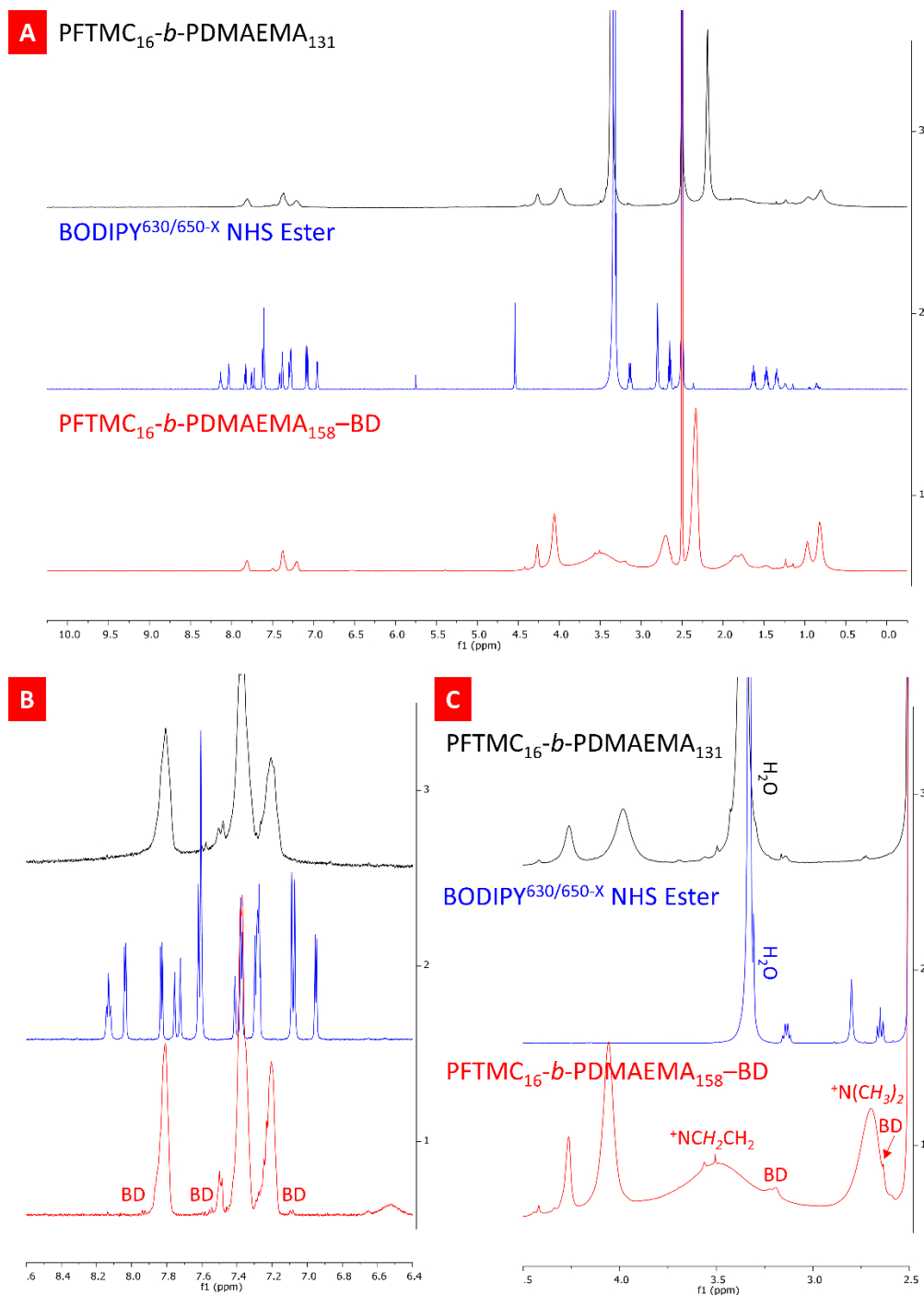
Figure S27. Stacked ¹H-NMR spectra of PFTMC$_{16}$-*b*-PDMAEMA$_{131}$ (**P1**, black trace), BODIPY$^{630/650-X}$ NHS Ester (blue trace) and PFTMC$_{16}$-*b*-PDMAEMA$_{158}$-BD (**P2**, red trace) in DMSO-*d$_6$* (500 MHz). (A) Full spectra. (B) Expansion of region from 6.5 – 8.5 ppm. (C) Expansion of region from 2.5 – 4.5 ppm. Analysis of the spectra is complicated by self-assembly of the BODIPY$^{630/650-X}$ dye, as well as the shift in protonation state of the PDMAEMA corona. Nonetheless, the peaks corresponding to the BOPDIPY dye are labelled.
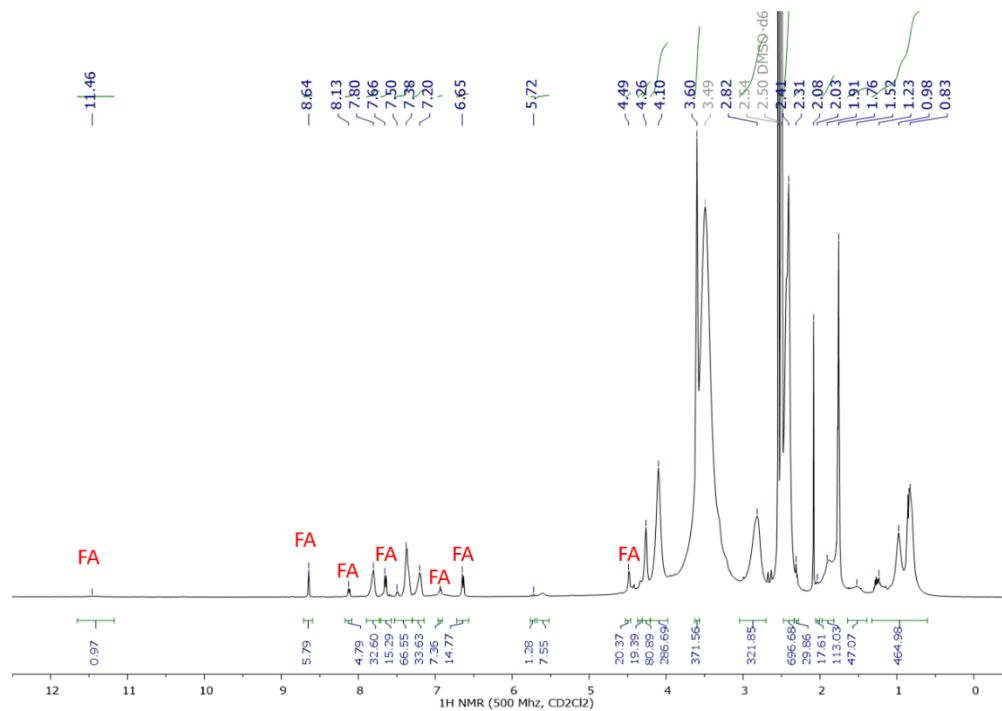
Figure S28. ^{1}H-NMR spectrum of PFTMC$_{16}$-b-PDMAEMA$_{161}$-FA$_7$ (**P3**) in DMSO-d_6 (500 MHz). Observable protons from folic acid are labelled.
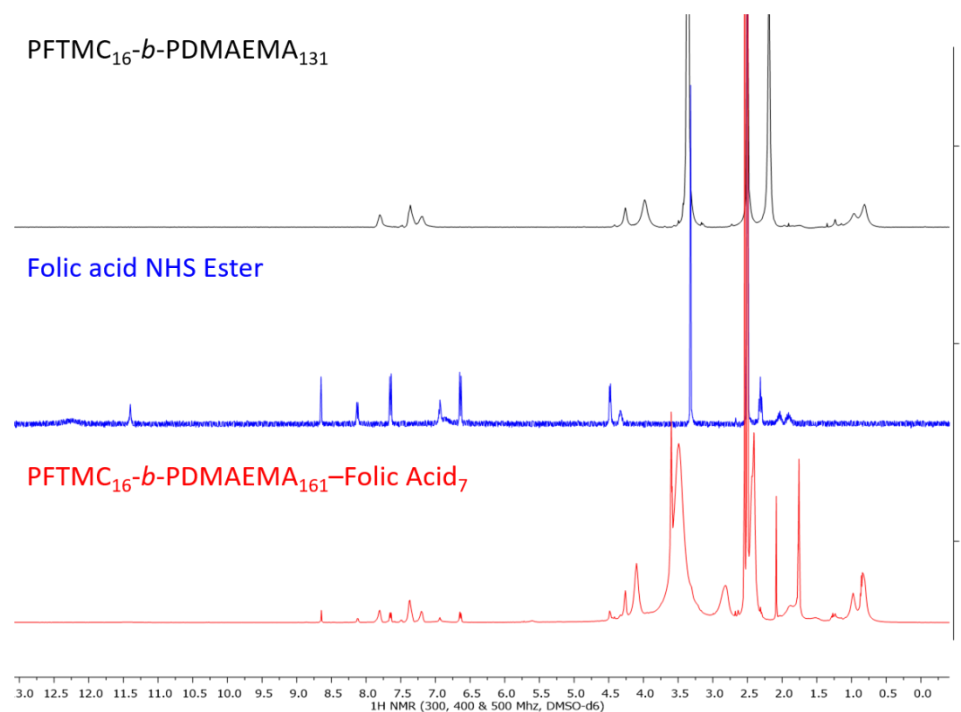
Figure S29. Stacked ^{1}H-NMR spectra of PFTMC$_{16}$-b-PDMAEMA$_{131}$ (**P1**, black trace), folic acid NHS ester (blue trace) and PFTMC$_{16}$-b-PDMAEMA$_{158}$-FA$_7$ (**P3**, red trace) in DMSO-d_6 (500 MHz).

Table S1. Molecular weight, composition, and characterization of the polymers studied in this work. BD = BODIPY[630/650-X], and FA = folic acid.

Name	Polymer	M_n (g/mol) via GPC	M_w (g/mol) via GPC	$Đ_M$ via GPC	M_n (g/mol) via NMR	PFTMC DP_n via NMR	PDMAEMA DP_n via NMR	M_n (g/mol) via MALDI-TOF	PFTMC DP_n via MALDI-TOF
	PFTMC$_{16}$-CTA	3,700	4,300	1.17	5,300	20	-	4,359	16
	PFTMC$_{16}$-b-(PDMAEMA · HCl)$_{124}$	-	-	-	28,300	16[a]	124	-	-
P1	PFTMC$_{16}$-b-PDMAEMA$_{131}$	9,700	15,000	1.55	24,900	16	131	-	-
	PDMAEMA$_{249}$	63,100	73,900	1.17	39,400	-	249	-	-
P2	PFTMC$_{16}$-b-PDMAEMA$_{158}$-BD	-	-	-	29,700	16[b]	158	-	-
P3	PFTMC$_{16}$-b-PDMAEMA$_{161}$-FA$_7$	-	-	-	32,700	16	161	-	-

[a] End-groups not visible in DMSO-d$_6$, so the DP$_n$ of this block is based on the post-workup DP$_n$ of **P1**.
[b] PFTMC end-group not visible in DMSO-d$_6$, so the DP$_n$ of this block is based on the DP$_n$ of **P1**.
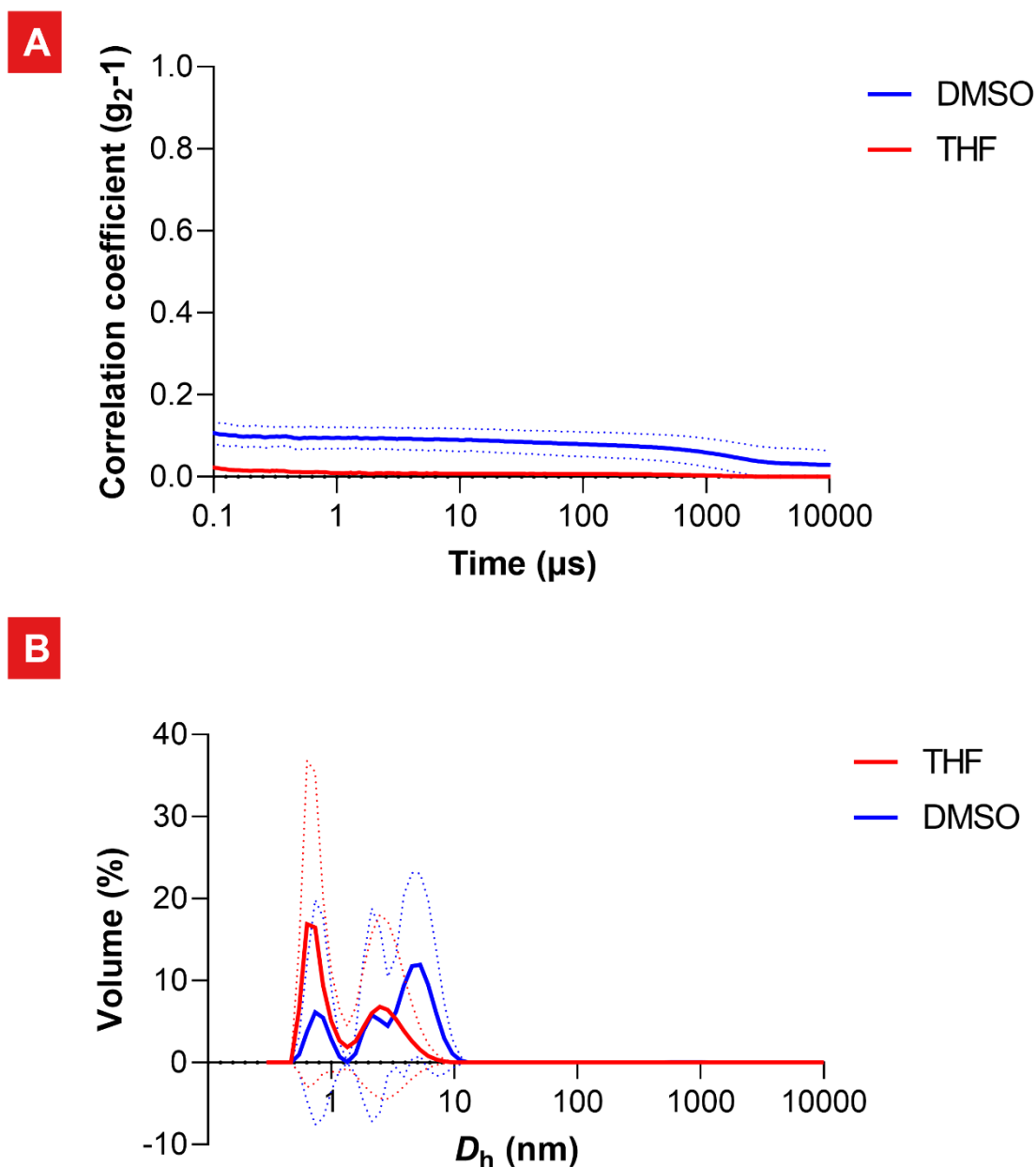
Figure S30. Determination of suitable common solvents for the self-assembly of **P1** via DLS. Samples of **P1** were investigated at 0.1 mg/mL, in THF and DMSO. (A) Correlograms for **P1** in THF (red) and DMSO (blue). The low correlation coefficient (<0.1 g_2-1) indicates weak scattering – a lack of a detectable sample. (B) The associated volume-based size plots for **P1** in THF (red) and DMSO (blue) at 25 °C. Whilst these plots are not reliable due to the weak scattering (observed in A), the sizes obtained were nonetheless less than 10 nm. The volume-based size plots were calculated using polystyrene latex as the material. The average of 5 runs is plotted on the graphs as a solid line, with the 95% confidence interval plotted as dotted lines.
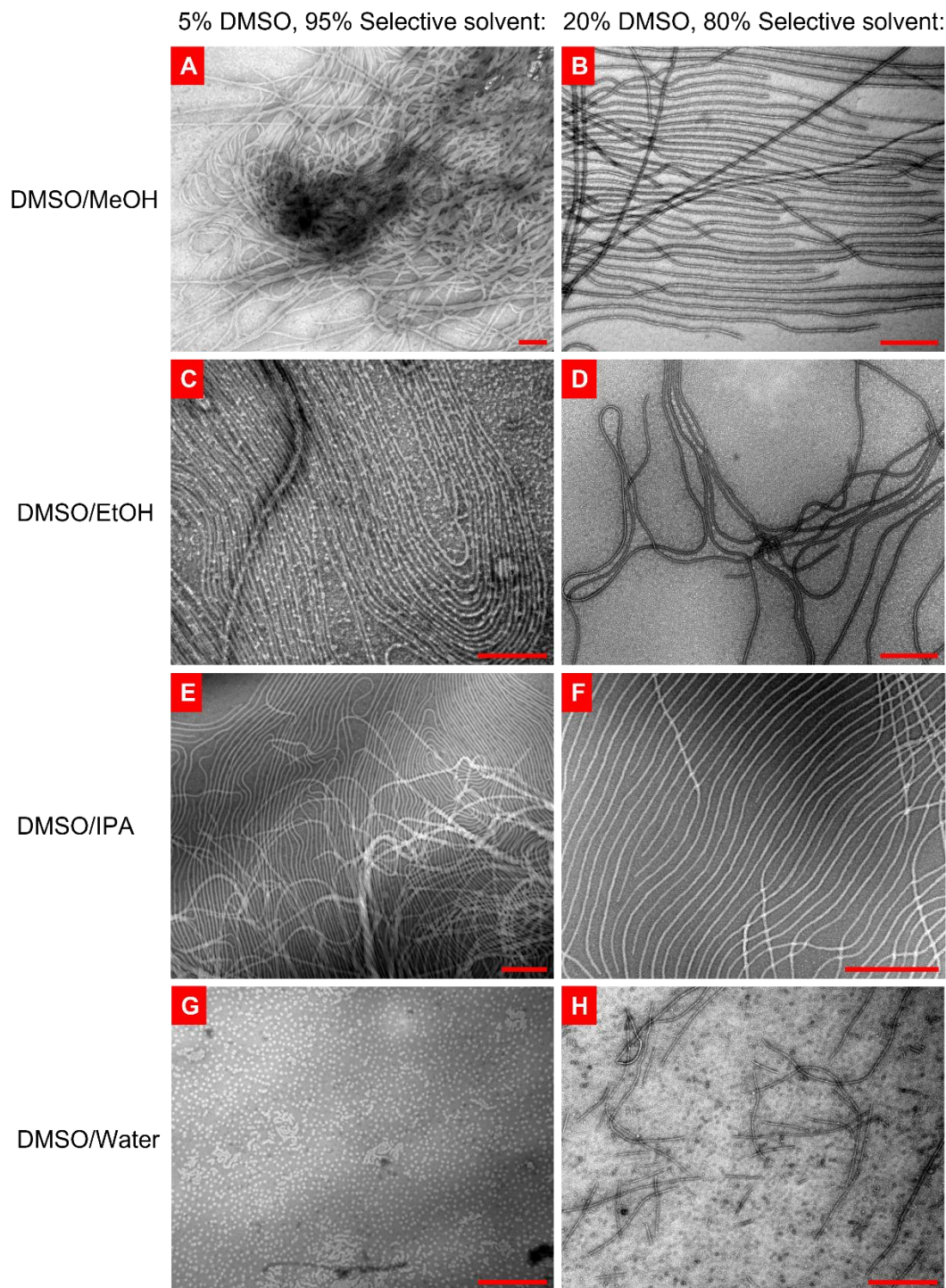
5% DMSO, 95% Selective solvent: 20% DMSO, 80% Selective solvent:

DMSO/MeOH

DMSO/EtOH

DMSO/IPA

DMSO/Water

Figure S31. Conditions screened for the spontaneous self-nucleation of **P1**. TEM micrographs of the assemblies formed after annealing at 70°C for 30 min, using DMSO as a common solvent (at 5%, and 20% *v/v*), and (A-B) MeOH, (C-D) EtOH, (E-F) iPrOH, and (G-H) H_2O as selective solvents for the PDMAEMA corona-forming block. Scale bars = 500nm. All samples were stained with uranyl acetate (3 wt% in EtOH).

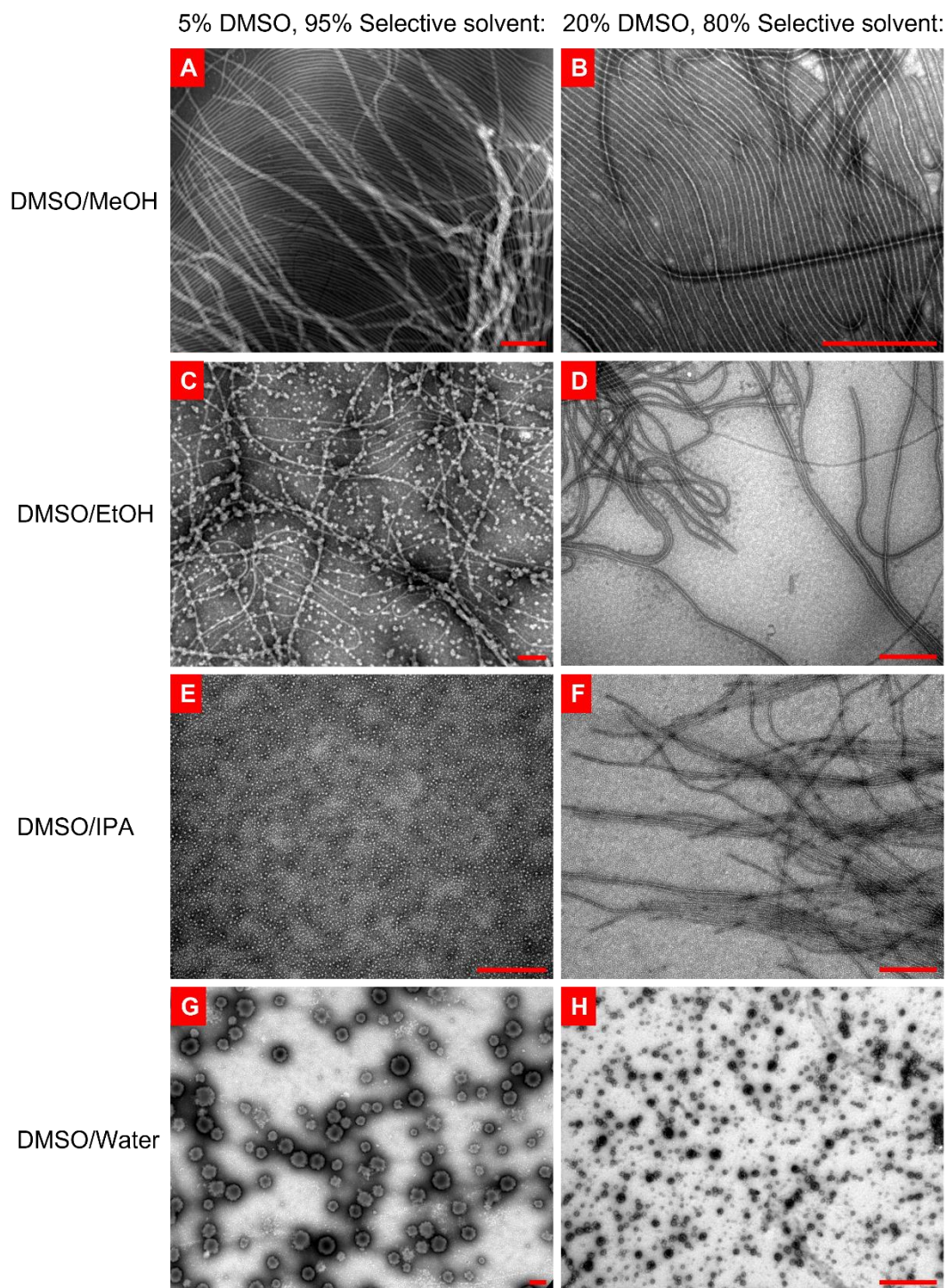5% DMSO, 95% Selective solvent: 20% DMSO, 80% Selective solvent:

Figure S32. Conditions screened for the spontaneous self-nucleation of **P1**. TEM micrographs of the assemblies formed after mixing at 23°C, using DMSO as a common solvent (at 5%, and 20% *v/v*), and (A-B) MeOH, (C-D) EtOH, (E-F) iPrOH, and (G-H) H_2O as selective solvents for the PDMAEMA corona-forming block. Scale bars = 500nm. All samples were stained with uranyl acetate (3 wt% in EtOH).
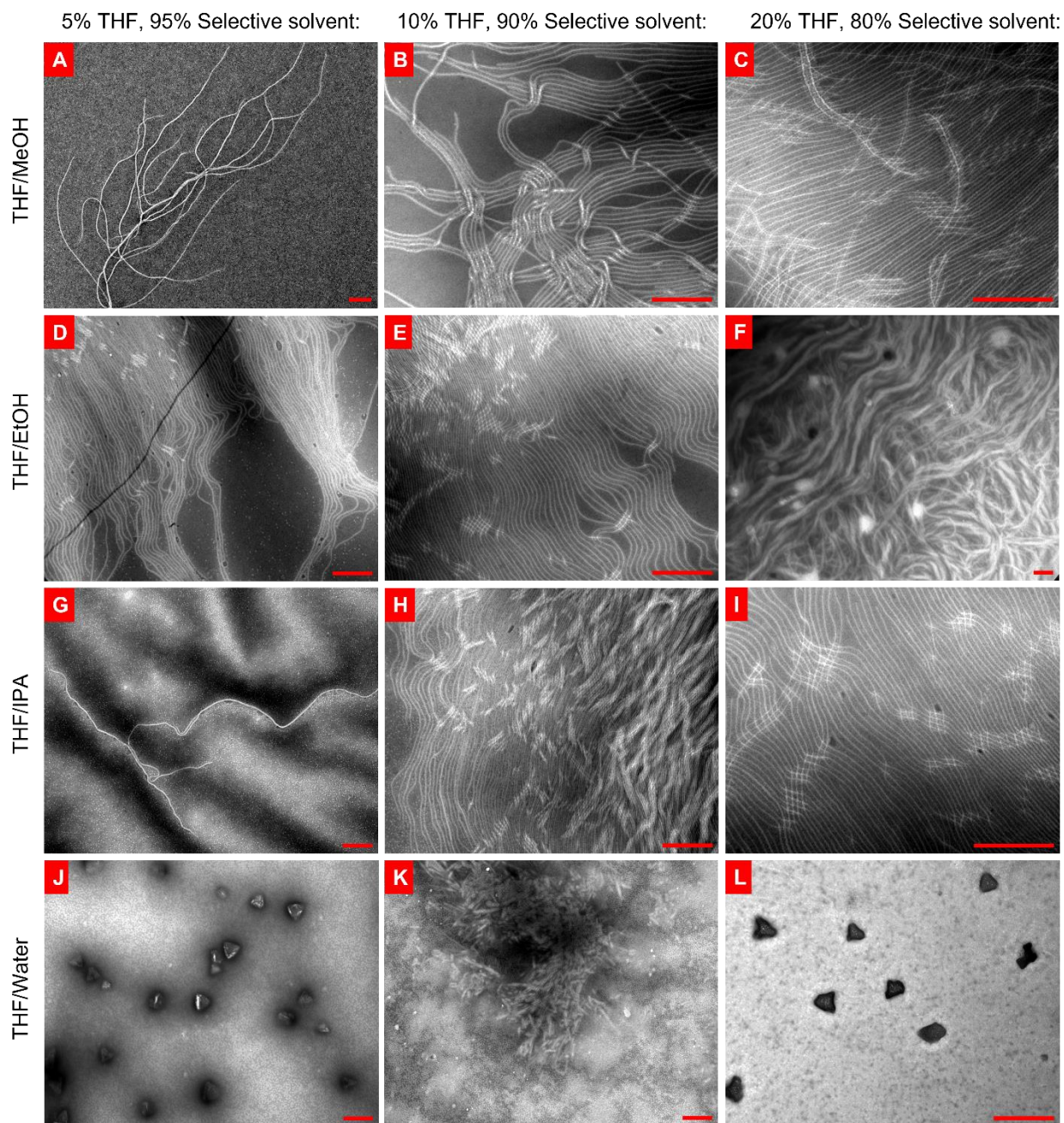
Figure S33. Conditions screened for the spontaneous self-nucleation of **P1**. TEM micrographs of the assemblies formed after annealing at 70°C for 30 min, using THF as a common solvent (at 5%, 10%, and 20% *v/v*), and (A-C) MeOH, (D-F) EtOH, (G-I) iPrOH, and (J-L) H$_2$O as selective solvents for the PDMAEMA corona-forming block. Scale bars = 500nm. All samples were stained with uranyl acetate (3 wt% in EtOH).
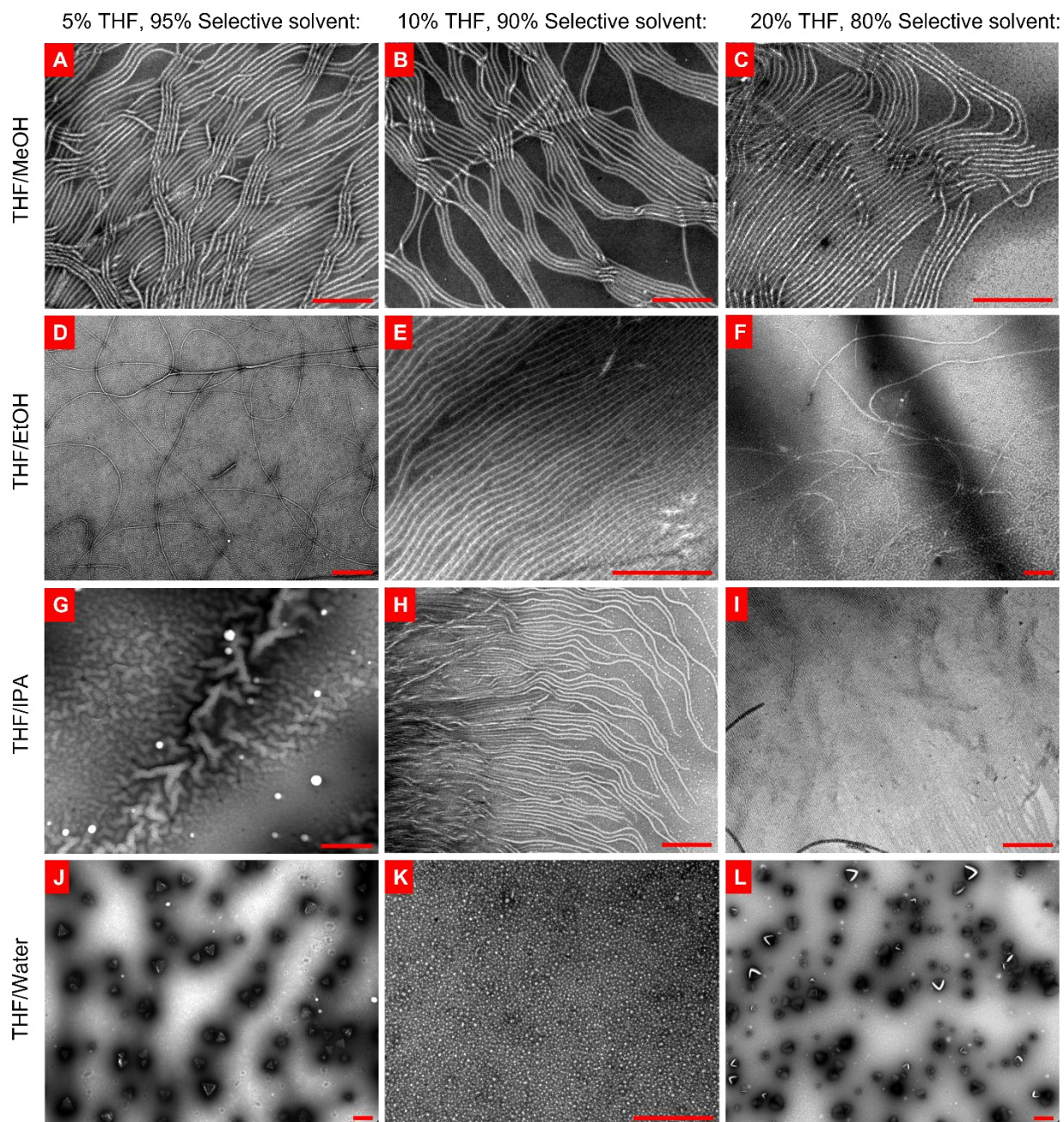
Figure S34. Conditions screened for the spontaneous self-nucleation of **P1**. TEM micrographs of the assemblies formed after mixing at 23°C, using THF as a common solvent (at 5%, 10%, and 20% *v/v*), and (A-C) MeOH, (D-F) EtOH, (G-I) iPrOH, and (J-L) H_2O as selective solvents for the PDMAEMA corona-forming block. Scale bars = 500nm. All samples were stained with uranyl acetate (3 wt% in EtOH).
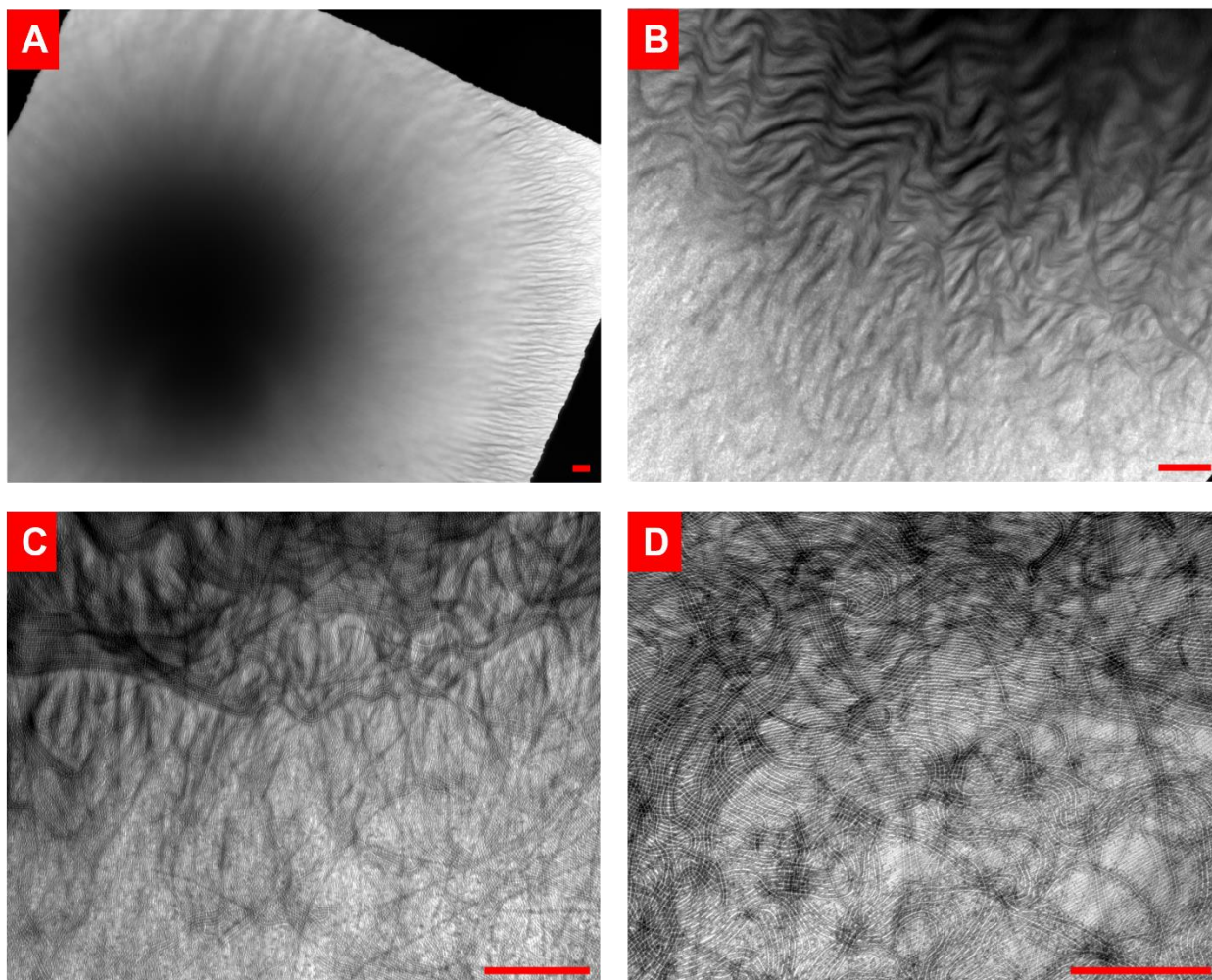
Figure S35. Example of large (10 – 50 µm) spherical supermicelle aggregates of disperse **P1** nanofibers. This sample was prepared in THF/EtOH (10:90 *v/v*) after annealing at 70°C for 30 min. (A-D) increasing magnification of a single supermicelle aggregate. Scale bars = 1000nm. All samples were stained with uranyl acetate (3 wt% in EtOH).
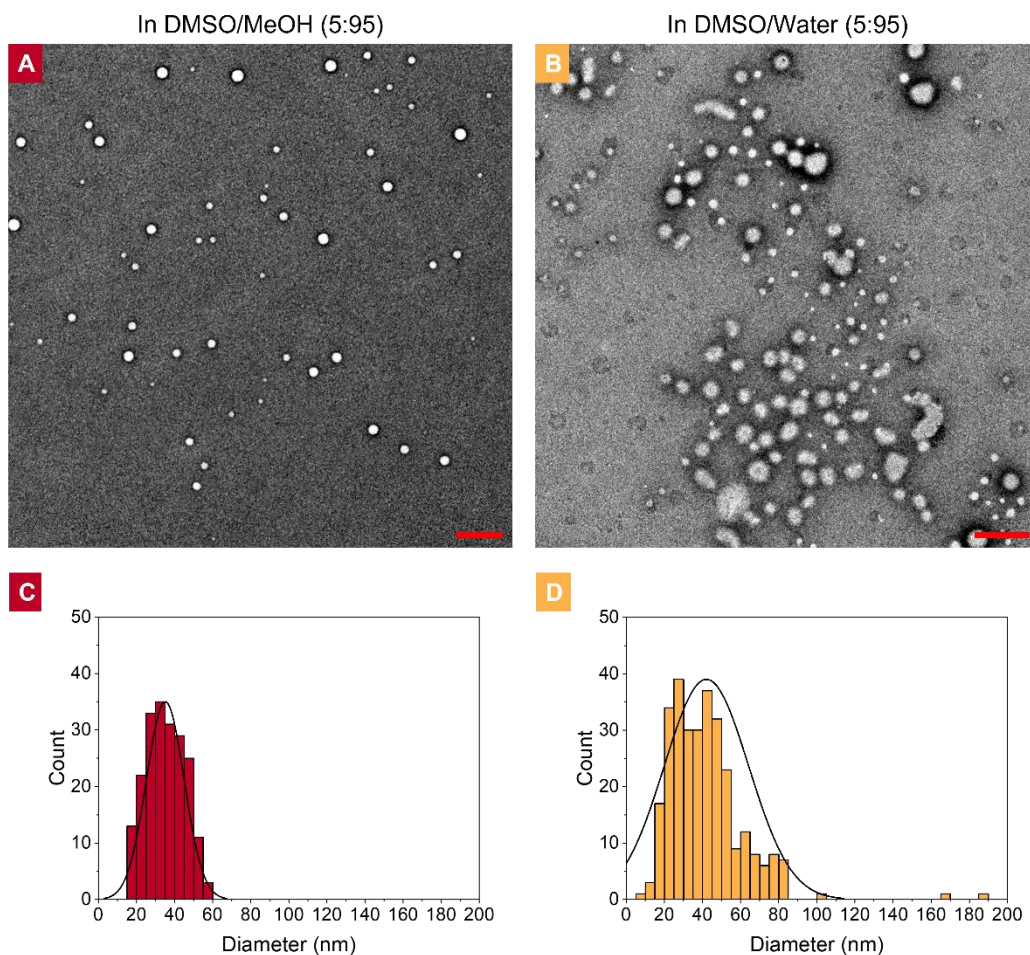
Figure S36. Nanospheres formed from the spontaneous self-nucleation of PFTMC$_{16}$-*b*-(PDMAEMA · HCl)$_{124}$. TEM micrographs of the assemblies formed after annealing at 70°C for 30 min, using DMSO as a common solvent, and (A) MeOH, or (B) H$_2$O as selective solvents. (C-D) Histograms of the diameter of the particles in (C) A (D_n = 35 nm, Đ$_D$ = 1.08, σ = 10 nm), and (D) B (D_n = 42 nm, Đ$_D$ = 1.28, σ = 22 nm). Scale bars = 200nm. Both samples were stained with uranyl acetate (3 wt% in EtOH).
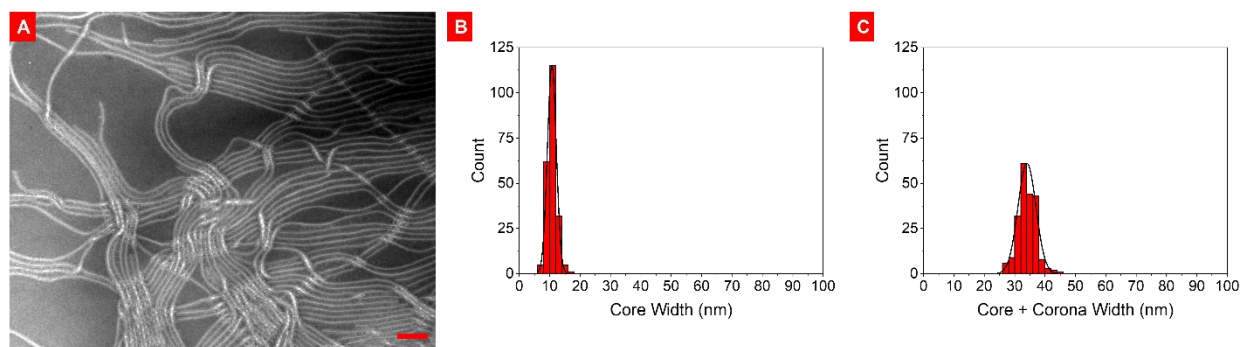
Figure S37. (A) TEM micrograph and (B-C) contour width histograms of the disperse **P1** nanofibers formed in THF/MeOH (10:90 *v/v*) after annealing at 70°C for 30 min. (B) the width of the PFTMC nanofiber core ($W_n = 11$ nm, $Đ_W = 1.02$, $\sigma_W = 1$ nm) and (C) the overall nanofiber width, that is the nanofiber core + corona ($W_n = 34$ nm, $Đ_W = 1.01$, $\sigma_W = 3$ nm). This equated to a corona width of ca. 12nm. For reference, a fully extended carbon chain 262 atoms long (for PDMAEMA$_{131}$) would be expected to be ca. 40 nm based on a C-C bond length of 0.154 nm. Thus, the PDMAEMA$_{131}$ corona appears to be in a contracted state after drying, roughly 3.3 times shorter than its fully extended length. Scale bar = 200nm. The sample was stained with uranyl acetate (3 wt% in EtOH).
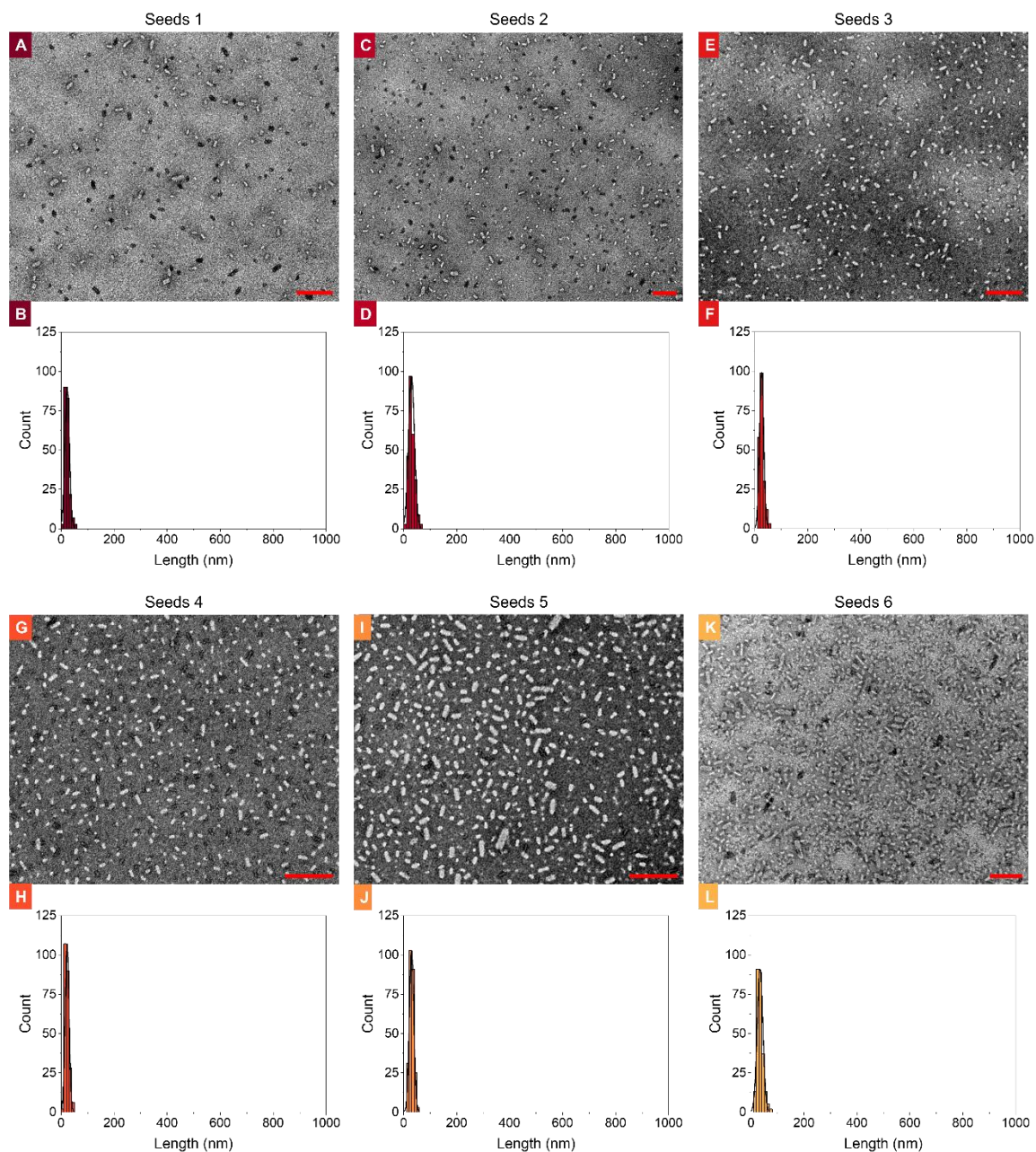
Figure S38. P1 seed nanofibers used to produce length-controlled nanofibers. (A, C, E, G, I, K) TEM micrographs and (B, D, F, H, J, L) contour length histograms of: (A-B) **seeds 1** (THF/MeOH 5:95 *v/v*, 1 mg/mL, 2 step procedure); (C-D) **seeds 2** (DMSO/MeOH 20:80 *v/v*, 1 mg/mL, 2 step procedure); (E-F) **seeds 3** (THF/MeOH 5:95 *v/v*, 1 mg/mL, 1 step procedure); (G-H) **seeds 4** (THF/MeOH 5:95 *v/v*, 10 mg/mL, 1 step procedure); (I-J) **seeds 5** (THF/MeOH 20:80 *v/v*, 10 mg/mL, 1 step procedure); (K-L) **seeds 6** (THF/MeOH 10:90 *v/v*, 10 mg/mL, 2 step procedure). Length and dispersity data is in Table S2. Scale bars = 200nm. All samples were stained with uranyl acetate (3 wt% in EtOH).
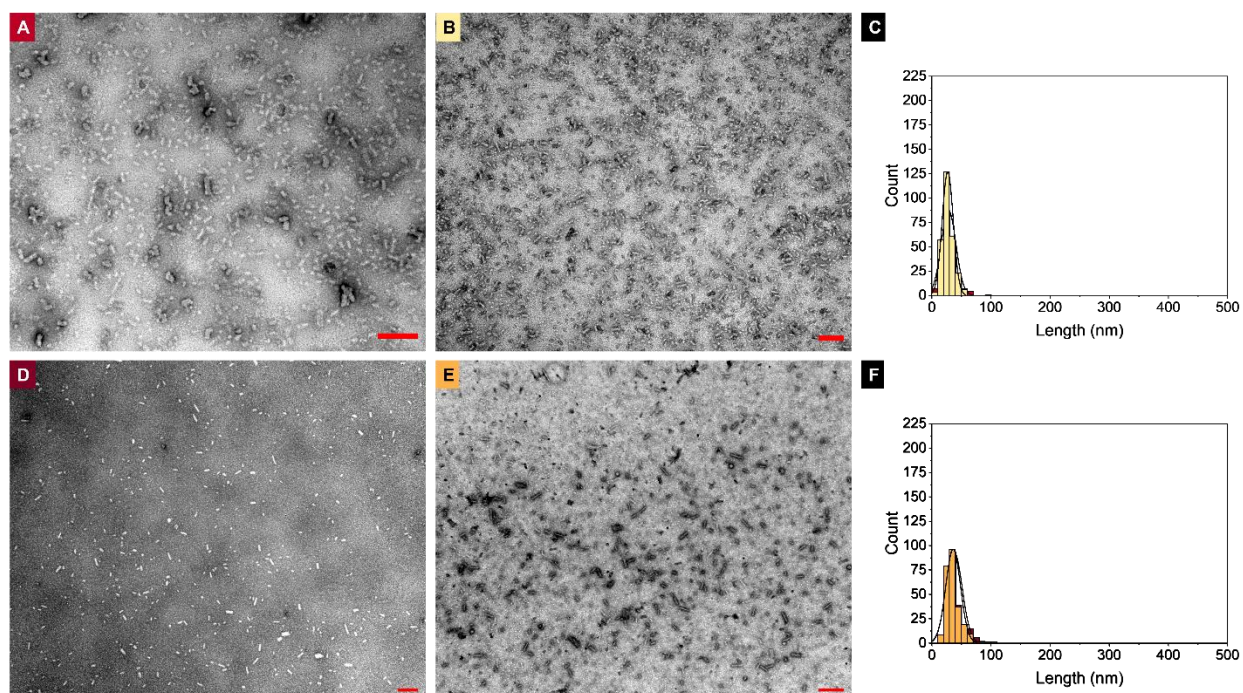
Figure S39. P1 nanofibers **seeds 7** and **seeds 8** transferred into water. (A-B) TEM micrographs of **seeds 7** in (A) THF/MeOH (10:90 *v/v*, 2 step procedure) and (B) after dialysis into H_2O; (C) contour length histograms of **seeds 7** in A-B; (D-E) TEM micrographs of **seeds 8** in (D) THF/MeOH (10:90 *v/v*, 2 step procedure) and (E) after transfer into H_2O; (F) contour length histograms of **seeds 7** in D-E. Length and dispersity data is in Table S2. Scale bars = 200nm. All samples were stained with uranyl acetate (3 wt% in EtOH).
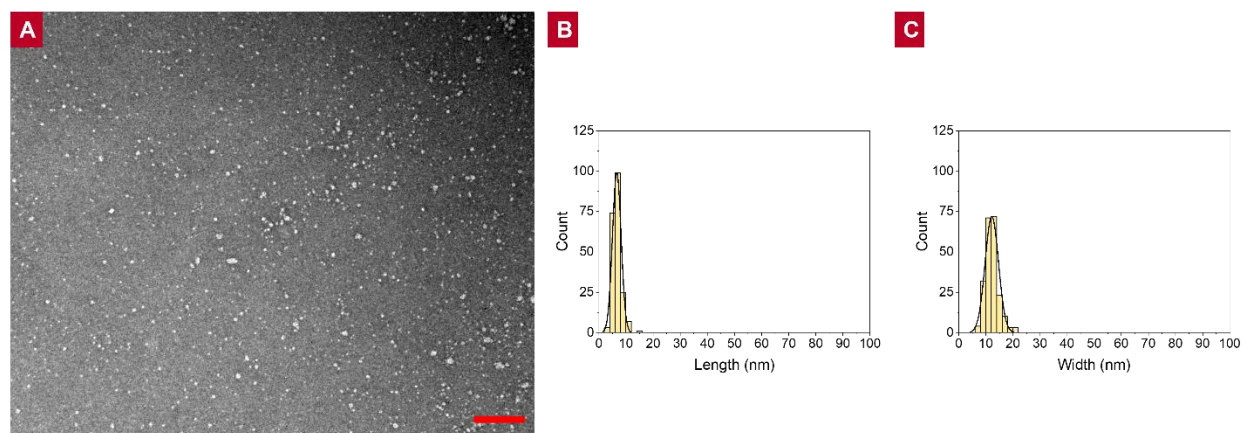

Figure S40. P1 nanofiber **seeds 7b** after **seeds 7** were further sonicated for 3 h in water (sample was aged for 7 months at 25°C between transfer to water and sonication). (A) TEM micrograph of **seeds 7b** in water; (B) contour length histogram of **seeds7b** ($L_n = 7$ nm, $Đ_L = 1.06$, $\sigma_L = 2$ nm) and (C) contour width histogram of **seeds7b** ($W_n = 12$ nm, $Đ_W = 1.04$, $\sigma_W = 2$ nm). Length and

dispersity data is also in Table S2. Scale bars = 200nm. All samples were stained with uranyl acetate (3 wt% in EtOH).

Table S2. Statistical analysis of the contour lengths and dispersities of the seed nanofibers studied in this work, produced from PFTMC$_{16}$-b-PDMAEMA$_{131}$ (**P1**).

TEM Micrograph	Label	n	L_n (nm)	L_w (nm)	$Đ_L$	σ (nm)	σ / L_n	Sonication time
S38-A	**seeds 1**	208	22	26	1.15	9	0.38	3 h
S38-C	**seeds 2**	249	29	34	1.15	11	0.38	10 h
S38-E	**seeds 3**	202	25	28	1.10	8	0.32	3 h
S38-G	**seeds 4**	233	22	25	1.11	7	0.33	3 h
S38-I	**seeds 5**	253	30	32	1.08	8	0.28	3 h
S38-K	**seeds 6**	250	34	37	1.10	11	0.32	3 h 45 min
S39-A	**seeds 7**	234	28	33	1.20	12	0.45	3 h
S39-B	**seeds 7**[a]	277	27	30	1.12	9	0.35	n/a
S39-D	**seeds 8**	246	37	42	1.14	14	0.37	3 h
S39-E	**seeds 8**[a]	252	36	41	1.12	12	0.34	n/a
S40-A	**seeds 7b**[b]	209	7	7	1.06	2	0.24	3 + 3 h[b]

[a] This sample is in H$_2$O.

[b] This sample resulted from the sonication of **seeds7** in H$_2$O for a further 3 h, for a total of 6 h sonication time.
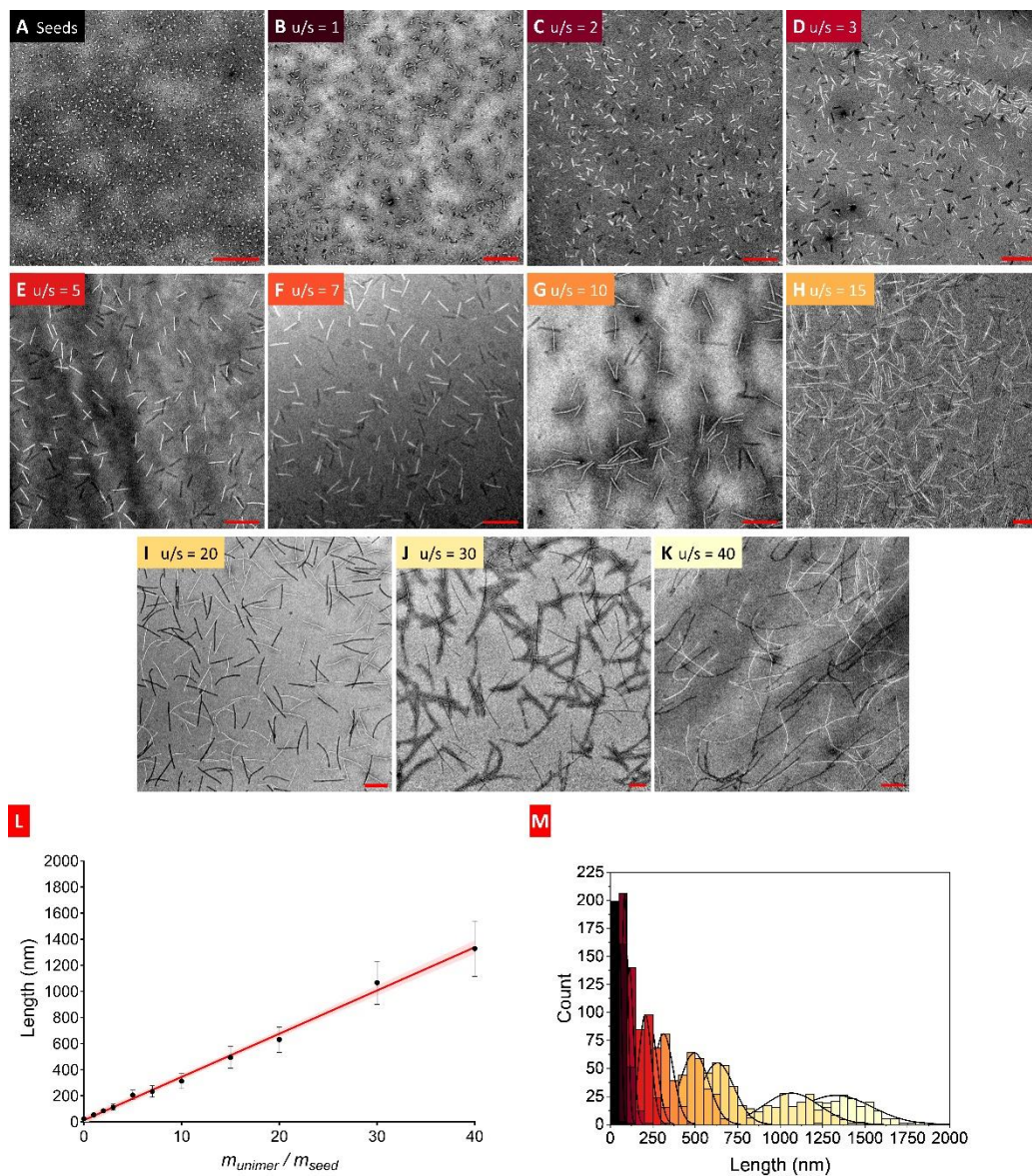
Figure S41. Preparation of low dispersity **P1** nanofibers of controlled lengths via living CDSA. (A) TEM micrographs of seed nanofibers **seeds3** (L_n = 25 nm, L_w/L_n = 1.10, σ = 8 nm) prepared via the one-step self-assembly and fragmentation of **P1**; (B-K) TEM micrographs of low dispersity nanofibers prepared at varied m_{unimer} / m_{seed} (u/s) ratios: (B) u/s = 1, (C) u/s = 2, (D) u/s = 3, (E) u/s = 5, (F) u/s = 7, (G) u/s = 10, (H) u/s = 15, (I) u/s = 20, (J) u/s = 30, (K) u/s = 40; (L) Plot of m_{unimer} / m_{seed} against L_n, highlighting the linear dependence of nanofiber length upon the m_{unimer} / m_{seed} ratio, with σ represented as the light red region; (M) Contour length histograms of the nanofibers in A-K, colour coded to the corresponding TEM images. Nanofibers were prepared in THF:MeOH (20:80 *v/v*) after mixing at room temperature. Scale bars = 500nm. All samples were stained with uranyl acetate (3 wt% in EtOH). For precise length data, see Table S3.

Table S3. Statistical analysis of the contour lengths and dispersities of the length-controlled nanofibers in Figure S41, produced via living CDSA from **P1**.

TEM Micrograph	m_{unimer} / m_{seed}	n	L_n (nm)	L_w (nm)	$Đ_L$	σ (nm)	σ / L_n	L_n / eq. (nm)[a]
S41A	0 (seeds)	202	25	28	1.10	8	0.32	25
S41B	1	265	54	57	1.05	12	0.22	27
S41C	2	206	85	89	1.05	19	0.22	28
S41D	3	226	112	117	1.05	24	0.22	28
S41E	5	224	206	212	1.03	37	0.18	34
S41F	7	225	233	241	1.03	43	0.19	29
S41G	10	227	313	324	1.03	57	0.18	28
S41H	15	261	495	509	1.03	83	0.17	31
S41I	20	262	631	646	1.02	98	0.16	30
S41J	30	201	1067	1092	1.02	165	0.16	34
S41K	40	218	1328	1362	1.02	212	0.16	32

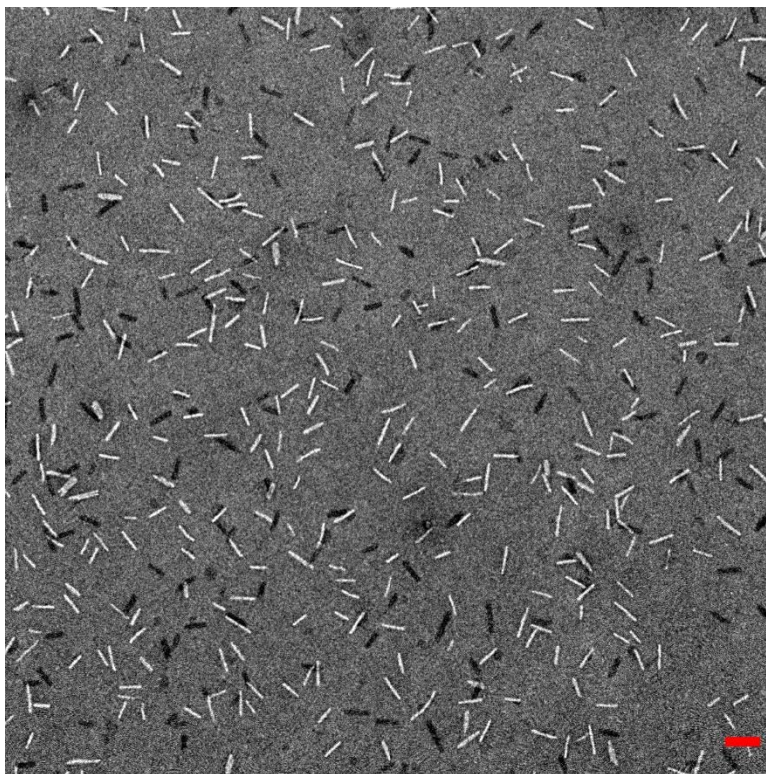[a] This is the length per equivalent of unimer added.

Figure S42. TEM micrograph of the low-dispersity **P1** nanofibers (L_n = 127 nm, $Đ_L$ = 1.03, σ = 23 nm) used for the AFM height analysis in Figure 4. The sample was prepared in THF:MeOH (20:80 *v/v*). Scale bar = 200nm. The sample was stained with uranyl acetate (3 wt% in EtOH).
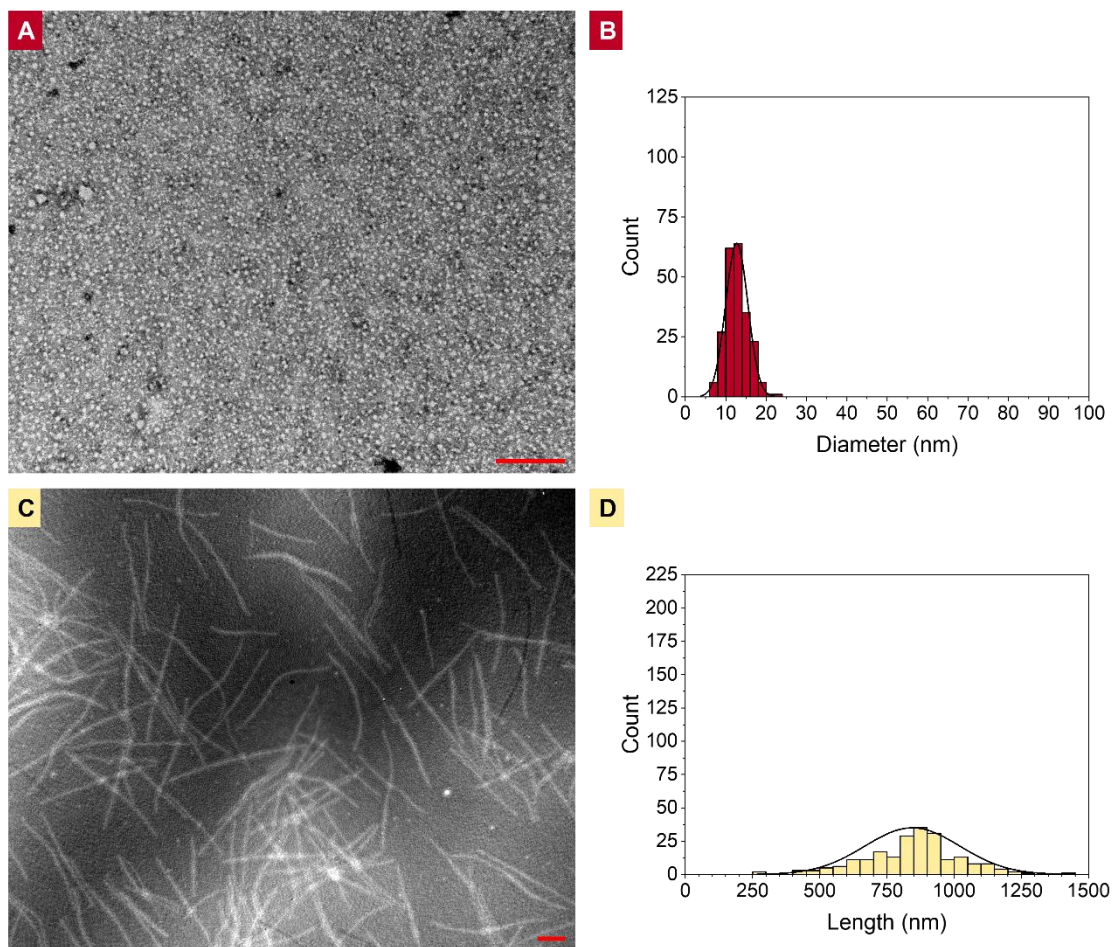
Figure S43. Attempted seeded growth from **P1** nanofiber **seeds 7b** ($L_n = 7$ nm, $Đ_L = 1.06$, $\sigma_L = 2$ nm) in (A-B) water and (C-D) THF/MeOH (5:95 v/v). (A) TEM micrograph of spherical micelles / small nanofiber fragments found upon addition of **P1** unimer to **seeds 7b** in water; (B) contour diameter histogram for the fragments/nanospheres observed ($D_n = 13$ nm, $Đ_D = 1.05$, $\sigma_D = 3$ nm); (C) TEM micrograph of nanofibers found upon addition of **P1** unimer to **seeds 7b** in THF/MeOH (5:95 v/v); (D) contour length histogram for the nanofibers ($L_n = 844$ nm, $Đ_L = 1.04$, $\sigma_L = 177$ nm). Scale bars = 200nm. All samples were stained with uranyl acetate (3 wt% in EtOH).
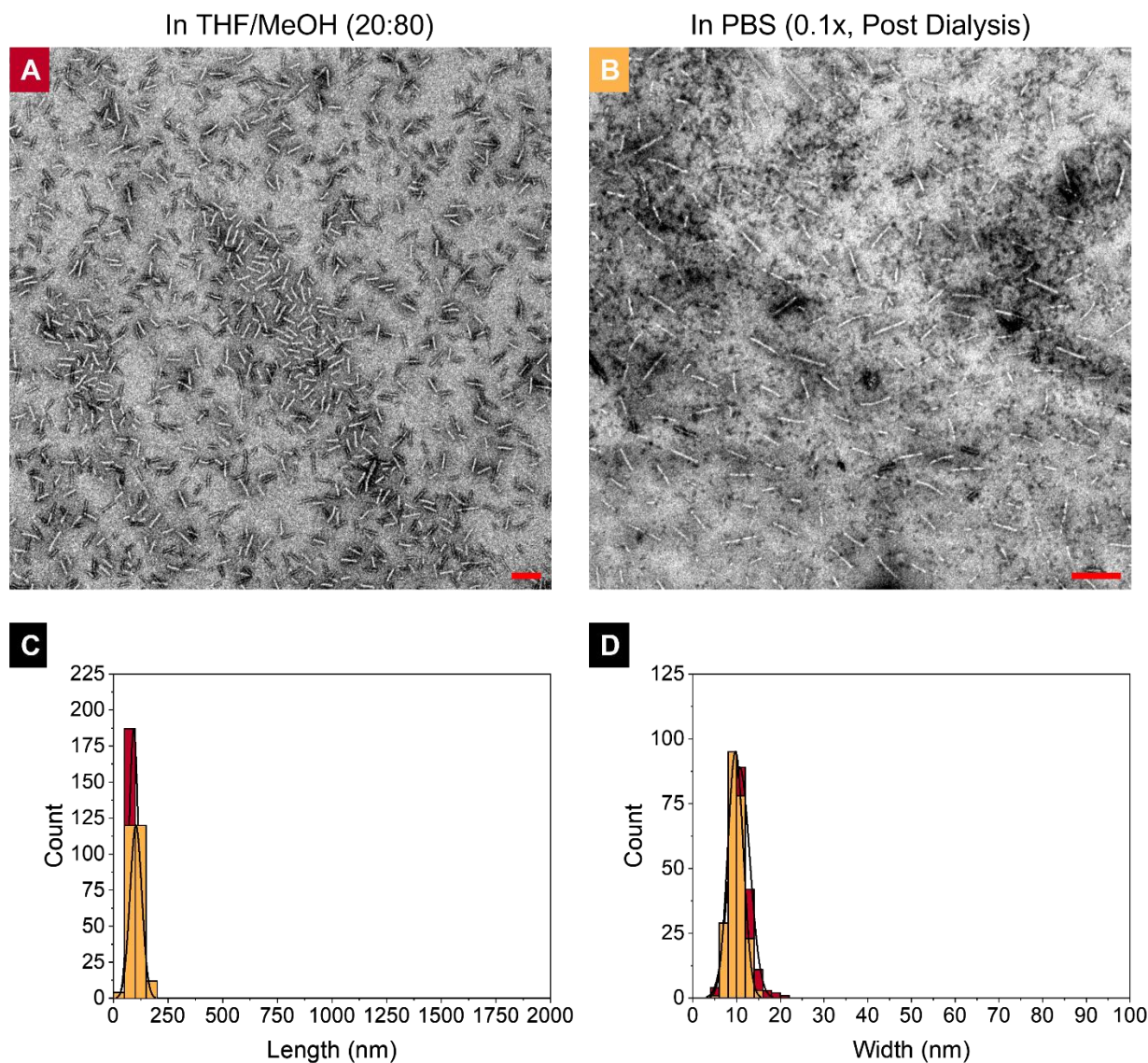
Figure S44. 103 nm low-dispersity length-controlled **P1** nanofibers used for biodegradability, stability, and cytotoxicity studies. (A-B) TEM micrographs of nanofibers in (A) THF/MeOH (20:80), and (B) in PBS after dialysis (diluted to 0.1x PBS for TEM analysis); (C) contour length and (D) contour width histograms before transfer into PBS (L_n = 93 nm, $Đ_L$ = 1.05, σ = 22 nm, W_n = 11 nm, $Đ_W$ = 1.05, σ = 2 nm) and after transfer into PBS (L_n = 103 nm, $Đ_L$ = 1.07, σ = 27 nm, W_n = 10 nm, $Đ_W$ = 1.03, σ = 2 nm). Scale bars = 200nm. All samples were stained with uranyl acetate (3 wt% in EtOH).
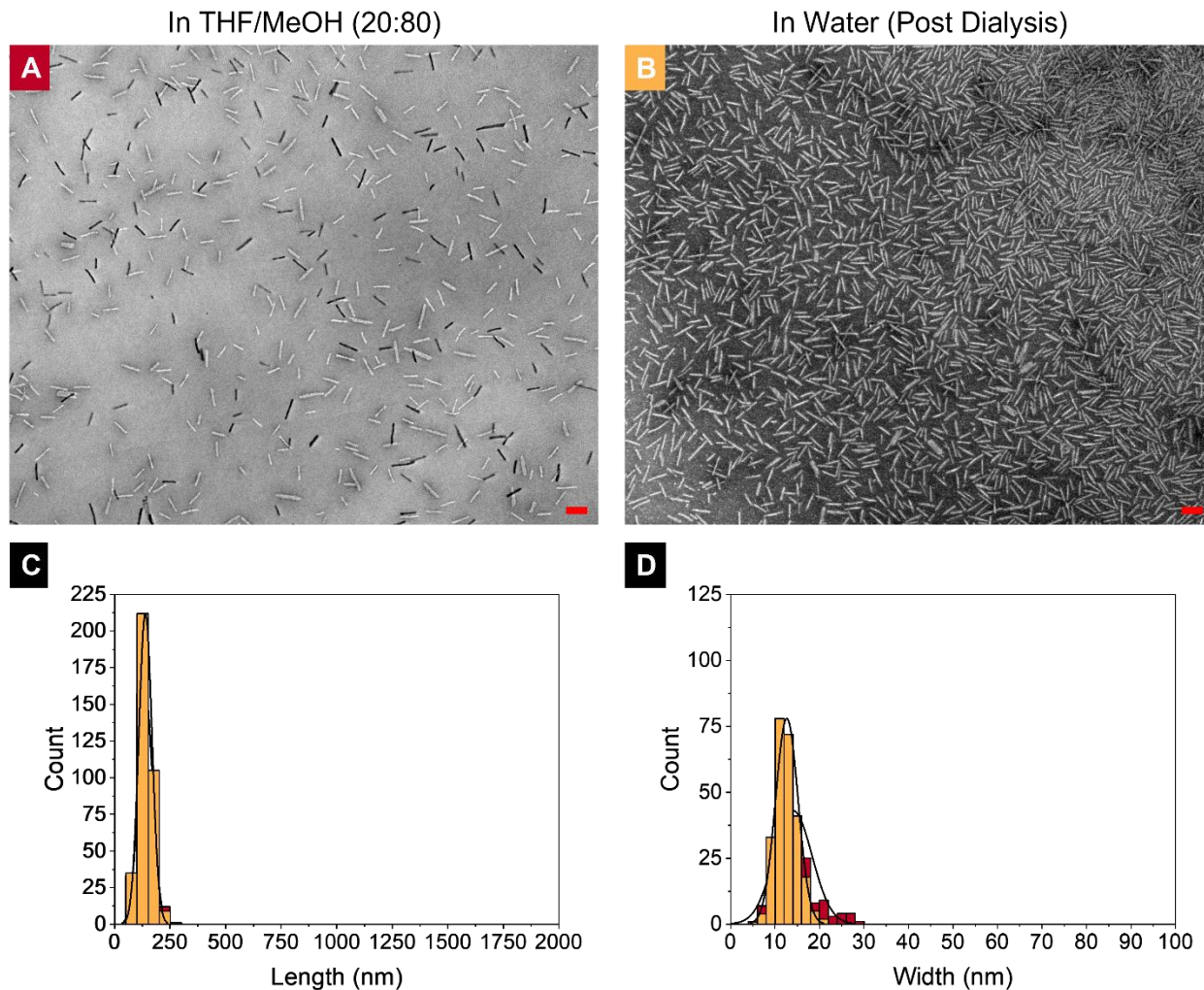
Figure S45. 137 nm low-dispersity length-controlled **P1** nanofibers used for biodegradability and stability studies. (A-B) TEM micrographs of nanofibers in (A) THF/MeOH (20:80), and (B) in water after dialysis; (C) contour length and (D) contour width histograms before transfer into water (L_n = 140 nm, $Đ_L$ = 1.05, σ = 32 nm, W_n = 14 nm, $Đ_W$ = 1.09, σ = 4 nm) and after transfer into water (L_n = 137 nm, $Đ_L$ = 1.05, σ = 30 nm, W_n = 13 nm, $Đ_W$ = 1.04, σ = 3 nm). Scale bars = 200nm. All samples were stained with uranyl acetate (3 wt% in EtOH).
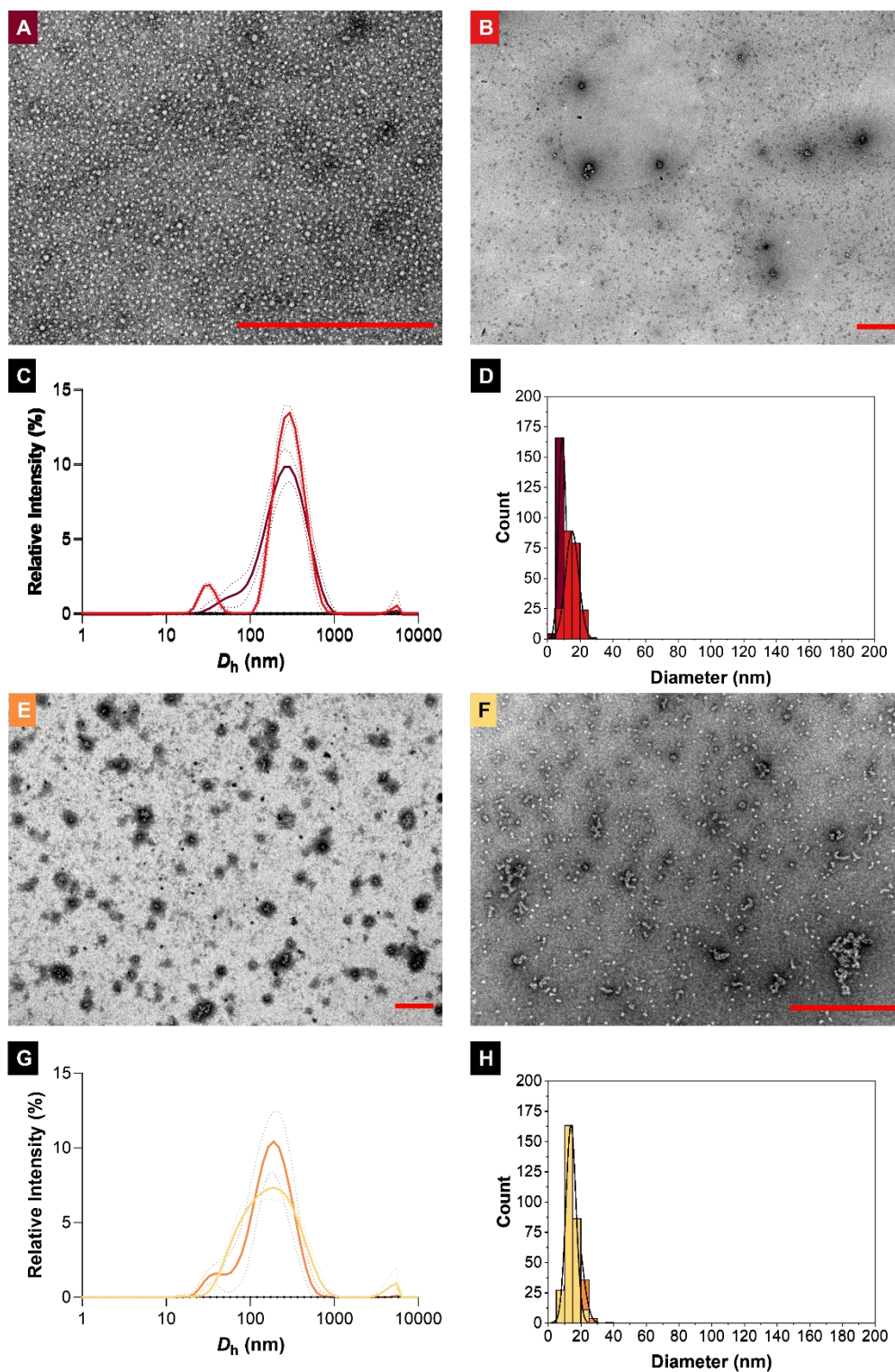
Figure S46. Preparation of **P1** nanospheres via dialysis from (A-D) THF and (E-H) DMSO into water. (A-B, E-F) TEM micrographs of **P1** nanospheres in water. (C, G) DLS intensity-based size distributions for samples in (C) A-B, and (G) E-F. The solid line represents the average of at least

5 repeats, and the dotted lines represent σ; (D, H) contour length histograms of the diameter of the nanospheres measured in (D) A-B and (H) E-F via TEM. Note that data from TEM represents the micelle core diameter not including the corona, whilst data from DLS includes the micelle core and corona. TEM micrographs, DLS plots, and histograms are all colour coded. Scale bars = 500nm. All samples were stained with uranyl acetate (3 wt% in EtOH). For precise measurement data, see Table S4.
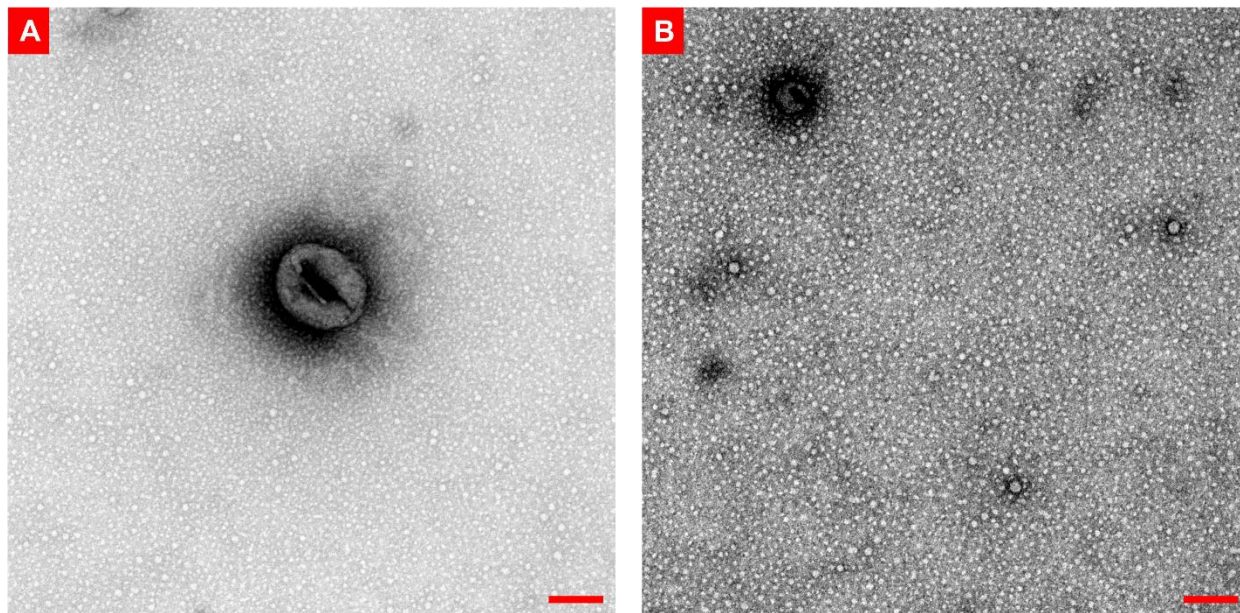

Figure S47. Evidence of larger spherical structures found in some samples of **P1** nanospheres via TEM. (A) High magnification TEM micrograph, and (B) lower magnification TEM micrograph of the larger spherical structures found in a sample of **P1** nanospheres ($D_n = 9$ nm, $Đ_D = 1.06$, $\sigma = 0.3$ nm). Some of these structures appeared to consist of multiple smaller nanospheres, with a resemblance to collapsed vesicles. These larger spherical structures were a small proportion of the sample, and it is unclear if these structures persist in solution. Scale bars = 100nm. All samples were stained with uranyl acetate (3 wt% in EtOH).

Table S4. Summary of the **P1** nanofiber and nanospheres studied in this work, including size analysis and characterization data. Entries 4 and 5 are representative examples of nanospheres prepared through dialysis from either THF (entry 4) or DMSO (entry 5). Error is represented as σ. The L_n and $Đ_L$ values for nanospheres represents the particle diameter. **P1** nanospheres prepared from THF (entry 4) had slightly larger D_h values via DLS than **P1** nanospheres prepared from DMSO (entry 5).

TEM	Morphology	L_n (nm)[a]	$Đ_L$	D_h in THF/MeOH (nm)[b]	D_h in water (nm)[b]	D_h in 5 mM NaCl (nm)[b]	ζ-potential in 5 mM NaCl (mV)
S40A	Nanofiber	7 ± 2	1.06	-	255 ± 70^{c}	193 ± 49^{c}	$+5.8 \pm 1.9$
S39B	Nanofiber	27 ± 9	1.12	-	85 ± 5.1	51 ± 0.9	$+18.6 \pm 0.3$
S39E	Nanofiber	36 ± 14	1.12	-	205 ± 12	195 ± 10	$+19.5 \pm 0.5$
S43B	Nanofiber	103 ± 27	1.07	-	124 ± 7.5^{d}	140 ± 4.7^{d}	$+26.4 \pm 1.1^{d}$
S44B	Nanofiber	137 ± 30	1.05	97 ± 0.7	77 ± 1.3	82 ± 1.4	$+17.6 \pm 0.6$
S45B	Sphere	15 ± 4	1.07	-	222 ± 12	192 ± 8.6	$+20.9 \pm 1.3$
S45F	Sphere	14 ± 3	1.05	-	136 ± 8.3	123 ± 3.3	$+25.5 \pm 0.4$

[a] Recorded via TEM, this represents the core dimensions, not including the corona.
[b] Recorded via DLS, this represents the core + corona dimensions.
[c] These results were recorded 2 weeks after sample preparation.
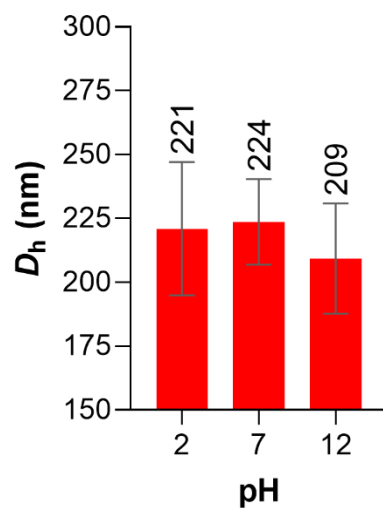[d] These results were recorded 20 months after sample preparation.

Figure S48. The effects of pH upon the hydrodynamic size of 36 nm **P1** nanofibers ($Đ_L = 1.12$, $\sigma = 14$ nm). At pH 2 (20 mM HNO_3 + 10 mM NaCl) and pH 7 (30 mM NaCl), the D_h is consistent, at around 220-225 nm. At pH 12 (20 mM NaOH + 10 mM NaCl), a contraction in D_h to 209 nm is observed that is consistent with a collapse of the PDMAEMA corona that occurs due to deprotonation of the PDMAEMA nitrogen. Data represents the mean of 5 independent runs with the 95% confidence interval (CI) as error.
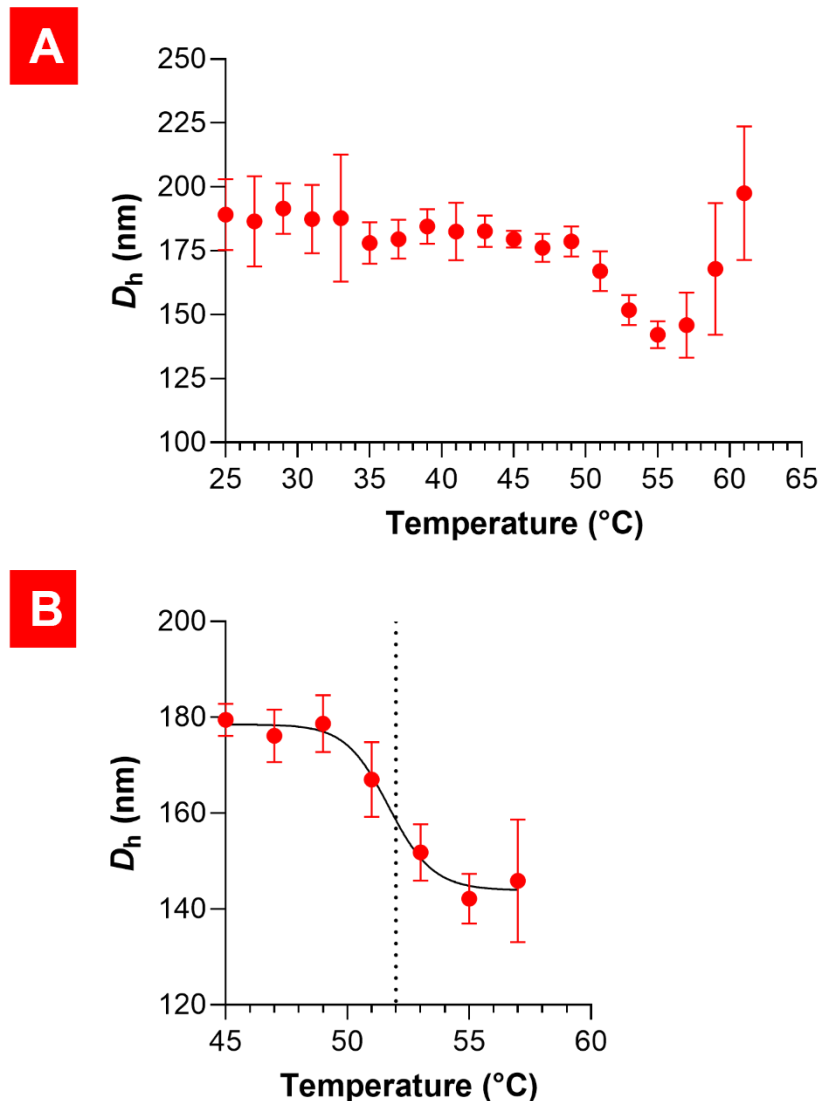
Figure S49. The effects of temperature upon the hydrodynamic size of 36 nm **P1** nanofibers ($Đ_L$ = 1.12, σ = 14 nm). (A) Plot of D_h against temperature. The sample was heated from 25 °C to 61 °C in 2 °C increments, with 2 minutes equilibration time between runs. Data represents the mean of 5 independent runs with the 95% CI as error. The D_h is largely consistent until 49 °C, when a decrease is observed between 49 °C and 55 °C from D_h = 180 nm to D_h = 142 nm. From 55 °C a rapid increase in aggregation is observed. (B) Expansion of the region between 45 °C and 57 °C used to estimate the lower critical solution temperature (LCST). This was performed using the '[inhibitor] vs. response - Variable slope (four parameters)' nonlinear regression analysis in GraphPad Prism 9. The estimated LCST is represented by the dotted line. Error is represented as the 95% CI.
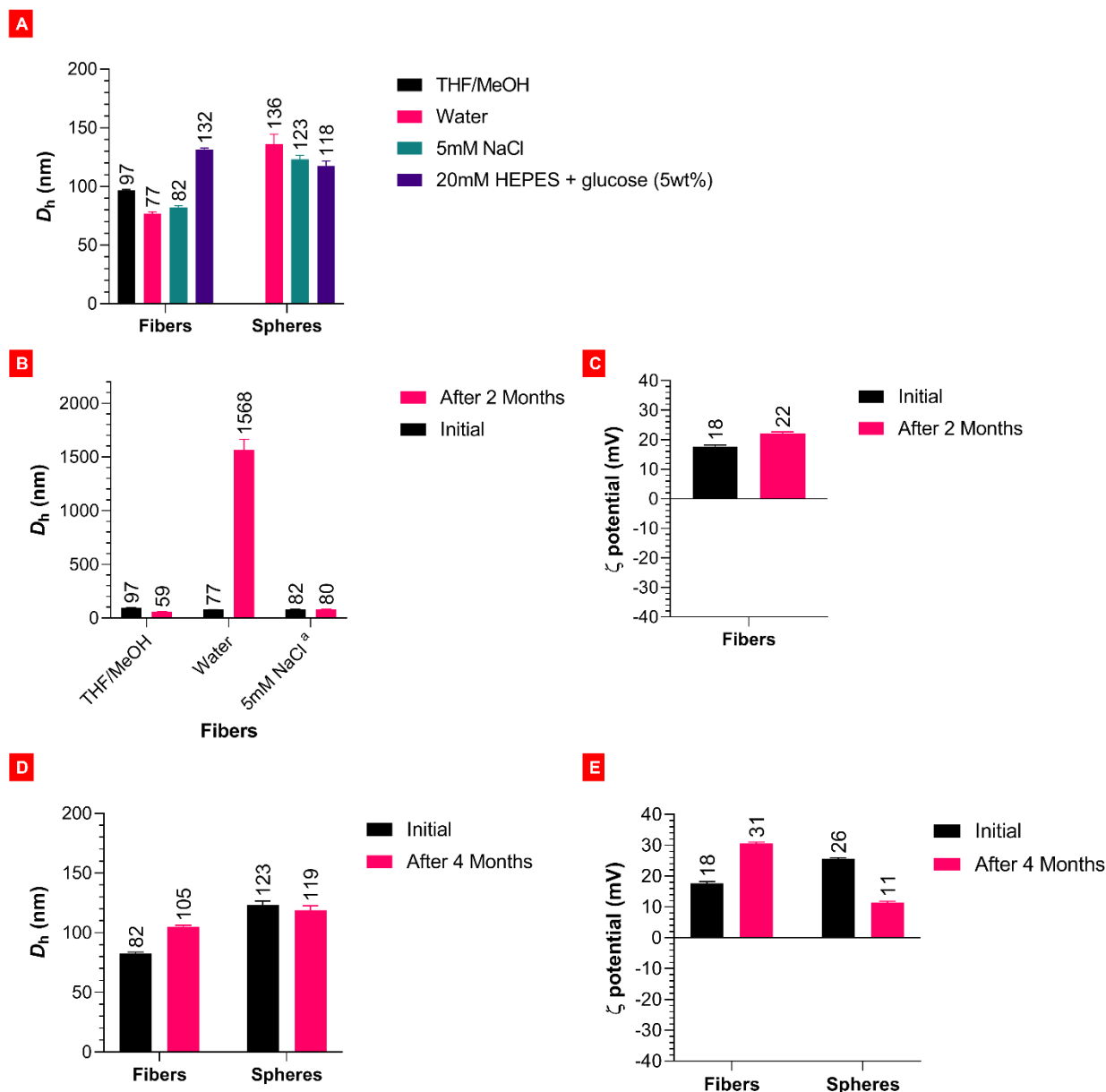
Figure S50. Examination of the colloidal stability and ζ-potential of 137 nm **P1** nanofibers ($Đ_L$ = 1.05, $σ$ = 30 nm) and 14 nm **P1** nanospheres ($Đ_D$ = 1.05, $σ$ = 3 nm) under various conditions via DLS. (A) Examination of the initial D_h of **P1** nanofibers and nanospheres under various solvents and buffers: THF/MeOH (20:80), water, 5mM NaCl, and 20 mM HEPES + glucose (5 wt%) pH 7.4 (HBG); (B) Changes in the D_h of 137 nm **P1** nanofibers over 2 months under various solvent conditions: THF/MeOH (20:80), water and 5mM NaCl; (C) Changes in the ζ-potential of 137 nm **P1** nanofibers over a 2 month period, in 5mM NaCl; (D-E) Changes in (D) the D_h and (E) the ζ-potential of 137 nm **P1** nanofibers and 14 nm **P1** nanospheres over a 4 month period in 5mM NaCl.
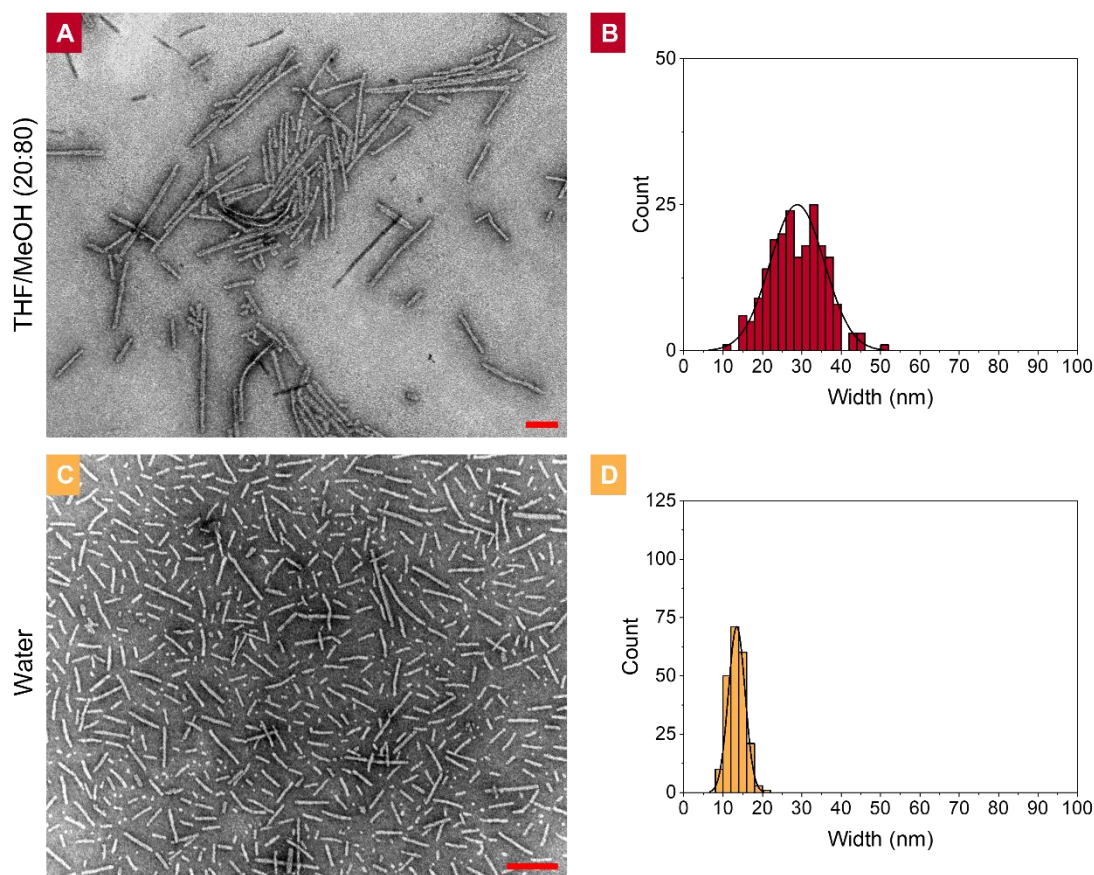
Figure S51. (A, C) TEM micrographs of the same **P1** nanofibers in (A) THF/MeOH (20:80 *v/v*) and (C) in water after 2 years of storage at 23°C; (B, D) Contour width histograms for (B) A (W_n = 29 nm, $Đ_W$ = 1.06, σ_W = 7 nm) and (D) B (W_n = 13 nm, $Đ_W$ = 1.02, σ_W = 2 nm). Scale bars = 200nm. Both samples were stained with uranyl acetate (3 wt% in EtOH). Contour length histograms for these samples are in Figure 6.
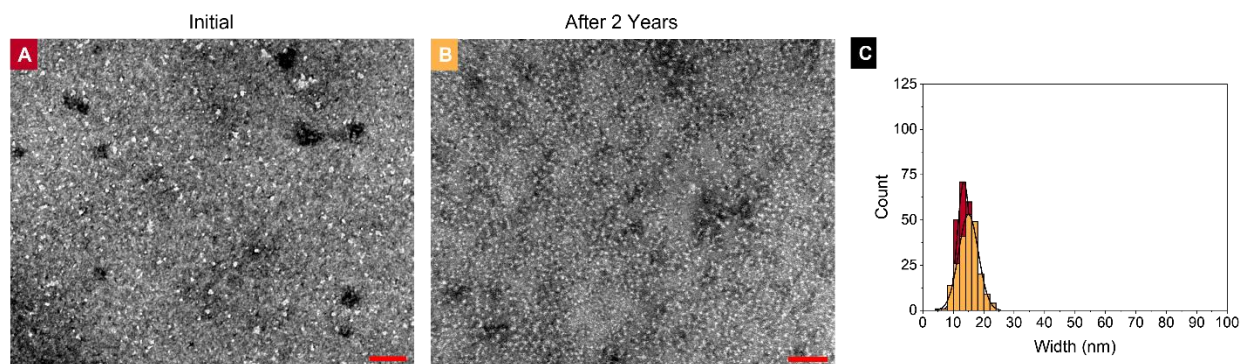

Figure S52. TEM micrographs of **P1** nanospheres in water either (A) initially, or (B) after 2 years of storage at 23°C; (C) Diameter histograms for A (D_n = 16 nm, $Đ_D$ = 1.08, σ = 5 nm, in red) and

B (D_n = 15 nm, $Đ_D$ = 1.05, $σ$ = 3 nm, in yellow). Scale bars = 200nm. Both samples were stained with uranyl acetate (3 wt% in EtOH).
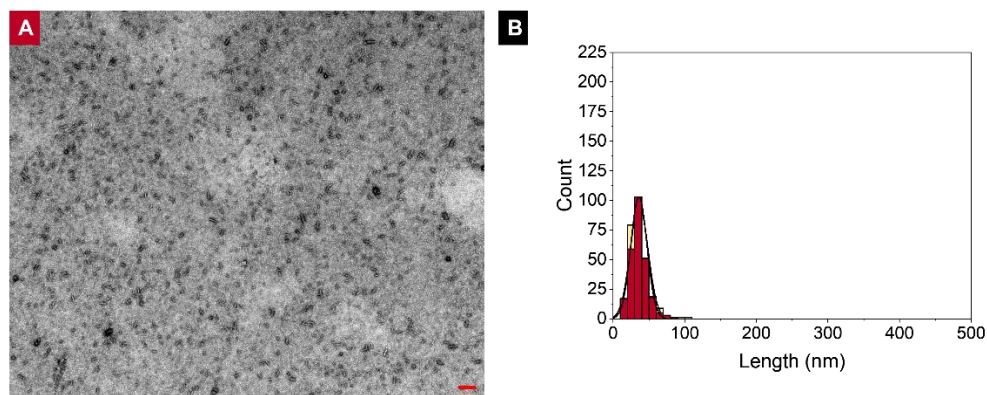

Figure S53. (A) TEM micrograph of **P1** nanofiber **seeds 8** after lyophilization to a solid, ageing for 24 h, and reconstitution in water. (B) contour length histogram for **P1** nanofiber **seeds 8** before (yellow) and after (red) lyophilization to a solid (L_n = 36 nm, $Đ_L$ = 1.12, $σ$ = 12 nm and L_n = 36 nm, $Đ_L$ = 1.10, $σ$ = 11 nm respectively). Scale bar = 200nm. The sample was stained with uranyl acetate (3 wt% in EtOH).
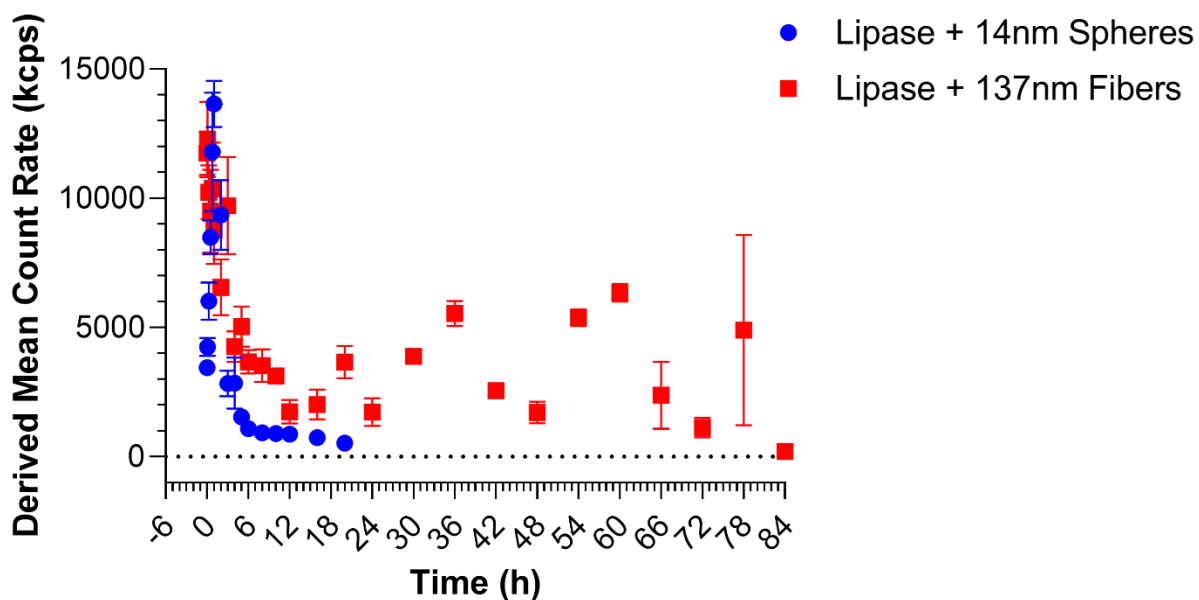

Figure S54. Assessing the degradation of 137 nm **P1** nanofibers ($Đ_L$ = 1.05, $σ$ = 30 nm) and 14 nm **P1** nanospheres ($Đ_D$ = 1.05, $σ$ = 3 nm) upon exposure to lipase from *Thermomyces lanuginosus* via DLS. Samples were exposed to lipase with activity levels of 1,000,000 U/L at 37°C in 5mM NaCl, and a size analysis was performed periodically. From the size data, the derived mean count

rate was plotted as a function of time. The derived mean count rate can be used as a measure of the number of particles remaining in solution. Each value represents the average of 5 repeats, with error represented as σ.
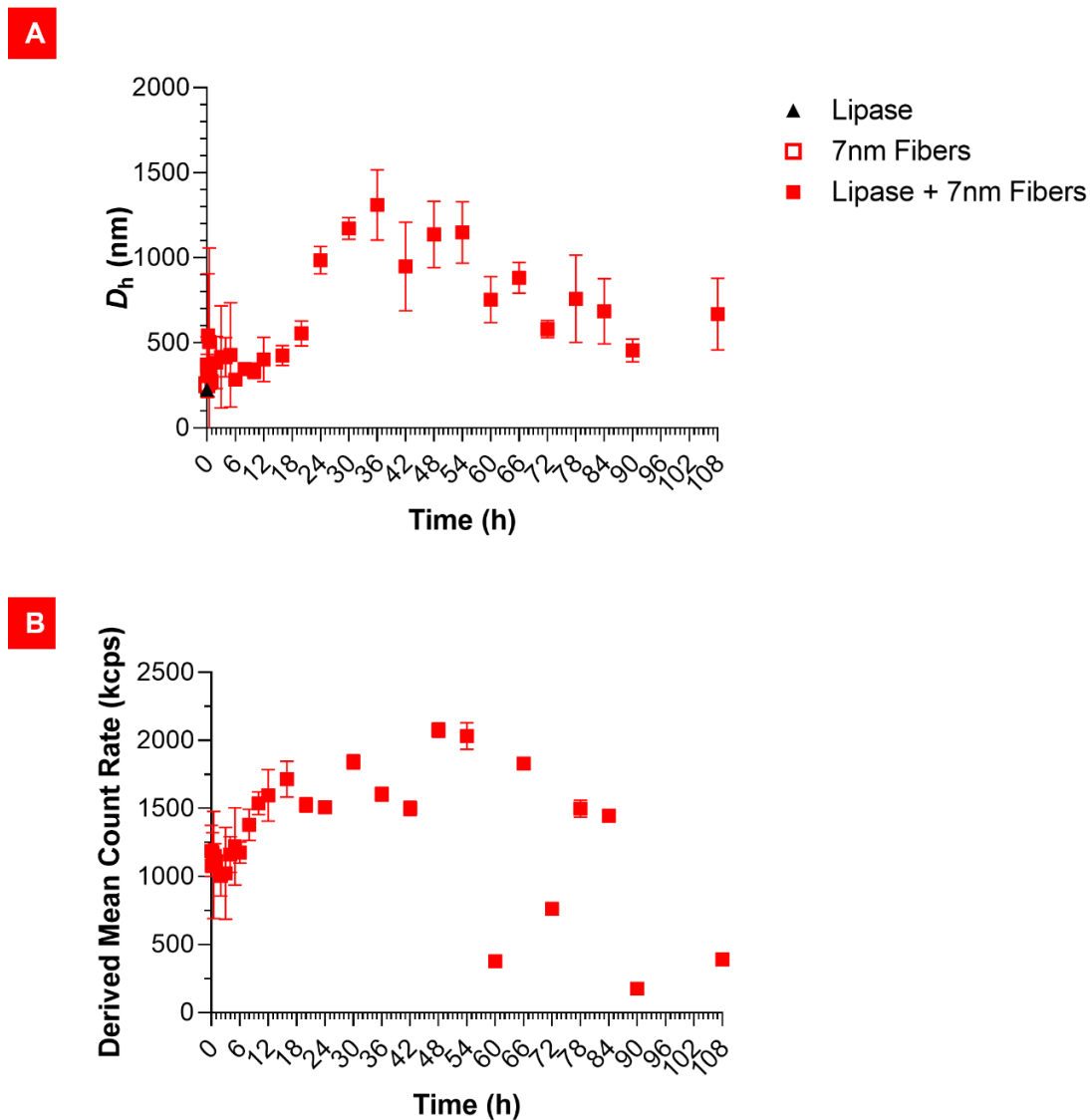

Figure S55. Assessing the degradation of 7 nm **P1** nanofibers ($Đ_L = 1.06$, $\sigma = 2$ nm) upon exposure to lipase from *Thermomyces lanuginosus* (TLL, 140 U/L) via DLS. Samples were incubated with lipase at 37°C in water, and (A) the D_h and (B) the derived mean count rate was measured periodically. Each value represents the average of 5 repeats, with error represented as σ. For reference, normal lipase levels in humans is typically <200 U/L.[S20] After 108 h, the instrument ceased to analyse the sample, instead repeatedly returning an 'invalid Z-average size' error (other samples worked fine).
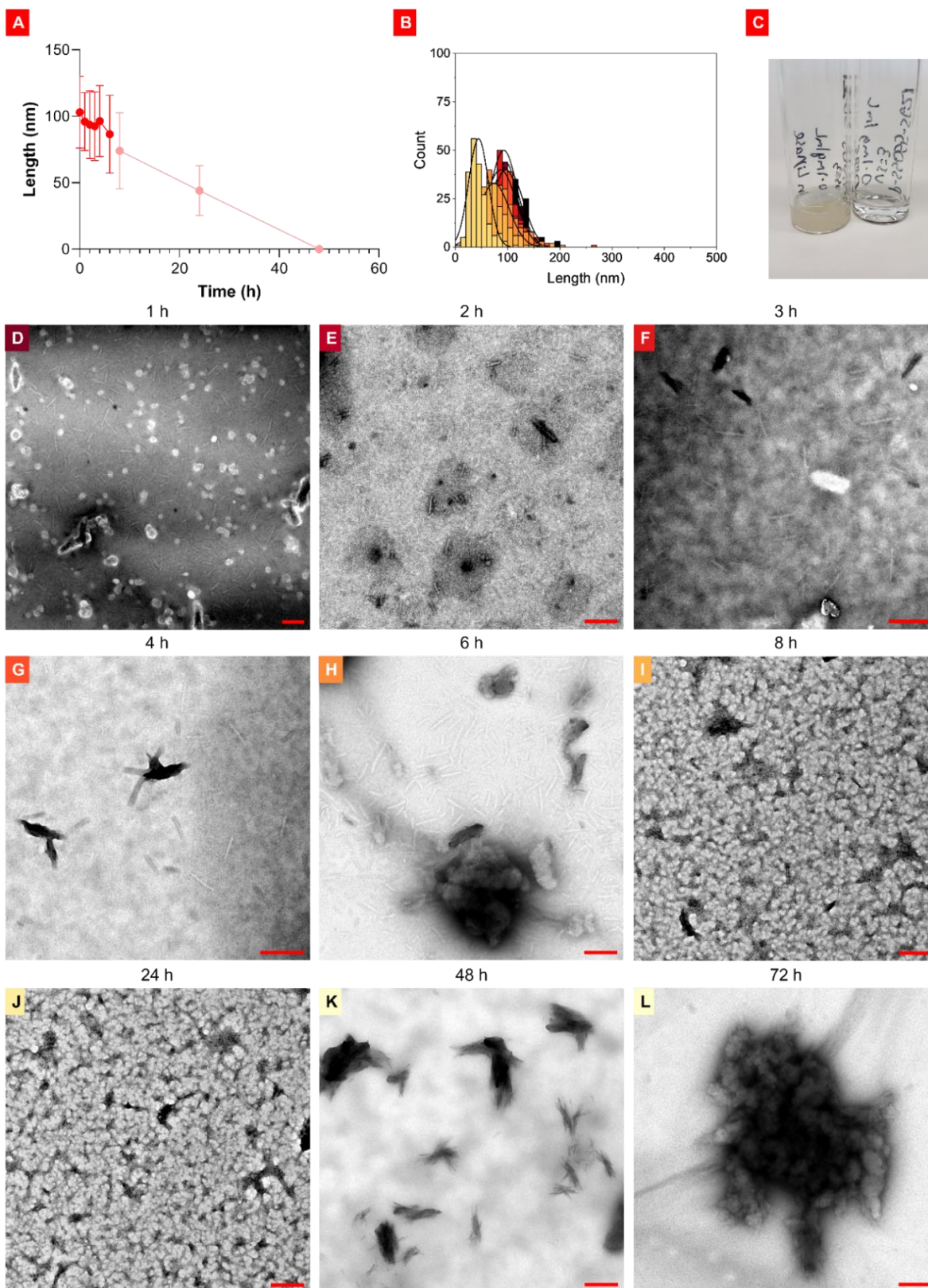
Figure S56. Assessing the degradation of 103 nm **P1** nanofibers ($Đ_L = 1.07$, $\sigma = 27$ nm) upon exposure to lipase from *Thermomyces lanuginosus* via TEM. Samples were exposed to lipase with

activity levels of $>9\times10^7$ U/L at 37°C in PBS, with aliquots taken for TEM (and MALDI-TOF MS) analysis periodically. (A) Plot of L_n against time, showing that nanofiber length decreases and dispersity increases over time. Dark red and light red indicate a high and low degree of confidence in the measurements respectively, as nanofibers were hard to definitively observe in samples from 8 and 24h, whilst none at all were observed for 48-72h; (B) Contour length histograms of the nanofiber measurements from D-L; (C) Photograph of the degradation solution after 72h (*left*) and nanofibers before the addition of lipase (*right*); (D-L) TEM micrographs of the degradation solution at various time intervals: after (D) 1h, (E) 2h, (F) 3h, (G) 4h, (H) 6h, (I) 8h, (J) 24h, (K) 48h and (L) 72h. Scale bars = 200nm. All samples were stained with uranyl acetate (3 wt% in EtOH).

Table S5. Statistical analysis of the contour lengths and dispersity of 103 nm **P1** nanofibers ($Đ_L = 1.07$, $\sigma = 27$ nm) obtained via TEM from the degradation study conducted in Figure S56. Timepoint 0 represents data from before lipase was added, whilst entries for 8h and 24h are coded red to indicate a lower degree of certainty of these measurements, due to nanofibers becoming harder to definitively observe in these samples. Note the continuously increasing $Đ_L$ and σ / L_n indicating an increase in sample dispersity.

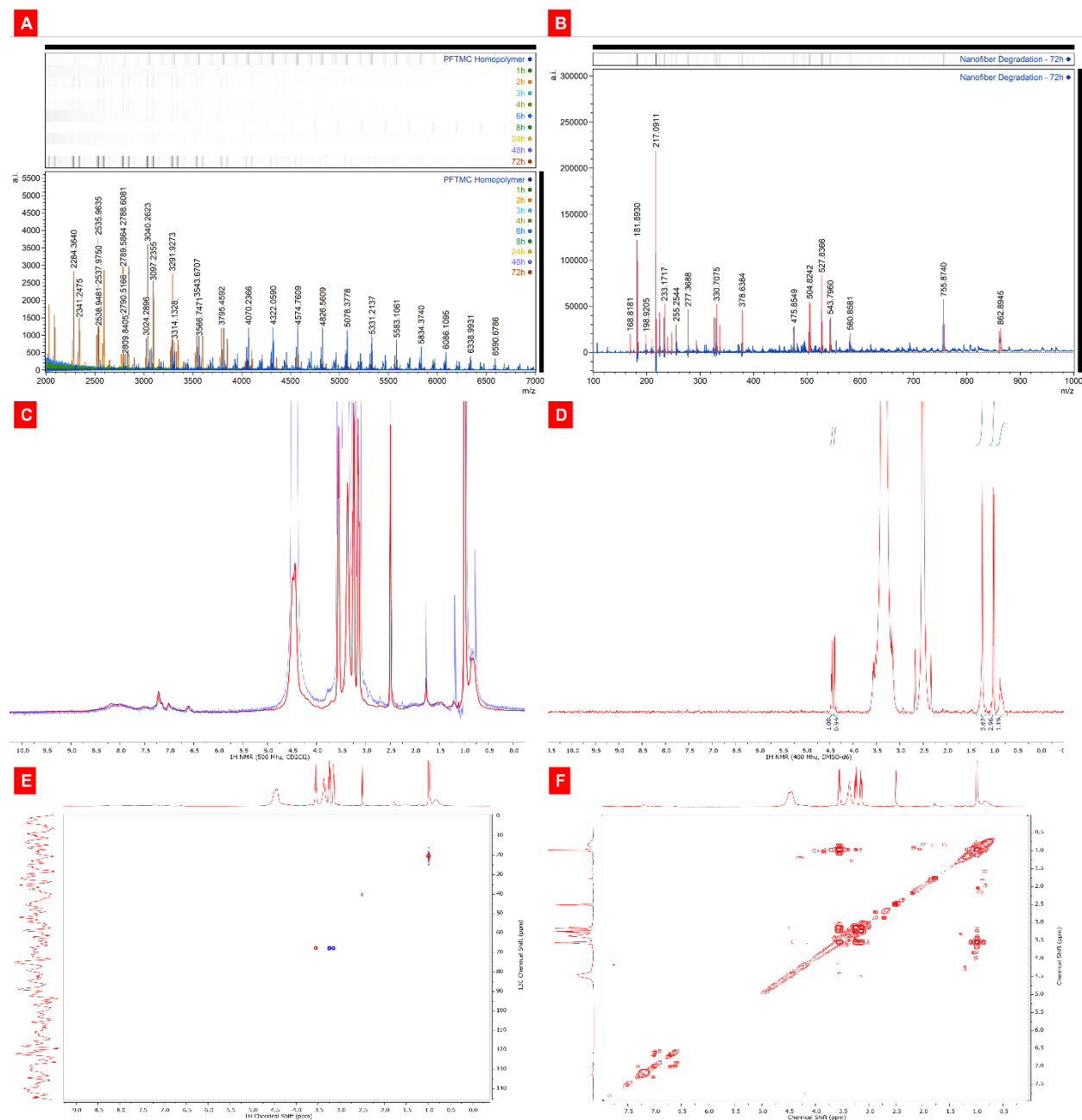| Timepoint (h)	n	L_n (nm)	L_w (nm)	$Đ_L$	σ (nm)	σ / L_n
0	256	103	110	1.07	27	0.26
1	216	96	101	1.05	22	0.22
2	208	94	101	1.07	26	0.27
3	235	93	100	1.08	26	0.28
4	209	97	104	1.08	27	0.28
6	238	86	96	1.12	29	0.34
8	201	74	85	1.15	29	0.39
24	201	44	52	1.18	19	0.43

Figure S57. Further analysis of the solution obtained from the degradation of 103 nm **P1** nanofibers ($Đ_L$ = 1.07, $σ$ = 27 nm) performed in Figure S56. (A-B) MALDI-TOF MS spectra of the degradation solution at various timepoints, revealing the presence of shorter PFTMC chains but no observable FTMC monomer. The faint signal at >4500 m/z for the 8h sample (green) corresponds to PFS impurities that were present on the MALDI plate; (C) ^{1}H-NMR of the degradation solution after 72h (red) which is mostly propylene glycol, with the ^{1}H-NMR of concentrated lipase solution overlaid (blue); (D) ^{1}H-NMR of the extracted organic components

from an analogous degradation experiment performed over 7 days, with no observable traces of **P1**; (E) ^{1}H-^{13}C HSQC NMR of the degradation solution after 72h from C; and (F) ^{1}H-^{1}H COSY NMR of the degradation solution after 72h from C.

Table S6. Cytotoxic effects of **P1** nanofibers and nanospheres, as well as PDMAEMA$_{113}$ and PEI$_{53}$ upon HeLa and WI-38 cells after 72h incubation. Reductive metabolism and cell viability were measured using almarBlue™ and calcein AM assays respectively. 103 nm **P1** nanofibers ($Đ_L = 1.07$, $\sigma = 27$ nm) were used for HeLa and WI-38, whilst 9-16 nm **P1** nanospheres ($Đ_L = 1.06 – 1.08$, $\sigma = 0.3 - 5$ nm) were used for HeLa and WI-38. The EC$_{50}$ values are reported in nM for all experiments, with the error in brackets, represented as the 95% confidence interval. Staurosporine was used as a positive control.

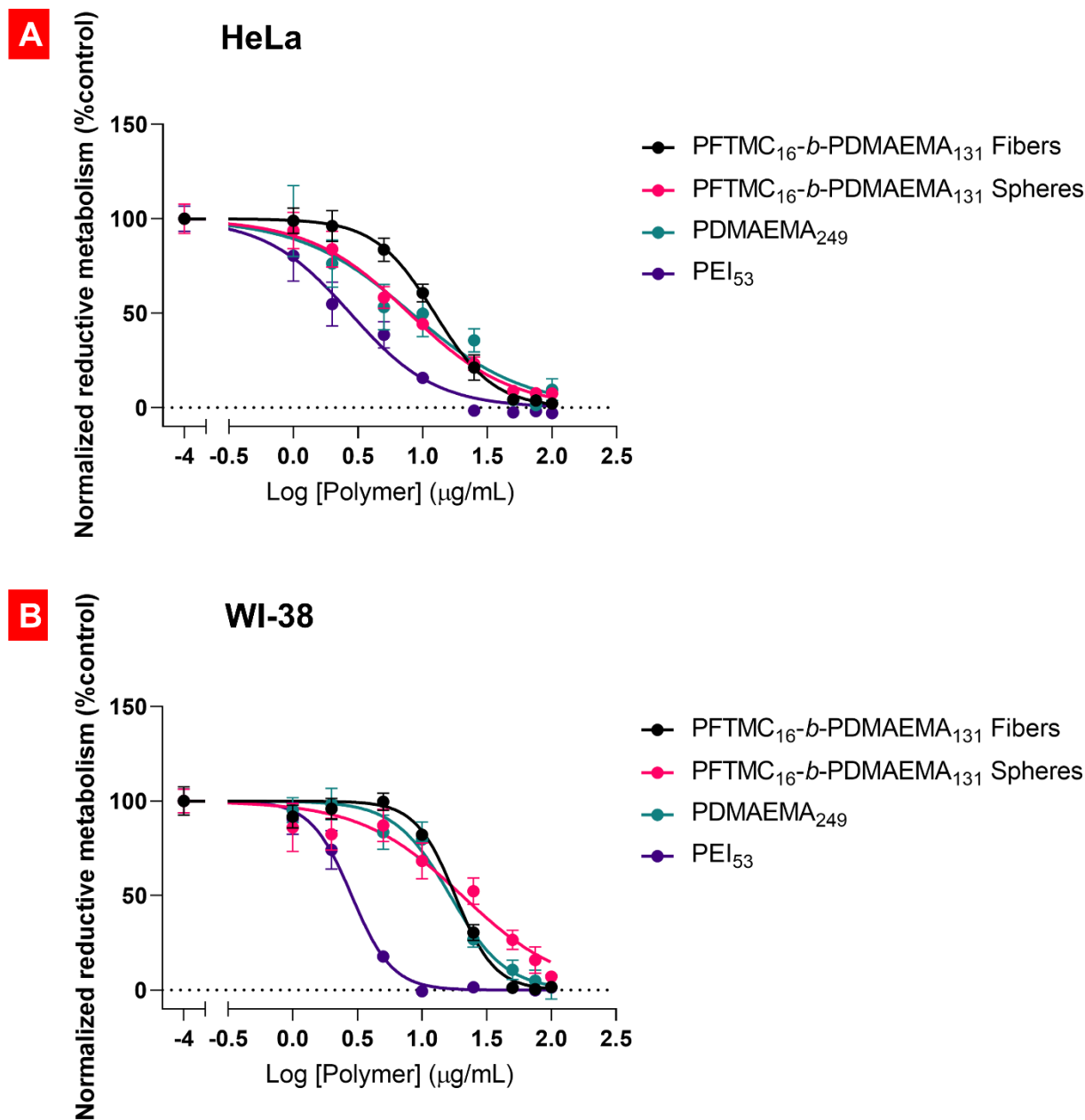| Sample	HeLa		WI-38	
	EC$_{50}$ alamarBlue™ (nM)	EC$_{50}$ Calcein AM (nM)	EC$_{50}$ alamarBlue™ (nM)	EC$_{50}$ Calcein AM (nM)
PFTMC$_{16}$-*b*-PDMAEMA$_{131}$ nanofibers	497 (460,537)	695 (591,813)	725 (680,774)	876 (788,962)
PFTMC$_{16}$-*b*-PDMAEMA$_{131}$ nanospheres	316 (282,354)	1385 (1249,1528)	820 (696,961)	281 (204,380)
PDMAEMA$_{249}$	455 (364,566)	2650 (2400,2879)	916 (824,1017)	560 (424,729)
PEI$_{53}$	110 (96,126)	374 (323,430)	114 (107,122)	68 (58,78)

Figure S58. Dose-response curves used to determine EC_{50} values for the cytotoxicity of **P1** nanofibers and nanospheres, as well as $PDMAEMA_{249}$ and PEI_{53} polymers upon (A) HeLa and (B) WI-38 cells after 72h incubation. Reductive metabolism was measured using an alamarBlue™ assay. Data was processed in GraphPad Prism 8 using the 'log(inhibitor) vs. normalized response - Variable slope (four parameters)' nonlinear regression analysis, and error is represented as the 95% confidence interval. The datapoint at -4 on the x-axis is the control (0 µg/mL).
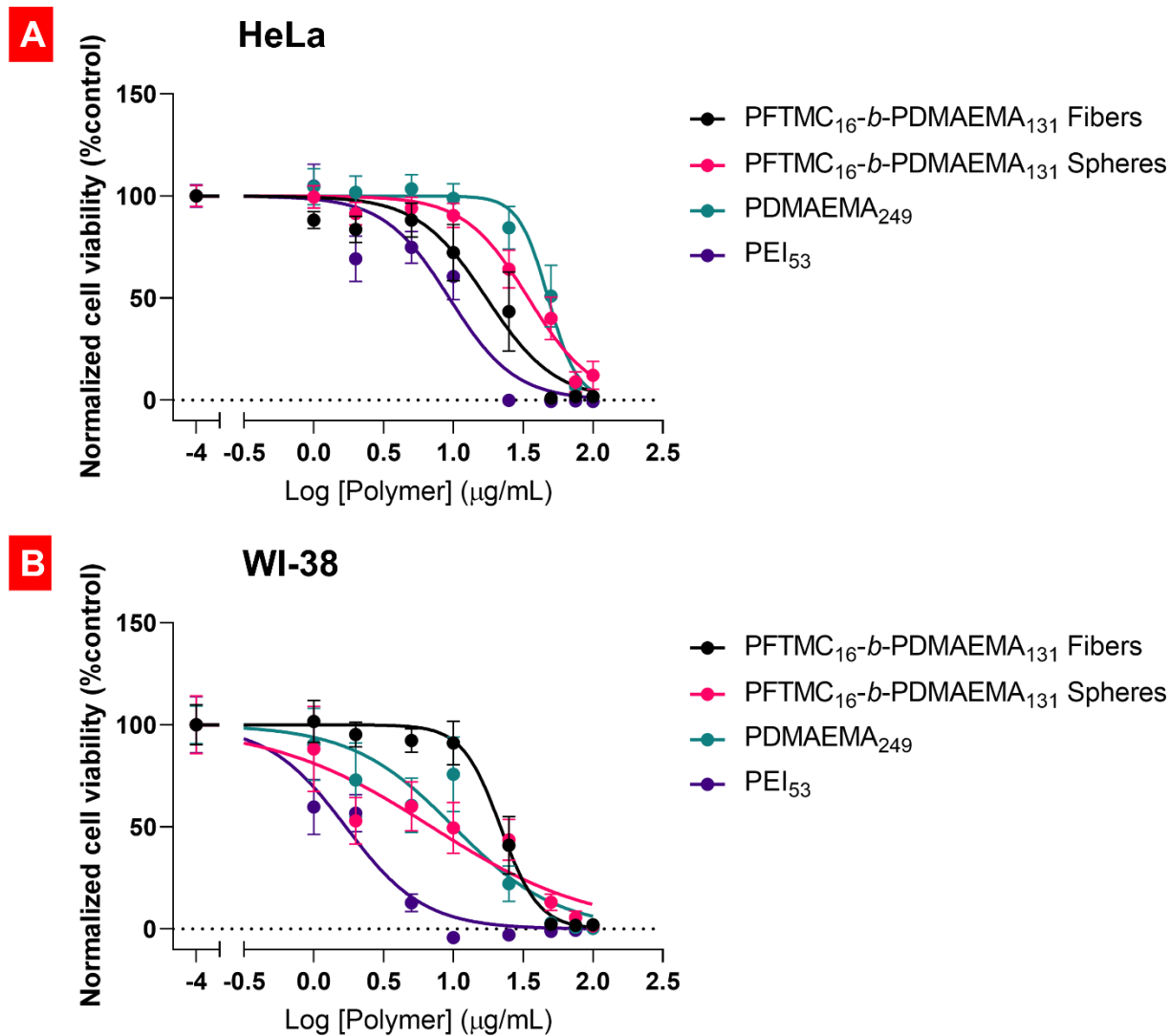
Figure S59. Dose-response curves used to determine EC_{50} values for the cytotoxicity of **P1** nanofibers and nanospheres, as well as $PDMAEMA_{249}$ and PEI_{53} polymers upon (A) HeLa and (B) WI-38 cells after 72h incubation. Cell viability was measured using a calcein AM assay. Data was processed in GraphPad Prism 8 using the 'log(inhibitor) vs. normalized response -- Variable slope (four parameters)' nonlinear regression analysis, and error is represented as the 95% confidence interval. The datapoint at -4 on the x-axis is the control (0 µg/mL).

Table S7. Summary of the segmented and blended micelles studied in this work, incorporating either **P2** containing BODIPY$^{630/650-X}$ or **P3** containing folic acid, into nanofibers or nanospheres produced from **P1**. Size and dispersity were determined via TEM, with error represented as σ.

Entry	Eq's P1	Eq's P2	Eq's P3	Morphology	L_n in THF/ MeOH 2:8 (nm)[a]	Đ in THF/ MeOH	L_n in Water (nm)[a]	Diameter (nm)[a]	Đ in Water
1	1	0	0	P1 Nanofiber	30 ± 8	1.08	-	-	-
2	1	2	0	P2-P1-P2 Triblock Nanofiber	51 ± 25	1.25	-	-	-
3	1	2	2	P3-P2-P1-P2-P3 Pentablock Nanofiber	101 ± 36	1.12	97 ± 44	-	1.20
4	1	0	0	P1 Nanofiber	22 ± 7	1.11	-	-	-
5[b]	1	2	2	(P2-*r*-P3)-P1-(P2-*r*-P3) Triblock Nanofiber	134 ± 42	1.10	77 ± 32	-	1.18
6	1	2	2	Random Blend Sphere	-	-	-	32 ± 11	1.11

[a] Recorded via TEM, this likely represents the core dimensions, not including the corona.
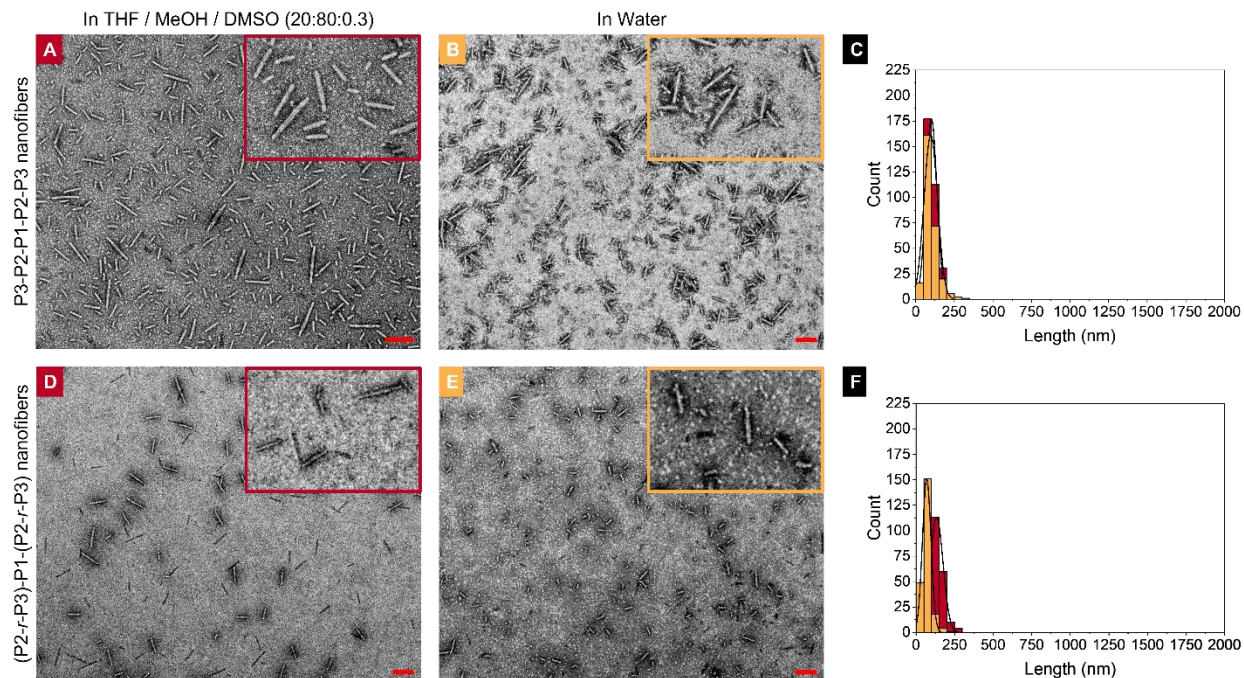[b] These nanofibers are a random blend of P2 and P3 grown from P1 seeds.

Figure S60. TEM micrographs of (A-C) pentablock segmented nanofibers and (D-F) blended nanofibers in (A, D) THF/MeOH/DMSO (20:80:0.3) and (B, E) water; (C) contour length histograms for A ($L_n = 101$ nm, $Đ_L = 1.12$, $\sigma = 36$ nm, in red) and B ($L_n = 97$ nm, $Đ_L = 1.20$, $\sigma = 44$ nm, in yellow); (F) Contour length histograms for D ($L_n = 134$ nm, $Đ_L = 1.10$, $\sigma = 42$ nm, in red) and E ($L_n = 77$ nm, $Đ_L = 1.18$, $\sigma = 32$ nm, in yellow). The ratio of polymers in both samples was: **P1**=1, **P2**=2, **P3**=2. Scale bars = 200nm. All images were stained with uranyl acetate (3 wt% in EtOH). Blended nanofibers exhibited more significant fragmentation and a reduction in length, whilst pentablock segmented nanofibers exhibited an increase in dispersity, but no significant change in length.
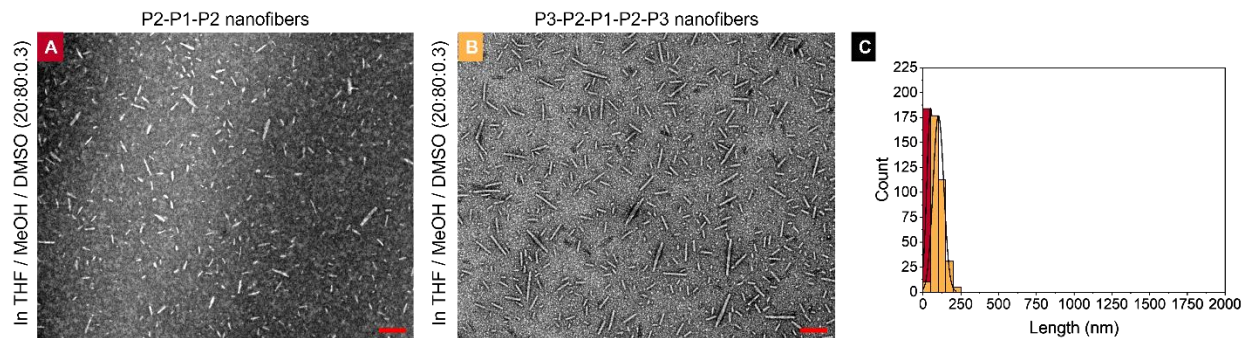

Figure S61. Preparation of 101 nm pentablock segmented nanofibers ($Đ_L = 1.12$, $\sigma = 36$ nm). (A-B) TEM micrographs of nanofibers (A) intermediate triblock nanofibers in

THF/MeOH/DMSO (2:88:10); (B) pentablock nanofibers in THF/MeOH/DMSO (2:88:10); (C) contour length histograms for A (L_n = 51 nm, $Đ_L$ = 1.25, σ = 25 nm) and B (L_n = 101 nm, $Đ_L$ = 1.12, σ = 36 nm). The 51 nm intermediate triblock nanofibers were prepared from 30 nm seeds ($Đ_L$ = 1.08, σ = 8 nm). Scale bars = 200nm. Both samples were stained with uranyl acetate (3 wt% in EtOH).
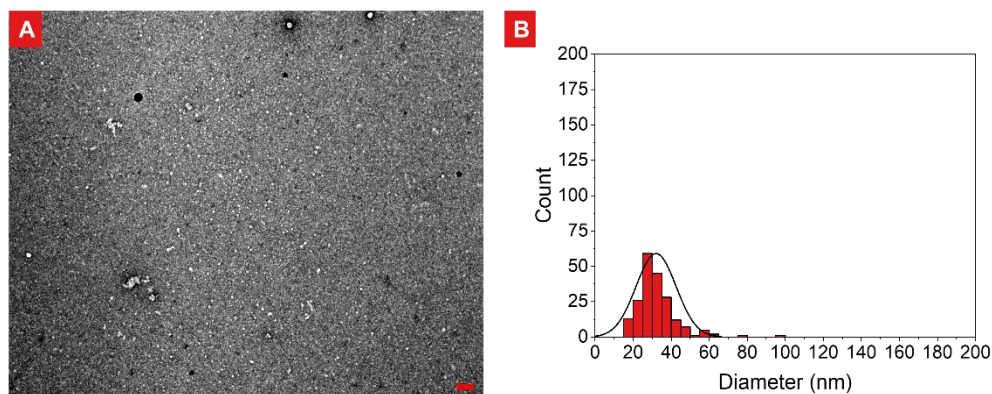

Figure S62. Blended nanospheres in water. (A) TEM micrograph and (B) diameter histogram (D_n = 32 nm, $Đ_L$ = 1.11, σ = 11 nm). The sample was stained with uranyl acetate (3 wt% in EtOH).

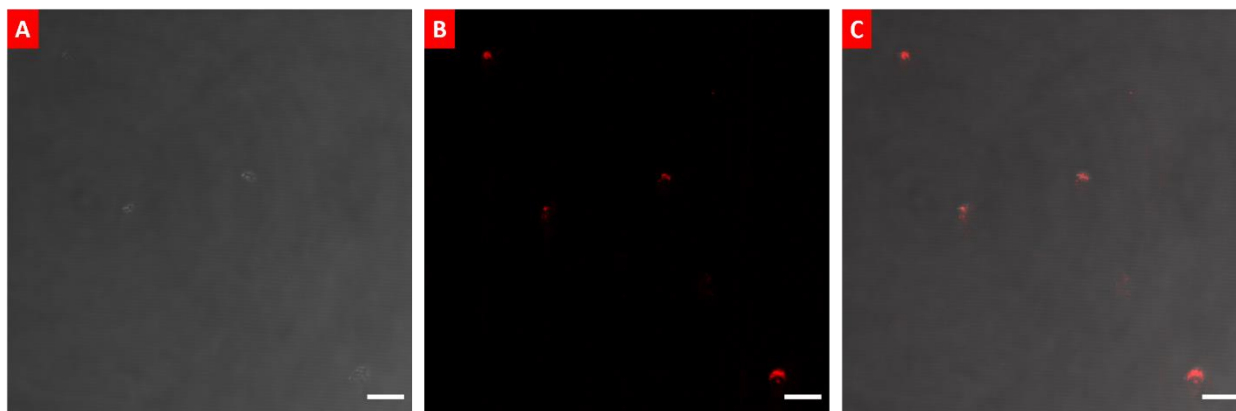**Figure S63.** CLSM z-projection of segmented nanofibers (L_n = 97 nm, $Đ_L$ = 1.20, σ = 44 nm, 0.1 mg/mL) in PBS (0.1× concentration). (A) Brightfield transmitted light channel; (B) BODIPY$^{630\text{-}650\text{-}X}$ fluorescence (λ_{ex} = 633 nm, λ_{em} = 640-700 nm); (C) overlay of images A-B. Scale bars = 10 μm.

References

S1   M. C. Arno, M. Inam, Z. Coe, G. Cambridge, L. J. Macdougall, R. Keogh, A. P. Dove and R. K. O'Reilly, *J. Am. Chem. Soc.*, 2017, **139**, 16980–16985.

S2   J. R. Finnegan, E. H. Pilkington, K. Alt, M. A. Rahim, S. J. Kent, T. P. Davis and K. Kempe, *Chem. Sci.*, 2021, **12**, 7350–7360.

S3   Z. M. Hudson, D. J. Lunn, M. A. Winnik and I. Manners, *Nat. Commun.*, 2014, **5**, 3372.

S4   J. D. Garcia-Hernandez, S. T. G. Street, Y. Kang, Y. Zhang and I. Manners, *Macromolecules*, 2021, **54**, 5784–5796.

S5   S. F. Mohd Yusoff, J. B. Gilroy, G. Cambridge, M. A. Winnik and I. Manners, *J. Am. Chem. Soc.*, 2011, **133**, 11220–11230.

S6   L. Gao, H. Gao, J. Lin, L. Wang, X. Wang, C. Yang and S. Lin, *Macromolecules*, 2020, **53**, 8992–8999.

S7   M. Luo, B. Jin, Y. Luo and X. Li, *Macromolecules*, 2021, **54**, 6845–6853.

S8   J. R. Finnegan, X. He, S. T. G. Street, J. D. Garcia-Hernandez, D. W. Hayward, R. L. Harniman, R. M. Richardson, G. R. Whittell and I. Manners, *J. Am. Chem. Soc.*, 2018, **140**, 17127–17140.

S9   J. M. Palomo, M. Fuentes, G. Fernández-Lorente, C. Mateo, J. M. Guisan and R. Fernández-Lafuente, *Biomacromolecules*, 2003, **4**, 1–6.

S10   S. Venkataraman, J. L. Hedrick and Y. Y. Yang, *Polym. Chem.*, 2014, **5**, 2035–2040.

S11   H. Lv, S. Zhang, B. Wang, S. Cui and J. Yan, *J. Control. Release*, 2006, **114**, 100–109.

S12   K. C. Remant Bahadur and H. Uludağ, in *Polymers and Nanomaterials for Gene Therapy*, Elsevier, 2016, pp. 29–54.

S13   S. T. G. Street, Y. He, X.-H. Jin, L. Hodgson, P. Verkade and I. Manners, *Chem. Sci.*, 2020, **11**, 8394–8408.

S14   A. M. Oliver, J. Gwyther, C. E. Boott, S. Davis, S. Pearce and I. Manners, *J. Am. Chem. Soc.*, 2018, **140**, 18104–18114.

S15   R. Deng, F. Liang, J. Zhu and Z. Yang, *Mater. Chem. Front.*, 2017, **1**, 431–443.

S16   A. B. Pangborn, M. A. Giardello, R. H. Grubbs, R. K. Rosen and F. J. Timmers, *Organometallics*, 1996, **15**, 1518–1520.

S17   W. C. Still, M. Kahn and A. Mitra, *J. Org. Chem.*, 1978, **43**, 2923–2925.

S18   WO 2016/193215 A1, 2016, p18.

S19   K. Nakazono, C. Yamashita, T. Ogawa, H. Iguchi and T. Takata, *Polym. J.*, 2015, **47**, 355–361.

S20   G. Lippi, M. Valentino and G. Cervellin, *Crit. Rev. Clin. Lab. Sci.*, 2012, **49**, 18–31.